

INFORMATION TO USERS

The most advanced technology has been used to photograph and reproduce this manuscript from the microfilm master. UMI films the text directly from the original or copy submitted. Thus, some thesis and dissertation copies are in typewriter face, while others may be from any type of computer printer.

The quality of this reproduction is dependent upon the quality of the copy submitted. Broken or indistinct print, colored or poor quality illustrations and photographs, print bleedthrough, substandard margins, and improper alignment can adversely affect reproduction.

In the unlikely event that the author did not send UMI a complete manuscript and there are missing pages, these will be noted. Also, if unauthorized copyright material had to be removed, a note will indicate the deletion.

Oversize materials (e.g., maps, drawings, charts) are reproduced by sectioning the original, beginning at the upper left-hand corner and continuing from left to right in equal sections with small overlaps. Each original is also photographed in one exposure and is included in reduced form at the back of the book.

Photographs included in the original manuscript have been reproduced xerographically in this copy. Higher quality 6" x 9" black and white photographic prints are available for any photographs or illustrations appearing in this copy for an additional charge. Contact UMI directly to order.

U·M·I

University Microfilms International
A Bell & Howell Information Company
300 North Zeeb Road, Ann Arbor, MI 48106-1346 USA
313/761-4700 800/521-0600

Order Number 9108146

**Interaction of the polysaccharide Xanthan with surfactants in
aqueous solution**

Mars, Laurent Robert, Ph.D.

City University of New York, 1990

Copyright ©1990 by Mars, Laurent Robert. All rights reserved.

U·M·I
300 N. Zeeb Rd.
Ann Arbor, MI 48106

A

**INTERACTION OF THE POLYSACCHARIDE XANTHAN
WITH SURFACTANTS IN AQUEOUS SOLUTION**

by

LAURENT R. MARS

**A dissertation submitted to the Graduate Faculty in Chemistry
in partial fulfillment of the requirements for the degree of
Doctor of Philosophy, The City University of New York.**

1990

© 1990

LAURENT R. MARS

All Rights Reserved

This manuscript has been read and accepted for the Graduate Faculty in Chemistry in satisfaction of the dissertation requirement for the degree of Doctor of Philosophy.

09/20/1990
date

Allen I. Rosano.
Chairman of Examining Committee

9/21/90
date

[Signature]
Executive Officer

[Signature]

David C. Loken

Supervisory Committee

The City University of New York

Abstract**INTERACTION OF THE POLYSACCHARIDE XANTHAN
WITH SURFACTANTS IN AQUEOUS SOLUTION**

by

Laurent R. Mars**Advisor: Professor Henri L. Rosano**

Polymer-Surfactant interactions are of considerable interest because of their chemical, biological, pharmaceutical, mineral-processing, and petroleum-engineering applications. The current investigation centered on the extent and mechanism of the interaction of the polymer Xanthan, an anionic polysaccharide widely used in industry because of its superior performance as an agent for rheology control, with three types of surfactants, nonionic, anionic, and cationic. Evidence of an interaction was obtained by observing a change either in the bulk properties of the polymer solutions upon addition of surfactant or in the surface properties of the surfactant solution upon addition of the polymer.

Interaction between Xanthan and a polyoxyethylene nonionic surfactant, Igepal CO-630, was found to occur when the surfactant is in its micellar form. Under conditions of salt concentration or pH that promote the helical conformation of Xanthan molecules, the degree of interaction is severely reduced, in fact becoming negligible. The proposed mechanism of interaction involves the formation of hydrogen bonds between the hydroxyl groups of Xanthan and the ether oxygens of the surfactant. Evidence of a specific interaction between Xanthan and the anionic surfactant Sodium dodecylsulfate was found only when divalent cations were added to the

solution. The weak interaction observed in this case is attributed to the divalent cations acting as bridges between the anionic groups of Xanthan and SDS. The effect of Ca^{2+} ions is more apparent in the monolayer experiments; when Xanthan is present along with Ca^{2+} ions in the subphase, the pressure and potential isotherms of an insoluble anionic film (arachidic acid at $\text{pH}=10$) are significantly altered. In contrast, the presence of Xanthan alone in the subphase does not affect these isotherms.

A significant interaction was observed between Xanthan and the cationic surfactant Cetyltrimethylammonium bromide (Stearyldimethylbenzylammonium chloride was used in monolayer experiments). Solubility experiments showed that precipitation occurs, due to charge neutralization, under conditions of excess surfactant. Further addition of surfactant does not resolubilize the precipitate. No precipitation is observed, however, when small amounts of Xanthan are added to a micellar surfactant solution, indicating that the polymer is preferentially binding to the micelles rather than to the monomer surfactant. In the pre-precipitation zone, the reduced viscosity of Xanthan solutions is lowered upon the addition of CTAB. This effect is comparable in magnitude to that produced by the addition of a simple salt (Tetramethylammonium chloride, or TMAC). The adsorption of CTAB on Xanthan therefore induces no surfactant-specific conformational change in the polysaccharide, and hydrophobic interactions can be ruled out. In the post-precipitation zone, the reduced viscosity of Xanthan + CTAB solutions is much lower than that of Xanthan + TMAC solutions. It may be concluded that the interaction between Xanthan and the cationic micelles imposes a more coiled-up conformation on the macromolecule. The surface tension of CTAB solutions is lowered upon the addition of Xanthan, due to the formation of

a highly surface-active polymer/surfactant complex. Similarly, the pressure-area isotherm of the cationic monolayer is expanded upon the introduction of Xanthan in the subphase. In contrast, the potential isotherm of the monolayer is only slightly affected by the presence of the polysaccharide. It may be concluded that the increase in surface pressure is due to an ion-exchange reaction (whereby a fraction of the counterions of the insoluble cationic surfactant are replaced by bulkier carboxylate groups of Xanthan), with very little or no penetration of segments of the polysaccharide molecules into the hydrophobic region of the monolayer. A thermodynamic treatment of the interaction between Xanthan and the cationic monolayer is proposed. The values obtained for the changes in partial standard free energy, enthalpy, and entropy clearly show that the interaction between Xanthan and the cationic monolayer is entropy driven.

Acknowledgements

--Would you like to go to the U.S.? Prof. Strauss asked abruptly, sticking his head through the door of the secretary's office where I was waiting for some form to be signed.

--Well, why not?

--All right! Consider yourself gone!

This brief and incongruous conversation happened in Paris, more than seven years ago, and it has somehow remained very vivid in my memory. And rightly so, for my life had just taken a turn as decisive as it was unexpected. Only months later would I learn of a certain Dr. Henri Rosano of New York, and more time would elapse before I learned that this same Dr. Rosano, with whom I was by now well acquainted, had suggested to my school's officials that they send him one of their soon-to-be-graduated students. So, before going any further, let me say with sincere gratitude: "Thank you, Dr. Rosano, for creating this opportunity, and thank you, Prof. Strauss, for choosing me. However casual your respective decisions, their impact on my life has been profound."

The years (too many of them, my mentor would certainly argue) spent under Dr. Rosano's tutelage have been rewarding both scientifically and in terms of my own personal development. As far as science was concerned, the field itself allowed me to explore several branches of chemistry. I never felt confined to a narrow, unidimensional area of research, and I greatly enjoyed finding myself at the boundary (or should I say interface) of distinct disciplines. This pluridisciplinary aspect of my work was magnified by my mentor's own attitude, which I find remarkable, of

unrelenting willingness to venture outside his primary area of expertise, despite the obvious temptation, after so many years of successful research, just to "keep rolling." Dr. Rosano represents to me the epitome of the polyvalent scientist who may not necessarily possess an encyclopedic knowledge but is capable of bringing together the expertise of scientists of different backgrounds, in order to solve whatever problem is given to him.

On the personal level, working with Dr. Rosano inevitably creates more than a professional relationship. Both supporters and detractors of this larger-than-life character would agree that he always speaks his mind. This attitude, which is far from being limited to scientific subjects, was very useful for me as I acquainted myself with a new culture. Our common cultural background combined with his own experiences as a newcomer in America helped me in my transition between old and new environments.

My years at City College were not without their many letdowns and periods of depression and frustration. Thanks to the unwavering support and love of my wife Grace, I was able to weather these difficult times.

During these years, I also forged a few friendships with my fellow graduate students. Time will tell if they survive the different directions that our lives are taking now. In any event, I will always remember fondly the good times we wasted discussing politics, music, or whatever nonscientific subject seemed preferable to our research.

If the style of my thesis ultimately reveals itself to be of greater value than the scientific contents, much credit is due to Martha Browne, despite her reluctance to admit it. Remaining errors or infelicities of style are entirely my own.

Table of Contents

Copyright	ii
Approval	iii
Abstract	iv
Acknowledgement	vii
Table of Contents	ix
List of Figures	xi
Chapter one: Introductory Remarks	1
1.1 The Research Project	1
1.2 Surfactant Solutions	3
1.2.1 Surface Properties and Self-association	3
1.2.2 Thermodynamic Models for Micellization	4
1.3 Polymer-Surfactant solutions	7
1.3.1 Introduction	7
1.3.2 Qualitative Description of Polymer-Surfactant Interactions..	8
1.3.3 Thermodynamics of Polymer-Surfactant Interactions.....	10
Chapter two: Characterization of the polysaccharide Xanthan	18
2.1 Introduction	18
2.2 Experimental	22
2.3 Results	23
2.3.1 NMR Spectroscopy	23
2.3.2 Viscosity	25
2.3.3 Photon Correlation Spectroscopy	25
2.4 Discussion	26

Chapter three: Bulk Properties of Xanthan/Surfactant solutions.....	35
3.1 Introduction	35
3.2 Experimental	38
3.3 Results	39
3.3.1 Non-ionic surfactant	39
3.3.2 Anionic Surfactant	40
3.3.3 Cationic Surfactant	40
3.4 Discussion	42
3.4.1 Nonionic Surfactant	42
3.4.2 Anionic Surfactant	44
3.4.3 Cationic Surfactant	45
Chapter four: Surface Properties of Xanthan/Surfactant Solutions.....	56
4.1 Introduction	56
4.2 Experimental	58
4.3 Results	60
4.3.1 Surface tension	60
4.3.2 Monolayers	61
4.3.2.1 Nonionic Film	61
4.3.2.2 Anionic Film	62
4.3.2.3 Cationic Film	63
4.4 Discussion	65
4.4.1 Nonionic and Anionic surfactants	65
4.4.2 Cationic Surfactants	67
References	101

List of Figures

Chapter 2

Figure 2.1	Molecular structure of Xanthan	28
Figure 2.2	Schematic illustration of a) the ordered and disordered conformations of Xanthan, and b) the gel-like structure formed by Xanthan molecules	29
Figure 2.3	Instrument configuration for Photon Correlation Spectroscopy	30
Figure 2.4	NMR spectrum of Xanthan in D ₂ O	31
Figure 2.5	Reduced viscosity of Xanthan in 0.01M NaCl solution vs. shear rate	32
Figure 2.6	Zero-shear reduced viscosity of Xanthan solutions vs. Xanthan concentration	33
Figure 2.7	z-average translational diffusion coefficient of Xanthan in 0.01M NaCl solution vs. sample time	34

Chapter 3

Figure 3.1	Reduced viscosity of Xanthan + Igepal CO-630 solutions vs surfactant concentration	50
Figure 3.2	Reduced viscosity of Xanthan in 0.01M Igepal CO-630 solution vs. Xanthan concentration	51

Figure 3.3	Reduced viscosity of Xanthan + SDS solutions vs. surfactant concentration	52
Figure 3.4	Reduced viscosity of Xanthan + SDS + 2×10^{-4} M CaCl ₂ solutions vs. surfactant concentration	53
Figure 3.5	Solubility diagram of Xanthan + CTAB solutions	54
Figure 3.6	Reduced viscosity of 0.10g/l Xanthan + CTAB solutions vs. surfactant concentration	55
 Chapter 4		
Figure 4.1	Schematic illustration of the effect of the interaction between a neutral polymer and an ionic surfactant on the surface tension of the solutions	74
Figure 4.2	Schematic illustration of the effect of the interaction between an anionic polymer and a cationic surfactant on the surface tension of the solutions	75
Figure 4.3	Experimental setup used for the monolayer experiments....	76
Figure 4.4	Surface tension of Xanthan + Tween 60 solutions vs. surfactant concentration	77
Figure 4.5	Surface tension of Xanthan + SDS solutions vs. surfactant concentration	78
Figure 4.6	Surface tension of Xanthan + CTAB solutions at pH=7 vs. surfactant concentration	79

Figure 4.7	Surface tension of Xanthan + CTAB solutions at pH=3 vs. surfactant concentration	80
Figure 4.8	Π -A and ΔV -A isotherms of palmitic acid at pH=3 on 0.10g/l Xanthan subphase	81
Figure 4.9	Π -A and ΔV -A isotherms of palmitic acid at pH=7 on 0.10g/l Xanthan subphase	82
Figure 4.10	Π -A and ΔV -A isotherms of arachidic acid at pH=10 on 0.10g/l Xanthan subphase	83
Figure 4.11	Π -A and ΔV -A isotherms of arachidic acid at pH=10 on 0.10g/l Xanthan + CaCl ₂ subphase	84
Figure 4.12	Π -A and ΔV -A isotherms of Stearyldimethylbenzylam- monium chloride at pH=3 on 0.04g/l Xanthan subphase ...	85
Figure 4.13	Π -A and ΔV -A isotherms of Stearyldimethylbenzylammo- nium chloride at pH=10 on 0.04g/l Xanthan subphase ...	86
Figure 4.14	$\Delta\Pi$ vs. Π_i for Stearyldimethylbenzylammonium chloride on 0.04g/l Xanthan at pH=3 and pH=10	87
Figure 4.15	Π -A and ΔV -A isotherms of Stearyldimethylbenzyl- ammonium chloride at 10°C, 15°C, 25°C, and 31°C on 0.40g/l Xanthan subphase	88
Figure 4.16	$\Delta\Pi$ vs. Π_i at 10°C, 15°C, 25°C, and 31°C on 0.40g/l Xanthan subphase	89

Figure 4.17 $\Delta\Pi$ vs. Π_i at 10°C and on 0.01g/l, 0.02g/l, 0.04g/l, and 0.40g/l Xanthan subphases	90
Figure 4.18 $\Delta\Pi$ vs. Π_i at 15°C and on 0.01g/l, 0.02g/l, 0.04g/l, and 0.40g/l Xanthan subphases	91
Figure 4.19 $\Delta\Pi$ vs. Π_i at 25°C and on 0.01g/l, 0.02g/l, 0.04g/l, and 0.40g/l Xanthan subphases	92
Figure 4.20 $\Delta\Pi$ vs. Π_i at 10°C and on 0.01g/l, 0.02g/l, 0.04g/l, and 0.40g/l Xanthan subphases	93
Figure 4.21 $\Delta\Pi$ vs. Xanthan concentration at constant Π_i , and T=10°C	94
Figure 4.22 $\Delta\Pi$ vs. Xanthan concentration at constant Π_i , and T=15°C	95
Figure 4.23 $\Delta\Pi$ vs. Xanthan concentration at constant Π_i , and T=25°C	96
Figure 4.24 $\Delta\Pi$ vs. Xanthan concentration at constant Π_i , and T=31°C	97
Figure 4.25 Schematic illustration of the arrangement of detergent ions at the air-water interface	98
Figure 4.26 $\Delta\bar{G}_{pen}^0$ vs. Π_i at 10°C, 15°C, 25°C, and 31°C	99
Figure 4.27 $\Delta\bar{G}_{pen}^0$ vs. temperature at constant Π_i	100

CHAPTER ONE

INTRODUCTORY REMARKS

1.1. THE RESEARCH PROJECT

The interaction in solution between surfactant molecules and either synthetic or biological macromolecules has been a topic of considerable interest over the past four decades in both academia and industry because of its relevance to biological, chemical, pharmaceutical, mineral-processing, and petroleum engineering applications (1-3). The simultaneous presence of surfactant and polymer molecules in solution can play a significant role in determining solution rheology, stability of colloidal dispersions, adsorption behavior at interfaces, and solubilization capacity of aqueous solutions, for example.

In type and magnitude, the interaction is governed primarily by the ionic character--cationic, anionic, or nonionic--of both polymer and surfactant molecules. It has been shown that the interaction patterns of charged polymers are quite different from those of neutral polymers, that the strength of the interaction is generally stronger with anionic surfactants than with their cationic analogs, and that nonionic surfactants either do not interact or do so very weakly. These well-established patterns have led previous investigators to concentrate primarily on three types of interactions out of the nine possible combinations of cationic, anionic, or nonionic polymers with cationic, anionic, or nonionic surfactants: those in which charged polymers interact with oppositely charged surfactants and those in which neutral polymers interact with anionic surfactants.

For the past 15 years or so, most newly-developed polysaccharides, whether anionic (Carboxymethyl cellulose), cationic (Polymer JR), or neutral (Hydroxymethyl cellulose), have been studied in their interaction with surfactants. In contrast, the anionic polysaccharide Xanthan, whose remarkable rheological properties in aqueous solution have found a wide range of industrial applications, has received little study as far as its interaction with surfactants is concerned. The complex, although well understood, behavior of this polymer in solution may explain this omission.

In my research, I sought to determine whether and how interactions take place between the polysaccharide Xanthan and nonionic, anionic, and cationic surfactants, using as an indicator any significant change in the main physico-chemical properties of one of the components (polymer or surfactant) upon addition of the other. This approach led naturally to a two-part investigation: a study of the effect of adding a surfactant on the bulk properties of Xanthan solutions and a study of the effect of adding Xanthan on the surface properties of surfactant solutions. The results are presented in chapters three and four, respectively.

This chapter first reviews those properties of surfactant solutions that are relevant to the present study and briefly presents some of the thermodynamical models for surfactant aggregation that have been used as a basis for developing theories of polymer/surfactant interactions. A qualitative description of polymer/surfactant interactions follows, with a discussion of theoretical models that have been proposed in recent years.

1.2. SURFACTANT SOLUTIONS

1.2.1. SURFACE PROPERTIES AND SELF-ASSOCIATION

Surface-active compounds, or surfactants, are molecules with both a hydrophobic part (usually a long hydrocarbon chain, referred to as the surfactant tail) and a hydrophilic part (either a polar or an ionic group). The term "surface active" arises from their preference for occupying a position at the solution interface, one that minimizes the energetically unfavorable contact between water molecules and their hydrophobic parts. The resulting excess concentration (compared to the bulk concentration) of surfactant in the neighborhood of the surface has the effect of lowering the surface (or interfacial) tension of the aqueous solution.

Surfactants are usually classified as nonionic or ionic. In nonionic surfactants, the hydrophilic part is a polar group such as amine-oxide or ether. The class of ionic surfactants can be subdivided into anionic compounds (e.g., sulfate, sulfonate, or carboxylate), cationic compounds (e.g., quaternary ammonium), and zwitterions (in which both anionic and cationic groups are present).

At low concentrations (typically, $1 \times 10^{-2} \text{M}$ or less), surfactant molecules are singly dispersed in solution. As the surfactant concentration is increased, however, a point is reached at which the solution becomes saturated with monomer surfactant molecules and any further increase in concentration results in the spontaneous formation of stable aggregates called micelles. Micellization causes drastic changes in the various colligative properties of the surfactant solution (e.g., osmotic pressure, surface tension, and conductivity). The concept of critical micelle concentration, or cmc, inspired by these concentration-dependent phenomena, is defined (4) as the minimum surfactant concentration

necessary to form micelles. Hartley (5) was the first one to suggest, some forty years ago, that micelles are roughly spherical in shape. This notion has since been shown to be correct for concentrations close to the cmc. Different geometrical shapes are encountered, however, at surfactant concentrations far above the cmc.

The chief driving force in this aggregation process is a reduction of the hydrocarbon/water contact area of the surfactant alkyl chains. One of the main forces resisting micellization in the case of ionic surfactants is the coulombic repulsions created by the crowding together of the ionic headgroups at the periphery of the micelle. In the case of nonionic surfactants, dipole-dipole interactions and steric repulsions are the main resisting factors.

The process of micellization thus represents a delicate balance between forces favoring aggregation and those opposing it.

1.2.2. THERMODYNAMIC MODELS FOR MICELLIZATION

The first attempt at a quantitative treatment of micellization was made by Debye (6, 7). The many subsequent refinements (8-15) can be reduced in essence to three different approaches; these are summarized below, with greatest emphasis on the Mass Action model because of its direct application to polymer-surfactant interactions.

1.2.2.1. The Mass Action Model

The self-association process can be described by the following equation:



The equilibrium constant is given by

$$K_n = \frac{X_n}{X_1^n} \quad (1-2)$$

where X_1 is the molar fraction of singly dispersed surfactant molecules and X_n is the molar fraction of micelles containing n surfactant molecules.

The size distribution function of the micelles, $X_n(n)$, can be expressed in terms of the standard free energy change of micellization, $\Delta\mu_{mic}^0$, by

$$X_n = X_1^n \exp\left(-\frac{n\Delta\mu_{mic}^0}{kT}\right) \quad (1-3)$$

and the critical surfactant concentration X_{1cmc} at which micellization starts can be approximated by the expression (16, 17)

$$kT \ln X_{1cmc} \approx \Delta\mu_{mic}^0 = \mu_n^0 - \mu_1^0 \quad (1-4)$$

where μ_n^0 is the standard chemical potential of the surfactant molecule in the micelle and μ_1^0 is the standard chemical potential of the singly dispersed surfactant molecule.

It is convenient to define a so-called intrinsic equilibrium constant $k_n = (K_n)^{1/n}$. Since the molar fraction X_1 remains constant and equal to X_{1cmc} , it follows from eq. 1-3 and 1-4 that

$$k_n = \exp\left(-\frac{\Delta\mu_{mic}^0}{kT}\right) \quad (1-5)$$

Given an explicit equation for $\Delta\mu_{mic}^0$, as a function of the micelle size n , expressions for the size distribution function $X_n(n)$, the critical micelle concentration X_{1cmc} , and the intrinsic equilibrium constant k_n can therefore be derived from eq. 1-3, 1-4, and 1-5, respectively.

The standard free energy of micellization can be written as the sum of a number of contributions (18):

$$\Delta\mu_{mic}^0 = \Delta\mu_{hc/w}^0 - kT \ln\left(\frac{\Omega_{mic}}{\Omega_{hc}}\right) + \sigma(a - a_0) - kT \ln\left(1 - \frac{a_p}{a}\right) + \Delta\mu_{electr} \quad (1-6)$$

The first term on the right-hand side of eq.1-6 represents the standard free energy change when the surfactant tail is transferred from water to a liquid hydrocarbon phase. The second term accounts for the decreased conformational freedom for the surfactant tail in the micelle (Ω_{mic}) compared to that in liquid hydrocarbon (Ω_{hc}). The third term represents the free energy of formation of the micelle/water interface, with σ the interfacial tension, a the molecular area at the micelle surface, and a_p the molecular area occupied by the surfactant headgroup. The fourth term is a measure of the steric repulsions between the polar headgroups at the micellar surface. The last term accounts for the electrostatic interactions among the headgroups.

1.2.2.2. Other Models

The Pseudo-phase separation model considers the formation of micelles as a phase separation. At equilibrium, the chemical potentials of the surfactant molecules in the aqueous phase and in the micellar phase must be equal:

$$\mu_{mic} = \mu_{aq} \quad (1-7)$$

Both terms in eq.1-7 can be expressed in terms of the molar fractions of surfactant in aqueous and micellar phases, and the resulting expression is identical to eq.1-3 obtained with the mass-action model. However, the two approaches are equivalent only in the treatment of nonionic surfactant solutions. In the case of ionic surfactants, eq.1-1 must be modified in order to account for the surfactant counterions participating in the equilibrium, and the two models are no longer equivalent (except for micelles of large size, for which the two models are again in agreement).

A third model, based on Hill's (15) theory of the thermodynamics of small systems, has been proposed (19), in which micelles of various sizes and shapes are in a dynamic equilibrium determined by intensive environmental variables including temperature, pressure, and chemical potential of the singly dispersed surfactant molecules. Whereas the mass-action and phase separation models are valid only in the concentration range near the cmc where micelles are small, spherical, and monodispersed, this method has the advantage of accounting for the coexistence of micelles with different sizes and shapes, a condition generally encountered at surfactant concentrations greatly exceeding the cmc.

1.3. POLYMER-SURFACTANT SOLUTIONS

1.3.1. INTRODUCTION

The foundation of the current research in polymer-surfactant interaction can be traced back to the 40's, when protein-ionic surfactant systems were first studied. Two observations--that maximum interaction occurred when protein and surfactant molecules carried opposite charges, and that resolubilization could be made to follow precipitation of the polymer-surfactant complex by the addition of excess surfactant (20)--led to emphasis on the role of coulombic forces in the binding of the surfactant onto the macromolecule and on the effect of such interaction on the protein conformation.

In the 50's and 60's, a great deal of work was done on mixtures of neutral synthetic polymers and ionic surfactants (21, 22). The behavior of such systems was shown to be primarily governed by two critical surfactant concentrations, the first corresponding to the onset of polymer-surfactant

complex formation, the second to the saturation of the polymer with surfactant. Although no specific part of the macromolecule could be clearly identified as a binding site, the concept, inherited from the earlier studies on protein-surfactant mixtures, was used in interpreting data and formulating theoretical models.

Finally, the advent in the early 70's of a range of new polyelectrolytes (mainly natural polysaccharides and synthetic vinyl polymers) gave rise to a surge of interest in charged polymers-ionic surfactants systems that has grown steadily ever since.

1.3.2. QUALITATIVE DESCRIPTION OF POLYMER-SURFACTANT INTERACTIONS

Mixing surfactants and polymers in aqueous solution leads, under certain circumstances, to complex formation through binding or adsorption of the surfactant molecules--either individually or as aggregates--onto the macromolecule. Both the occurrence and the strength of such interactions depend on the properties of polymer, surfactant, and dissolving medium. Nonionic surfactants either do not interact with polymers or do so very weakly (23-25), while ionic surfactants bind to both uncharged and oppositely charged polymers, anionic surfactants interacting more strongly than cationic ones of the same hydrophobic moiety (26). The interaction patterns differ, however, according to the ionic nature of the polymer.

With neutral polymers, complex formation occurs only above a critical surfactant concentration, which is lower than the surfactant cmc and independent of the polymer concentration. The surfactant concentration at which the polymer becomes saturated is directly proportional to the polymer concentration and can therefore be either lower or higher than the

cmc. In the latter case, micellization of unbound surfactant molecules starts competing with the binding process, preventing the polymer molecules from becoming saturated. The interaction process is highly cooperative, as indicated by the steep slope of the binding isotherms (27). Such observations have led to the conclusion that surfactant molecules were actually binding to the macromolecule as surfactant clusters rather than as individual molecules. Studies using NMR (28) and neutron-scattering (29) techniques have lent support to the existence of such polymer-micelle complexes. Indirect estimates of the size of these clusters (30,31) showed that they were smaller than the free micelles occurring in polymer-free solutions.

Because polymer-bound micelles occur at lower surfactant concentration than do free micelles, the presence of polymer in solution can be interpreted as promoting micellization through favorable hydrophobic interactions. The polymer-surfactant complex can be viewed as consisting of a macromolecule wrapped around surfactant aggregates, with the hydrophobic segments partially penetrating the interfacial regions of the micelles, thereby decreasing the contact area between water and the hydrocarbon core of the micelle. Furthermore, sufficient flexibility of the macromolecule could, ideally, allow ion-dipole interaction between its hydrophilic segments and the ionic headgroups of the surfactant, resulting in the lowering of ionic repulsions between the latter.

With oppositely charged polymers, binding occurs at much lower surfactant concentrations. As more surfactant is added, charge neutralization is eventually reached and the complex precipitates. Often, a further increase in surfactant concentration can resolubilize the precipitate

as a polyelectrolyte complex with a net charge opposite that of the original polymer (32). For such systems, the binding isotherm generally starts with a low slope and becomes very steep around the point of half saturation. Addition of a neutral salt usually has the effect of shifting the isotherm to higher surfactant concentrations and of increasing the steepness of the slope, indicating that electrical shielding of the charges reduces the affinity of binding while enhancing the cooperativity of the process (33-35). These results have been interpreted in terms of ionic and hydrophobic interactions. While the primary driving force can be viewed as electrostatic, the process is strongly reinforced by the association of alkyl chains of the adsorbing species. We can thus identify two distinct modes of adsorption: one, at low surfactant concentration, in which individual surfactant molecules bind to the polymer through ionic attraction alone, and a second, at higher concentrations, in which cluster-like adsorption is due primarily to hydrophobic interactions between bound surfactant molecules.

1.3.3. THERMODYNAMICS OF POLYMER-SURFACTANT INTERACTION

Various attempts have been made to provide a theoretical framework within which to interpret the wealth of data gathered over the past twenty years or so. The differences observed between neutral polymer-surfactant solutions and charged polymer-surfactant solutions have been a major obstacle towards a unified theory for polymer-surfactant interactions, however, and most attempts have accordingly been limited to one or the other of the two systems.

1.3.3.1. Nonionic Polymers

The similarities between the formation of polymer-bound clusters and micellization have led most investigators to use equations derived for the latter process, modifying them to account for the presence of polymer in solution. Such theoretical attempts have resulted in models requiring a knowledge of the system's macromolecular geometry that is not available, and curve-fitting parameters must therefore be introduced. The first models to be developed used a mass action law approach (31, 36). Their major drawback lay in the requirement that the total concentration of binding sites on the polymer molecule be known. This quantity can be determined experimentally through saturation of the polymer with bound surfactant, but this is not always possible to achieve.

More recently, Nagarajan (37) and Ruckenstein (38) have proposed similar models based on the theory of micellization that they had previously developed (13, 17, 18). Nagarajan hypothesized that micellar aggregates form in the free space of the coiled macromolecule. Undefined segments of the macromolecule can penetrate the interfacial region of the surfactant clusters, with two opposite effects: on the one hand, a decrease in the contact area between the hydrocarbon core and water, and on the other, an increase in steric repulsions between the surfactant headgroups. If the former effect outweighs the latter, polymer-bound surfactant clusters will form. These effects are accounted for by modifying the expression derived for the change in standard chemical potential (see eq. 1-6) of the surfactant molecules upon micellization, as follows:

$$\Delta\mu_{mic}^0 = \Delta\mu_{hc/w}^0 - kT \ln \left(\frac{\Omega_{mic}}{\Omega_{hc}} \right) + \sigma(a - a_s - a_{pol}) - kT \ln \left(1 - \frac{a_p + a_{pol}}{a} \right) + \Delta\mu_{electr} \quad (1-8)$$

The parameter a_{pol} represents the area per surfactant molecule occupied by the polymer at the micellar interface, and it can be interpreted as a measure of the polymer's ability to adopt a configuration compatible with the micellar surface. Values of a_{pol} are obtained by fitting the model equations to experimental data.

Ruckenstein (38) based his model on the same original expression for $\Delta\mu_{mic}^0$, but instead of considering the polymer molecule penetrating the surfactant aggregates, he assumed that the presence of the macromolecule wrapped around the surfactant clusters results in a change in interfacial energy. The term $\sigma(a - a_0)$ in eq. 1-6 is therefore replaced by

$$(\sigma - \Delta\sigma)(a - a_p) + \sigma(a_p - a_h) + a_p \Delta\sigma_p \quad \text{when } a_p > a_h \quad (1-9a)$$

and

$$(\sigma - \Delta\sigma)(a - a_p) + a_p \Delta\sigma_p \quad \text{when } a_p < a_h \quad (1-9b)$$

where $\Delta\sigma$ and $\Delta\sigma_p$ are the changes in interfacial tension between the hydrocarbon core and water and between surfactant headgroups and water, respectively, caused by the presence of the polymer. The value of $\Delta\sigma$ can be estimated by measuring the change in interfacial tension between a hydrocarbon phase and water upon addition of the polymer to the water phase, and $\Delta\sigma_p$ is taken as equal to $\Delta\sigma$.

According to this model, polymer-surfactant complexation will occur if the energy increase due to unfavorable interaction between surfactant headgroups and the macromolecule is more than compensated by the energy

decrease caused by a reduction of the contact area between the hydrocarbon core of the surfactant aggregates and water.

Both models, then, use the set of equations derived for polymer-free micellization (see section 1.2.2.1) to determine the size of bound micelles (g_b), the critical surfactant concentration (X_{1mic}), and the intrinsic equilibrium constant (K_b).

The mass balance equation describing the equilibrium among free micelles, polymer-bound micelles, and monomeric surfactant can be written as

$$X_t = X_1 + g_f(K_f X_1)^{g_f} + g_b n X_p \left(\frac{(K_b X_1)^{g_b}}{1 + (K_b X_1)^{g_b}} \right) \quad (1-10)$$

where X_t and X_1 are the total and singly dispersed surfactant concentrations, respectively. The second term on the right-hand side of eq. 1-10 represents the concentration of surfactant in free micelles; the third term, the concentration of surfactant in bound micelles.

Although these models agree satisfactorily with the experimental data, their major drawback lies in the use of parameters that are either impossible to measure independently or grossly estimated. Moreover, both approaches neglect the shielding effect of the polymer on the ionic repulsions between surfactant headgroups.

Hall (40) has recently extended his treatment of charged colloidal systems (39) to describe polymer-surfactant interactions. His basic approach is to derive an expression for the Donnan equilibrium between a solution of charged colloidal species (polymer-surfactant complexes and

free micelles) plus supporting electrolyte and a colloid-free electrolyte solution of polymer plus surfactant. The theory does not regard the bound surfactant molecules as forming well-defined aggregates, instead considering a situation in which the surfactant binds either individually or collectively (bound clusters), and only two types of colloidal species coexist in solution: polymer molecules saturated exclusively with clustered surfactant and polymer molecules containing exclusively monomeric surfactant ("all or none" approximation). Hall derives equations relating the shape of the binding isotherm to the distribution of bound surfactant ions among the macromolecules and allowing the calculation of enthalpies of binding from the temperature dependence of the binding equilibria. The theory predicts, inter alia, that (a) the amount of bound surfactant may decrease when free micelles start forming, and (b) the surfactant monomer concentration may exhibit two maxima. Although experimental data (41) have confirmed some of this theory's predictions, currently available data are insufficient to allow a systematic comparison with experiment. But Hall's "all or none" assumption hardly seems justified given the strong experimental evidence (42-44) for an equal distribution of bound surfactant molecules among macromolecules.

1.3.3.2. Charged Polymers

Working independently, several authors (45, 46) have proposed similar theoretical accounts of the cooperative binding of surfactants onto polyions, all essentially based on the Zimm-Bragg theory of helix-coil transition in polypeptides (47). Both phenomena exhibit a strong cooperative character and can be described by a nucleation and growth

mechanism. The mass balance equation for a surfactant ion binding to a polymer site can be written as



The apparent binding constant (K_a) is defined as

$$K_a = \frac{\theta}{C_f(1-\theta)} \quad (1-12)$$

where θ is the fraction of occupied sites and C_f denotes the equilibrium concentration of free surfactant. Assuming that the cooperativity of the process can be reduced to nearest neighbor interactions, we must consider two different situations: i) binding to a site with two unoccupied nearest neighbors, and ii) binding to a site adjacent to an occupied site. The two equilibria can be written as



and



where 0 and 1 represent unoccupied and occupied sites, respectively, and u is defined as the cooperativity parameter. Following Zimm-Bragg theory, two parameters, s and σ , are introduced to express the statistical weights of the two states, (01) and (11), contributing to the partition function as σs and s respectively (the unit quantity being given to the state (00)). These parameters are related to the equilibrium constants by

$$s = Ku C_f \quad \text{and} \quad \sigma = 1/u$$

The matrix method yields an expression for the partition function in terms of s and σ , and the following relationships can be derived:

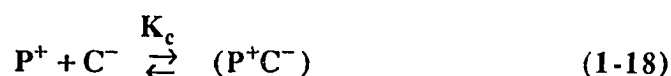
$$\theta = \frac{1}{2} + \frac{s-1}{2 \left[(1-s)^2 + \frac{4s}{u} \right]^{1/2}} \quad (1-15)$$

$$\left(\frac{d\theta}{d \ln C_f} \right)_{\theta=1/2} = \frac{1}{4} \sqrt{u} \quad (1-16)$$

$$K = \frac{1}{u(C_f)_{\theta=1/2}} \quad (1-17)$$

Equations 1-16 and 1-17 are solved for u and K by using the experimental binding isotherm. The values obtained can, in turn, be used in eq. 1-15 to yield the theoretical isotherm. In most cases, the agreement is satisfactory for low θ values. Above $\theta = 0.6$, the theoretical isotherm usually overestimates the amount of bound surfactant, indicating that the nearest-neighbor cooperative interaction approximation no longer holds near saturation, most likely because of steric effects.

The model's predictions of the dependence of (K , u) on the amount of added salt are not borne out by experimental data. The competitive, non-cooperative binding of a counterion bearing the same charge as the surfactant ion can be described by the following equation:



The new intrinsic binding constant, K' , is now dependent on the added salt concentration:

$$K' = \frac{K}{1 + K_c [C]} \quad (1-19)$$

In the presence of excess salt, the mass-action treatment yields

$$\ln K' \propto -\ln [C] \quad (1-20)$$

But experimental data show that the slope of $\ln K'$ vs $\ln [C]$ is actually less than 1 (0.6 to 0.8). This last result indicates that a theoretical

treatment must take into account such specific ionic interactions as ionic condensation (48).

Very recently, Delville (49) has presented a refined version of the same model. Two additive effects are considered simultaneously: on the one hand, the electrostatic condensation of surfactant ions in the vicinity of the polyelectrolyte, which is treated by means of the Poisson-Boltzman equation plus cell model; on the other hand, the cooperative binding of surfactant on the polyion, which is treated as described above. Delville has applied this model to the DTAB/DNA system; steric effects for this particular system were accounted for by considering cooperative interactions with the second nearest neighbor only, binding on two adjacent sites being ruled out. The model showed excellent agreement with the experimental isotherm over the whole range of surfactant concentration. It remains to be seen whether it can be applied to other systems with equal success.

CHAPTER TWO

CHARACTERIZATION OF THE POLYSACCHARIDE XANTHAN

2.1 INTRODUCTION

Xanthan gum is an anionic polysaccharide produced commercially by fermentation of the bacterium *Xanthomonas Campestris*, which occurs in nature as a plant pathogen. The discovery of this biopolymer can be traced back to the late 50's, when the Northern Regional Research Center (NRRC) of the U.S. Department of Agriculture was extensively involved in the production, from micro-organisms, of new types of extracellular polysaccharides. The ability of micro-organisms to synthesize polysaccharides from simple and complex organic substrates is widespread. Three types can be distinguished: intracellular polysaccharides located inside or as part of the cytoplasmic membrane; cell-wall polysaccharides; and exocellular polysaccharides located outside the cell wall, either covalently attached to the cell or secreted unattached into the growth medium. For practical reasons, including the relative costs of purification procedures, the last type was explored first (1). *Xanthomonas Campestris* was originally discovered in rutabaga plants (2), and was subsequently found in related plants, including cabbage and cauliflower (3). Infected areas of the plants' vascular systems were coated with a sticky slime caused by an exuded polysaccharide, now known as Xanthan. The initial report, published in 1961 (4), and subsequent work

by the NRRC (5-7) showed that aqueous solutions of Xanthan exhibited unusual rheological properties such as high viscosity at low shear rates and a marked shear-thinning behavior. These properties, together with a retention of high viscosity at high ionic strengths and over a large range of temperature and pH, suggested a wide variety of industrial applications and led to commercial cultivation of micro-organisms for Xanthan production.

Xanthan's technological utility stems from its solution properties, which combine the ability to flow freely with that of holding particles in suspension over long periods of time by forming a tenuous gel-like structure at rest. The molecular origin of this behavior has been extensively studied over the past 20 years.

The primary structure of Xanthan has been shown (8,9) to consist of a (1->4)- β -D-glucose backbone with a trisaccharide substituent on alternate glucose residue (Fig. 2.1). This side chain is β -D-mannopyranosyl (1->4)- α -D-glucopyranosyl-(1->2)- β -D-mannopyranoside 6-O-acetate. The terminal D-mannose residue of the side-chain may have a pyruvic residue linked to the 4 and 6 positions. The degree of pyruvate substitution is variable and dependent on the bacterial strain and the fermentation conditions (10,11). The polymer undergoes a thermally induced conformational change in solution (12-15) from a disordered (stretched) chain conformation at high temperatures and low ionic strengths to an ordered (helical) conformation at physiologically relevant temperatures and salt concentrations. The transition midpoint temperature (or melting temperature), T_M , has been shown (13, 15) to vary linearly with the logarithm of the total salt concentration (polymer counterions plus

external salt) and is independent of the polymer concentration. This pattern of conformational change and T_M variance is typical of rod-like polyelectrolytes and has also been observed for DNA (16,17): the electrostatic repulsion between the polymer ionic groups is greater in the ordered conformation than in the disordered one because of the greater linear charge density imposed by the helical geometry. Addition of salt tends to reduce these repulsions, thereby stabilizing the ordered conformation.

The rheological properties of Xanthan solutions have been traced to the rigid, rod-like character of the molecule: the gel-like structure results from weak, non-covalent associations of ordered chains (Fig. 2.2), which may be enhanced by the addition of salt (18) or weakened by the addition of urea (19) without disruption of the ordered conformation (Fig. 2.2). Such side-by-side aggregation can occur in the case of rigid molecules, even if intermolecular attractions are slight, because it involves very little loss of entropy; with flexible polymers, in contrast, it is entropically too costly (20). Moreover, above a certain concentration threshold, alignment of chains in solution is geometrically necessary for long rigid molecules; other arrangements would result in steric clashes or molecular deformation. This has been confirmed by studies of birefringence of concentrated Xanthan solutions (15, 21, 22). The tendency for Xanthan molecules in the ordered conformation to aggregate also explains the important discrepancies in the molecular weights reported for the polysaccharide in earlier publications, as well as the considerable debate over the nature of the ordered structure: while X-ray diffraction analysis of oriented fibers of Xanthan showed (23) that in the condensed phase the molecule exists as a 5-fold helix in which the side-chains fold down to

align with the main chain, models involving either lateral association of single helices or coaxial association into a double helix were found equally compatible with the observed diffraction pattern (23, 24). Evidence from other techniques has been interpreted as supporting both the double-stranded helix (25-28) and the single-stranded structure (14, 15, 29). More recently, Rees et al. (30) have provided new evidence for the latter model: the increase in counterion condensation associated with the change to the ordered conformation, as calculated from the salt dependence of T_M , was found to agree with the theory of polyelectrolyte solutions developed by Manning (31-33) in the case of a 5_1 single helix but not for the alternative double-helix structure. Moreover, salt-jump kinetics measurements showed the transition to be first-order. The authors also succeeded in applying the Zimm-Bragg theory of helix-coil transition (34) to show that ordered and disordered regions within a Xanthan molecule could coexist at temperatures not too far below T_M . These results allowed them to interpret the sharp increase in the rate of ordering at temperatures approaching T_M as a change in the rate-determining step from a slow nucleation process (when Xanthan molecules are, at the start, completely disordered) to a faster growth process (when partial ordering already exists in the starting solution). Xanthan molecules should therefore be viewed as fully ordered helical rods only at temperatures well below T_M (typically, 70K below) and as broken rods at temperatures approaching T_M , rather than existing in a binary, all-or-none (helix or stretched) state.

As already mentioned, Xanthan samples may differ in molecular weight and acetate and pyruvate contents depending on the conditions under

which fermentation occurred. A characterization of the Xanthan samples used for our investigation of the polysaccharide interaction with surfactants is therefore necessary.

2.2. EXPERIMENTAL

2.2.1. Purification of Xanthan

Commercial Xanthan (Keltrol T) from the Kelco Co. (Clark, NJ) was dissolved in deionized water. After being heated at 90°C for two hours, the solution was filtered through 0.45 μ m Millipore filters in order to remove cellular debris. The solution was then dialyzed against deionized water for several days and freeze-dried. The yellow color of the commercial sample disappeared upon purification and the freeze-dried sample appeared white.

2.2.2. NMR Spectroscopy

High-resolution proton magnetic resonance spectra of Xanthan solutions in D₂O were recorded at 200 MHz on a IBM NR-200 spectrometer, using tetramethylsilane as the chemical shift reference. Integrated peak areas were referred to an external standard of p-dichlorobenzene in carbon tetrachloride, contained in a capillary located concentrically within the sample tube.

2.2.3. Viscosity Measurements

The solutions' viscosities were measured at various shear rates with a Brookfield viscometer. The temperature was kept constant at 25°C \pm 0.1°C.

2.2.4. Particle Size Measurements

Particle-size analysis of Xanthan solutions was carried out using the Photon Correlation Spectroscopy (PCS) technique. The apparatus was from Brookhaven Laboratories (the instrument configuration is shown in figure 2.3). The light source was a 5 mW Helium-Neon laser ($\lambda=638.2\text{nm}$). The beam was passed through a focusing lens and then directed towards the solution. The sample cells were made of quartz. The detection optics consisted of a field stop (FS), a primary pinhole (P1), a narrow-band optical filter (NBOF), and selectable pinholes (P2).

Signals from the photomultiplier (PMT) were first amplified and then discriminated to produce a uniform pulse train. The pulses were then fed into the correlator.

The data were analyzed by a microcomputer using the method of moments.

2.3. RESULTS

2.3.1. NMR Spectroscopy

Although the sugar ring protons of Xanthan give complex and overlapping NMR bands that cannot be used in a quantitative analysis, the O-acetate and pyruvate substituents located on the side-chains can serve as spectroscopic probes because their methyl groups yield sharp singlets that can easily be resolved and integrated. Polymer molecules whose rigid conformation restricts their molecular motion usually give broad lines not detectible with ordinary high-resolution NMR spectroscopy, however. In the case of Xanthan, this obstacle can be circumvented by bringing the

solution to a temperature above T_M , so that the ordered conformation no longer exists. Fig. 2.4 shows the NMR spectrum of a 0.10% Xanthan solution at different temperatures: at high temperatures, the solution gives two sharp singlets at $\delta 1.2$ ppm and $\delta 1.9$ ppm. These have previously been assigned to the methyl protons of the pyruvate and acetate groups, respectively (14,28). Upon cooling, both peak areas decrease and eventually disappear, as the rigid conformation is restored. The molar concentrations of pyruvate and acetate were calculated from their respective measured peak areas and that of the p-dichlorobenzene reference, using the equation:

$$c_p = \frac{4A_p}{3A_r} \frac{r_i^2}{R_i^2 - r_o^2} c_r \quad (2-1)$$

where A_p and A_r are the peak areas of the polymer and reference, respectively, and

r_i = inner radius of capillary

R_i = inner radius of NMR tube

r_o = outer radius of capillary

c_r = molar concentration of p-dichlorobenzene

c_p = molar concentration of either acetate or pyruvate

The mass of polymer per mole of acetate (M_{ac}) and the mass of polymer per mole of pyruvate (M_{py}) are computed from the known concentration of Xanthan, and the degrees of substitution, DS_{ac} and DS_{py} , are obtained by solving the following system of linear equations:

$$\begin{aligned}
 M_0 + m_{ac}DS_{ac} + m_{py}DS_{py} &= M_{ac}DS_{ac} \\
 M_0 + m_{ac}DS_{ac} + m_{py}DS_{py} &= M_{py}DS_{py}
 \end{aligned}
 \tag{2-2}$$

where M_0 represents the molecular mass of the five-sugar repeating unit of Xanthan when neither the acetate nor the pyruvate group is present, and m_{ac} (m_{py}) corresponds to the increase in molecular mass caused by substituting an acetate (pyruvate) group.

The resulting values are $DS_{ac} = 100\%$ and $DS_{py} = 85\%$.

2.3.2. Viscosity

The viscosity of Xanthan solutions in 0.01M NaCl was measured at various shear rates (Fig. 2.5). The values of the reduced viscosity extrapolated to zero shear rate were plotted against the polymer concentration (Fig. 2.6) and the zero-shear intrinsic viscosity was determined by extrapolation to zero concentration. A value of 7.2 l/g was obtained.

2.3.3. Photon Correlation Spectroscopy

Fig. 2.7 shows the values of the z-averaged translational diffusion coefficient, $\langle D_t \rangle_z$, obtained for Xanthan solutions at different sample times. All data were obtained at a scattering angle of 40° ; no zero-angle extrapolation was necessary since, in the $0-60^\circ$ region, the average half-width, $\bar{\Gamma}$, has been shown to vary linearly with the square of the amplitude of the wave-vector, K (35). For highly polydispersed systems, however, the values of $\langle D_t \rangle_z$ must be extrapolated to zero sample time (35), which yields a value of $\langle D_t \rangle_z = 2.2 \times 10^{-8} \text{ cm}^2 \text{ s}^{-1}$.

2.4. DISCUSSION

Our measurements of various properties of Xanthan solutions are generally in good agreement with the previously published results. The degree of pyruvate substitution of our sample is higher than most of the reported values, but at least one study (36) has reported an even higher value. The value of the zero-shear intrinsic viscosity (7.2 l/g) was obtained with Xanthan dissolved in 0.01M NaCl solutions. A direct comparison with the literature is not possible because of differences in experimental conditions. Holzwarth (37) found a value of 8 l/g for Xanthan in 0.5M NaCl + 0.04M PO₄ solution at 20°C, while Southwick et al. (38) reported values of 7 and 8 for Xanthan in 0.17M NaCl and 0.5M NaCl solutions (T=25°C), respectively. Our value is almost identical to these, and this is consistent with the results of Rinaudo and Milas (39), who found that the intrinsic viscosity (not extrapolated to zero shear) of Xanthan solutions remained approximately constant at NaCl concentrations greater than 0.01M.

Our values for the intrinsic viscosity and the translational diffusion coefficient were used to estimate the molecular weight of Xanthan by means of the Flory-Mandelkern equation (40):

$$([\eta]M_{D,\eta})^{1/3} = \frac{kT\beta}{\eta_0 D_t} \quad (2-3)$$

where $M_{D,\eta}$ = molecular weight

k = Boltzman constant

T = temperature

β = 2.5×10^6

η_0 = solvent viscosity

$M_{D,\eta}$ was found equal to 1.5×10^6 . The molecular weight thus defined is not equivalent to the weight-average molecular weight. The two quantities have been shown (41) to satisfy the following approximation:

$$M_{D,\eta} \approx (M_w)^{0.425} (M_D)^{0.575} \quad (2-4)$$

where M_w is the weight-average molecular weight and M_D is the diffusion-average molecular weight defined by

$$\langle D_t^0 \rangle_z = K_D (M_D)^{-b} \quad (2-5)$$

with K_D and b constants characteristic of the polymer studied. Since most of the reported values of Xanthan's molecular weight are weight averaged, no direct comparison with our value can be made. One study only (42) reported a value for the molecular weight of Xanthan (2.4×10^6) obtained by using the Flory-Mandelkern equation. The viscosity and light-scattering experiments were carried out in a different solvent (4M urea), however.

FIGURE 2.1: STRUCTURE OF XANTHAN

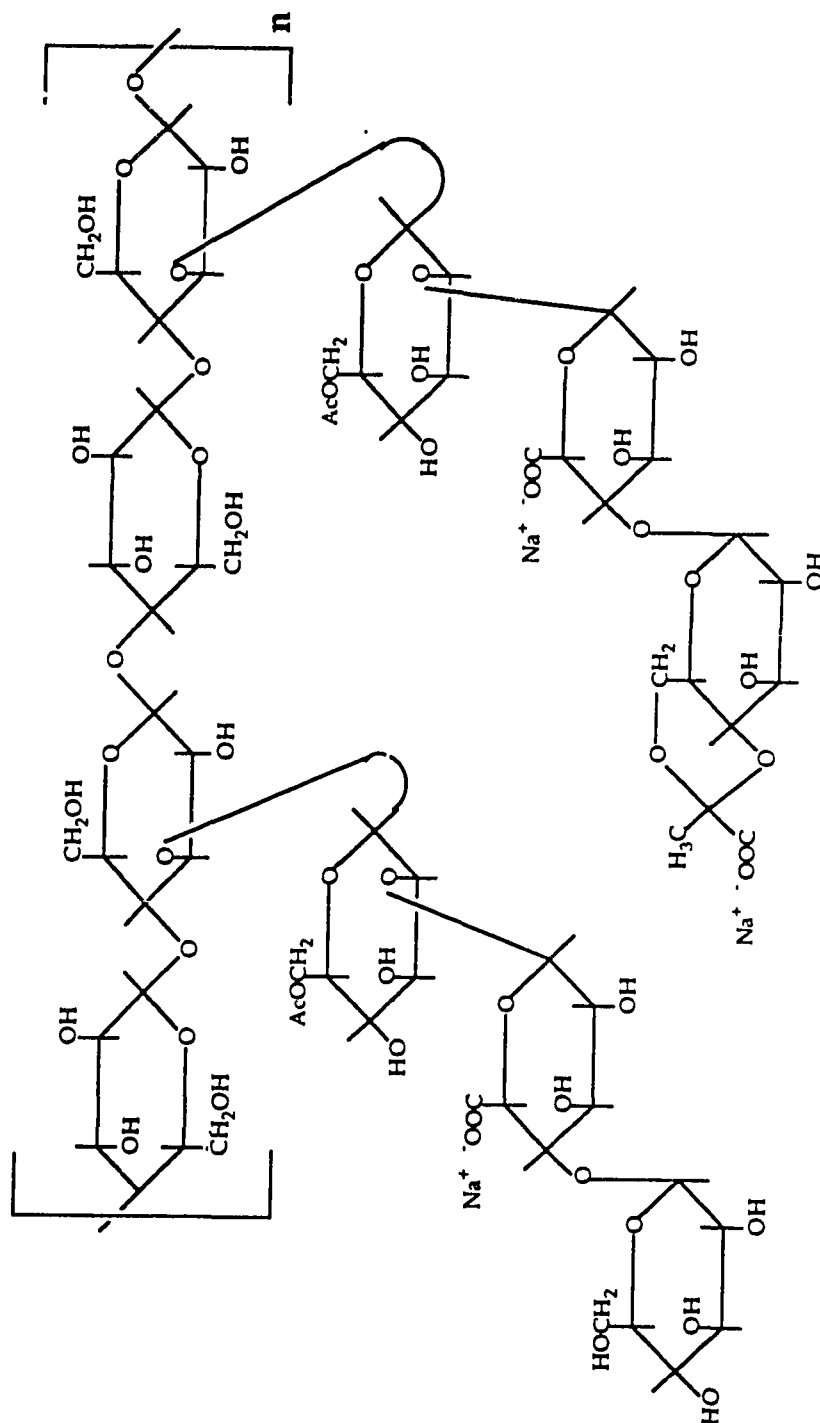


FIGURE 2.2: Schematic illustration of (a) the stretched conformation of Xanthan; (b) the partially ordered conformation; and (c) lateral association of ordered chain sequences yielding a weak gel-like network

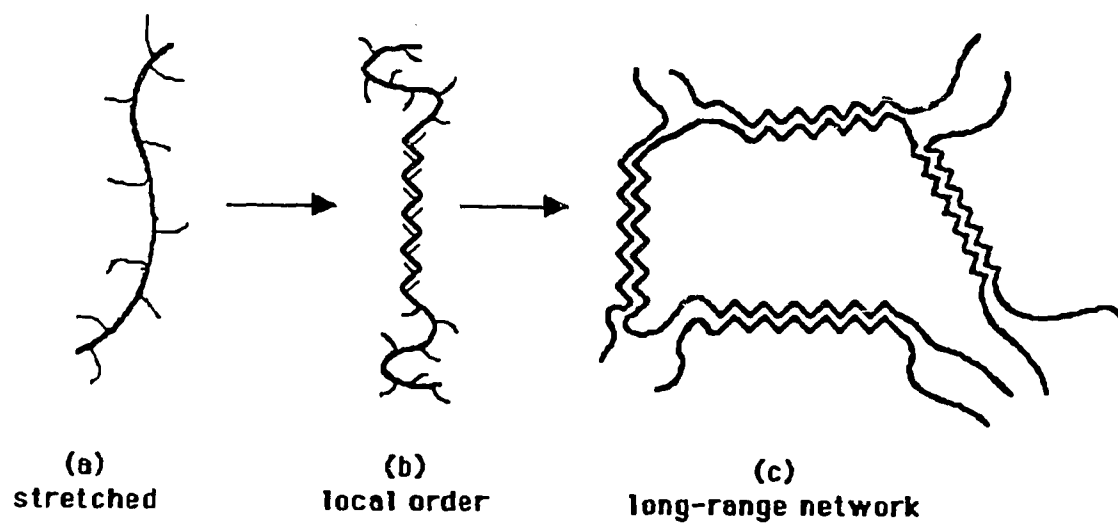
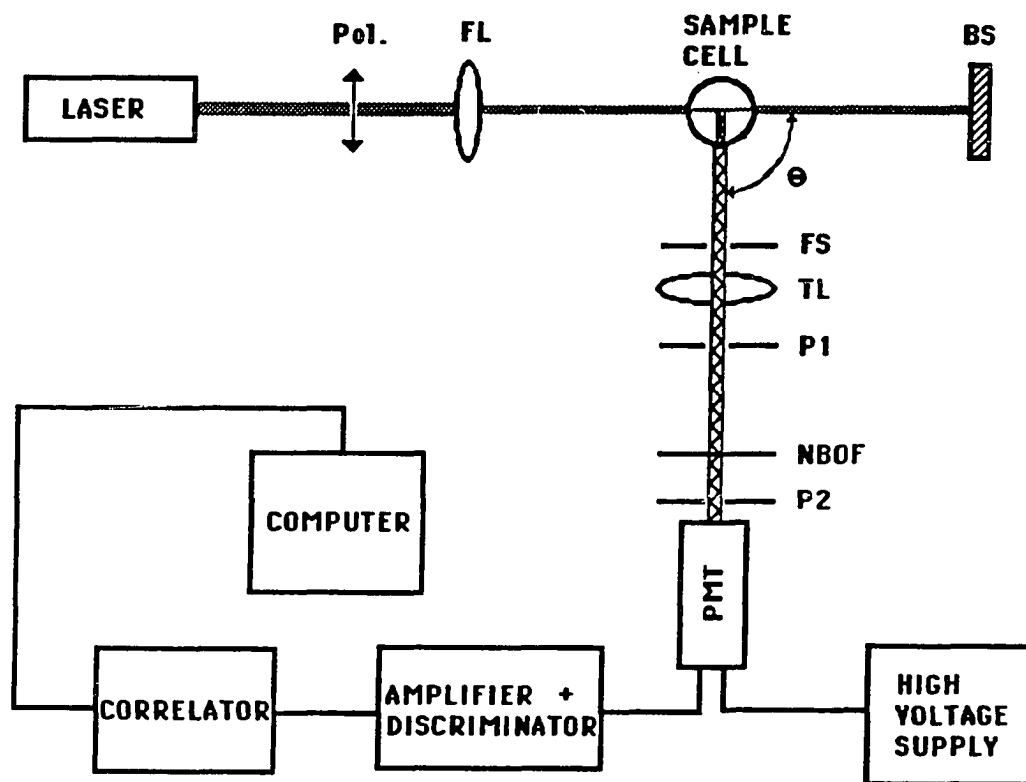


FIGURE 2.3: Instrument configuration for Photon Correlation Spectroscopy



LEGEND:

- Pol.:** Polarizer
- FL :** Focusing lens
- BS :** beam stop
- FS :** field stop
- TL :** transfer lens
- P1 :** primary pinhole
- P2 :** selectable pinhole
- NBOF:** narrow-band optical filter
- PMT :** photomultiplier tube

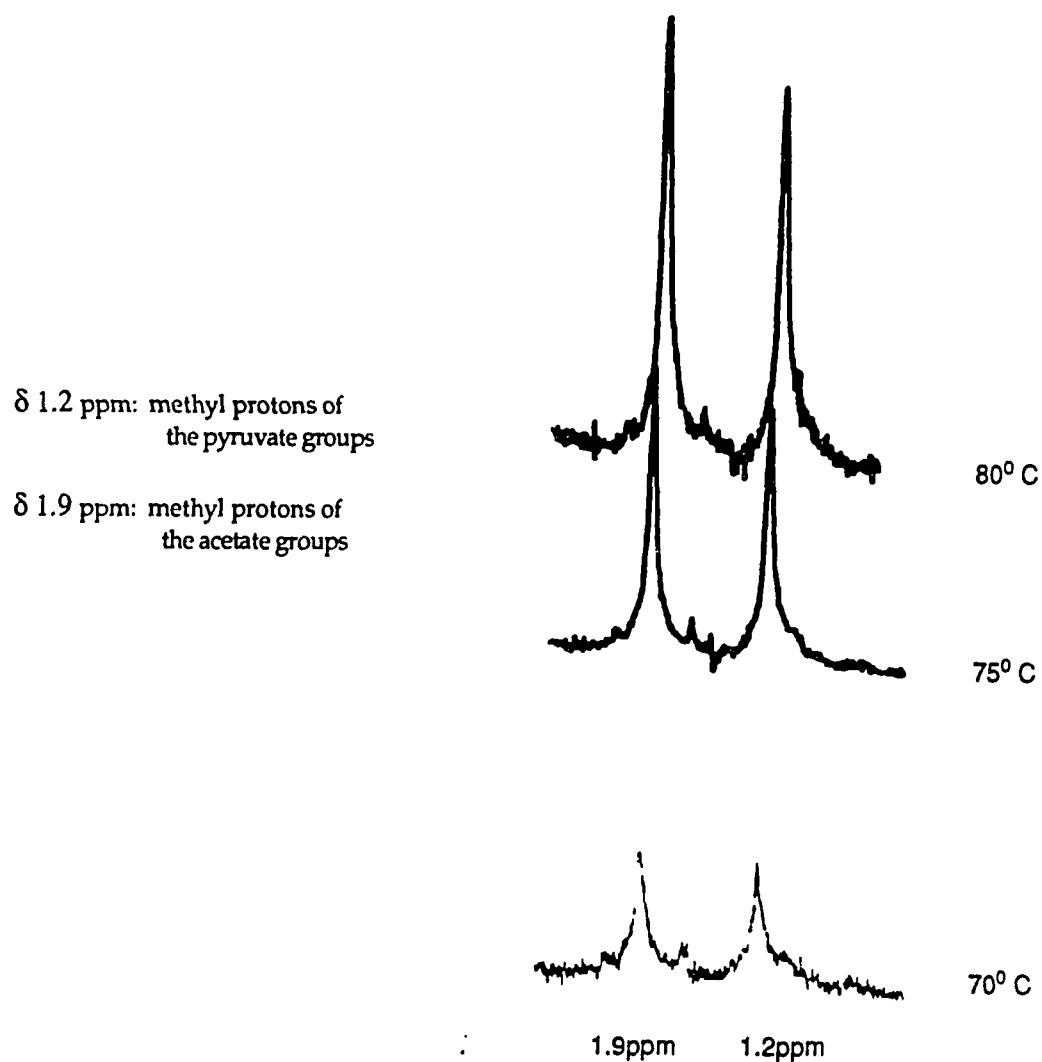
FIGURE 2.4: H-NMR Spectrum of Xanthan in D₂O

FIGURE 2.5: Viscosity of Xanthan in 0.01M NaCl solutions vs. shear rate

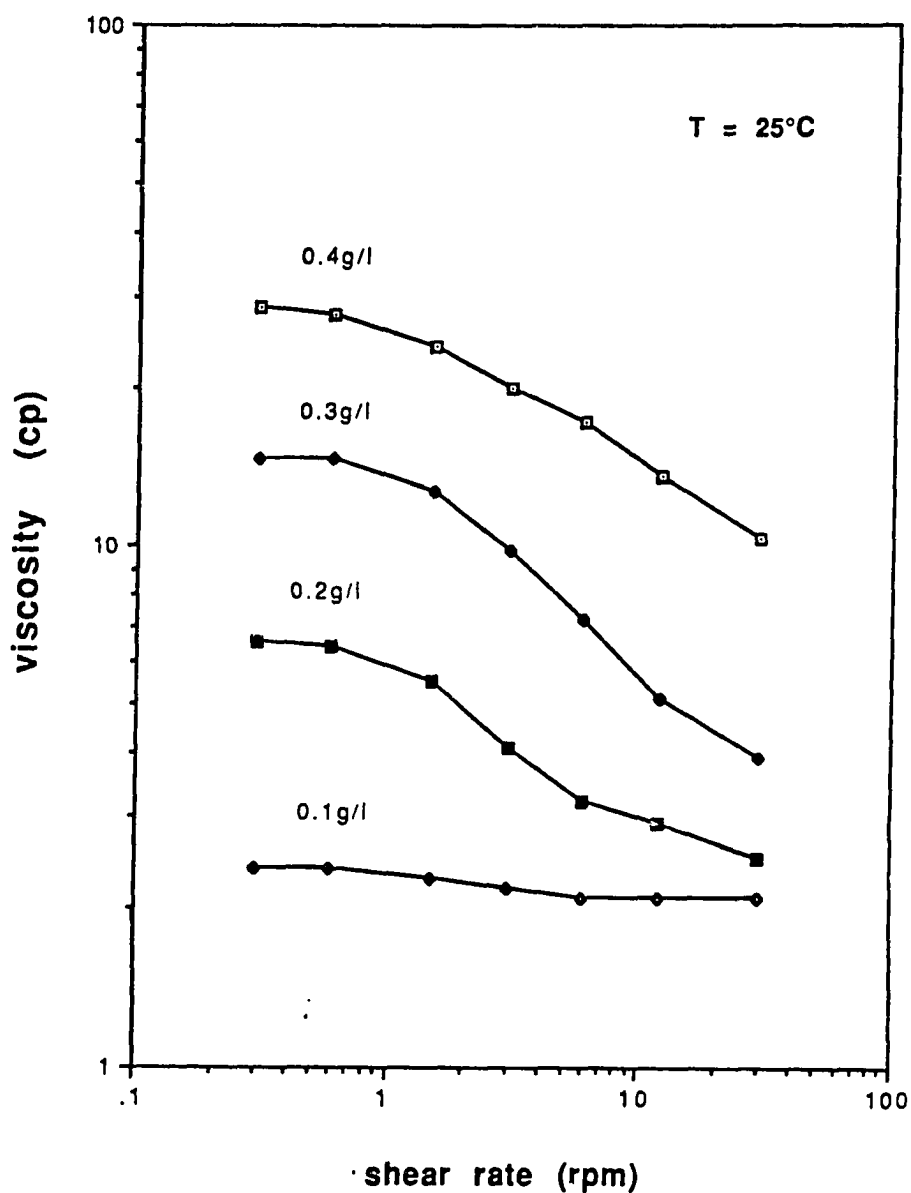


FIGURE 2.6: Plot of the zero-shear values of the reduced viscosity of Xanthan solutions in 0.01M NaCl vs. Xanthan concentration

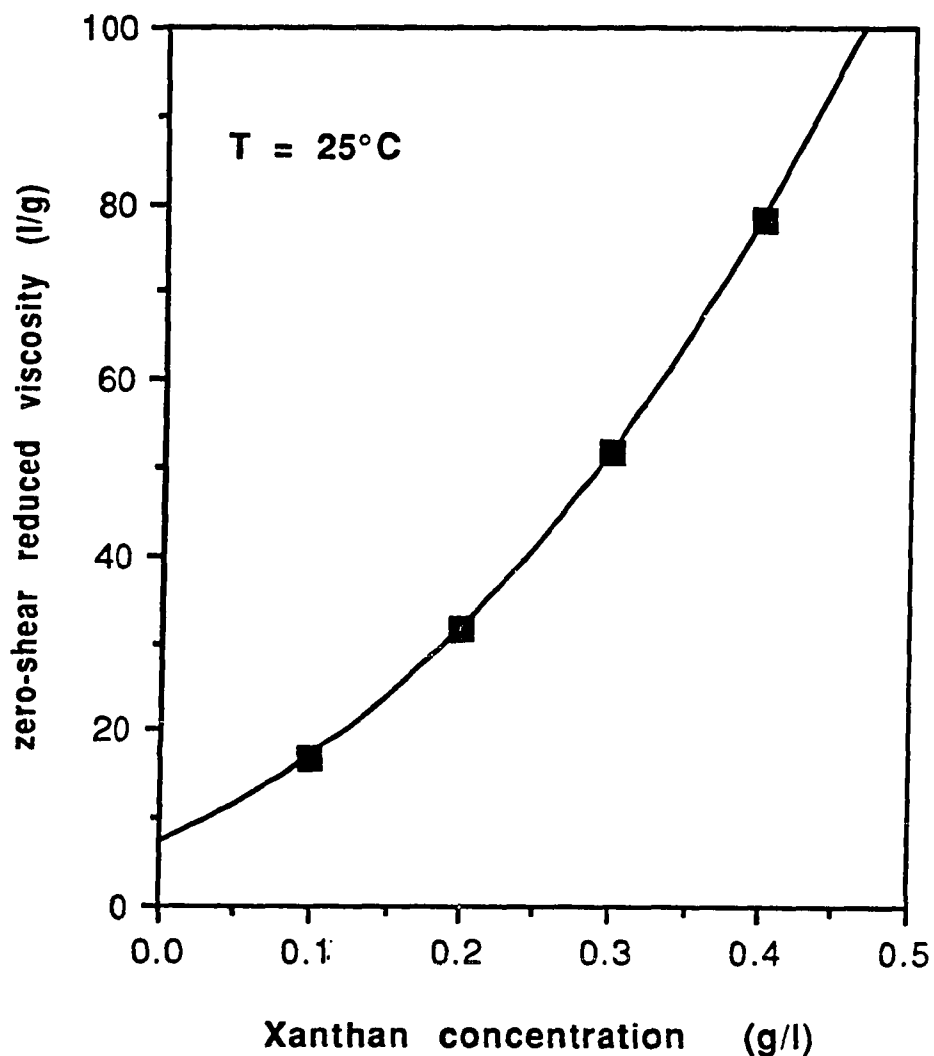
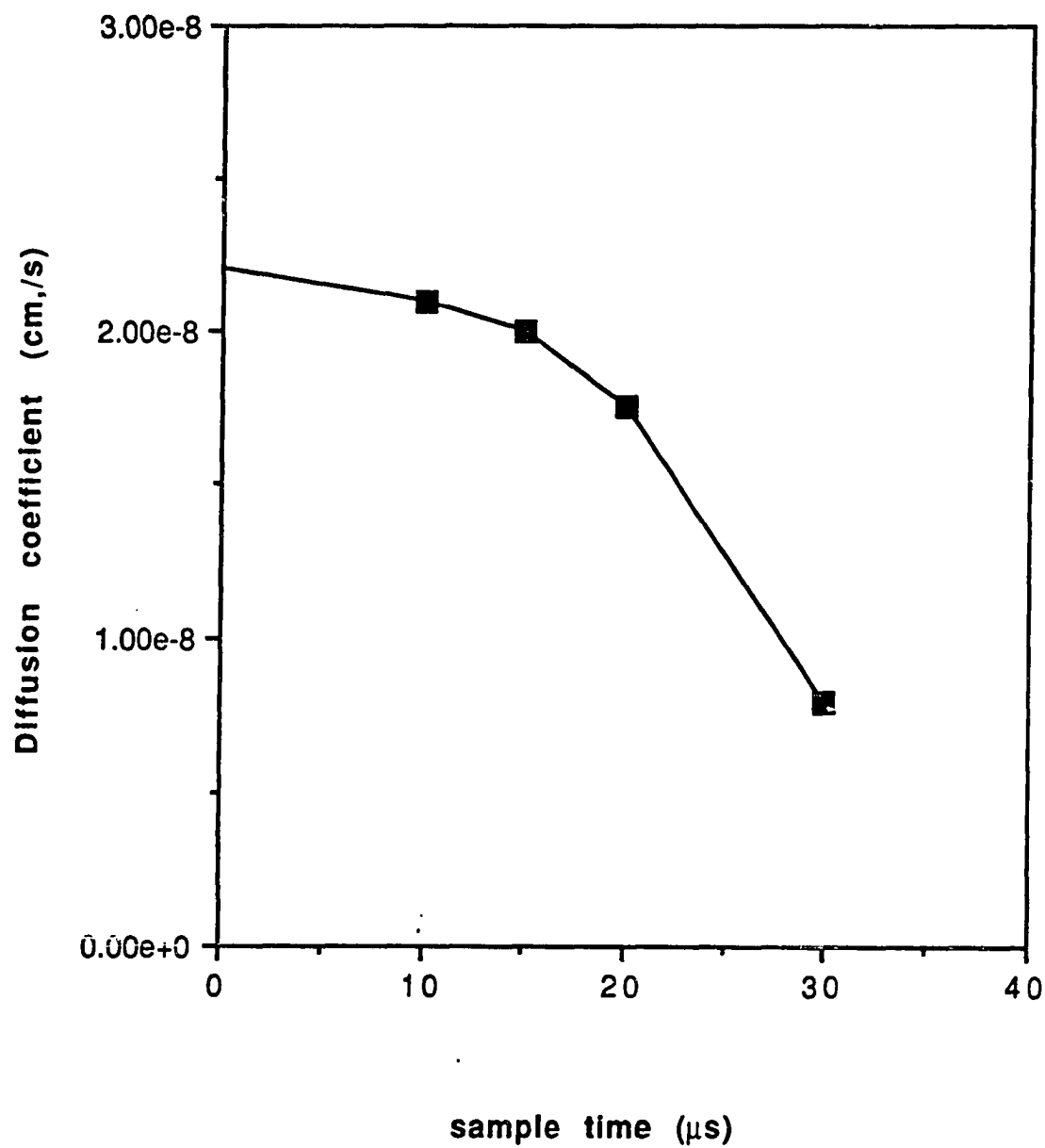


FIGURE 2.7: Diffusion coefficient of Xanthan in 0.01M NaCl at 25°C



CHAPTER THREE
BULK PROPERTIES
OF
XANTHAN/SURFACTANT SOLUTIONS

3.1 INTRODUCTION

The formation of a polymer/surfactant complex can be expected to influence the microenvironment of both components, and thus to affect their respective properties: self-association for the surfactant, conformation and intermolecular association for the macromolecule. Among the methods that have been used to investigate these effects are the following: solubilization of oil-soluble or fluorescent dyes (1-4), NMR spectroscopy (5), SANS (6), and, in the case of optically active macromolecules, circular dichroism and optical rotatory dispersion (7,8). But since the intrinsic viscosity of a polymer solution is a function of the radius of gyration (itself determined by the conformation of the macromolecule), simple rheological measurements can be used to study conformational changes induced by adsorption of surfactant. Goddard's extensive viscometric study of cationic polymer/anionic surfactant systems showed that addition of the surfactant can affect the polymer's rheological properties in different ways. A comparative study (6) of the interaction of SDS with an acrylamide β -methacryloxyethyltrimethylammonium chloride (Reten) and a quaternary nitrogen substituted cellulose ether (Polymer JR) showed that little change in conformation accompanied the binding of SDS to the former, whereas considerable changes were observed for the latter: at high polymer

concentrations (ca. 1%), the relative viscosity increased 200-fold and was shear dependent, indicating that the bound surfactant promoted intermolecular association, while, at lower polymer concentrations (ca. 0.1%), addition of SDS resulted in a lowered viscosity. The increase in viscosity observed at high polymer content is unlike anything reported in the literature to date, although this may be due to a lack of experimentation at sufficiently high polymer concentrations. In contrast, the lowering of viscosity observed with more dilute polymer solutions has been found to occur in other oppositely charged polymer/surfactant systems (9). This effect is not specific to ionic surfactants: it is well known that adding a simple salt to a polyelectrolyte solution causes a decrease in viscosity due to a "coiling up" of the macromolecule. However, viscosity measurements carried out by Abuin and Scaiano (2) on mixtures of Sodium Polystyrene Sulfonate (PSS) and Dodecyltrimethylammonium bromide (DTAB) showed that the effect of surfactant binding on the viscosity was much greater than that induced by the addition of an equivalent amount of tetramethylammonium bromide. These results imply that the effect of surfactant on the polymer solution viscosity cannot be interpreted solely as the consequence of electrostatic interactions (with shielding of the polymer ionic groups causing a reduction of the coil dimension). The authors suggested that the greater lowering of viscosity was due to the tendency of the bound surfactant molecules to associate through their hydrophobic chains to form small aggregates, thus forcing the polymer chain to adopt a more coiled conformation. Similar effects were observed by Bekturov (10), who studied the viscosity characteristics of a series of amphoteric polymers after the addition of anionic or cationic surfactants.

As was found with solutions of proteins below their isoelectric point that were mixed with anionic surfactants (11), the solubility behavior of oppositely charged surfactant and polyelectrolytes is complex. At low concentrations of surfactant, the polymer solution remains clear, although surface tension measurements indicate that binding of surfactant to the macromolecule occurs in this region. Continued addition of surfactant results in the appearance of a precipitate over a range of concentration, with maximum precipitation corresponding generally to a stoichiometric 1:1 charge ratio. Further addition of surfactant usually results in complete clarification of the solution as the precipitated complex is resolubilized. Many factors have been found to affect the above phenomena. For instance, Goddard (12) and Vanlerberghe (13) showed that redissolution of a polycation/SDS precipitate was very difficult, or impossible, when the charge density of the polymer was very high. So far as the surfactant is concerned, irregularities introduced into the surfactant structure, such as chain branching or polyetoxy chains inserted in the hydrophilic headgroup, can render the dissolution process incomplete (12). Although the formation of precipitates is often viewed as a nuisance, Goddard showed that a study of the precipitation phenomenon itself can yield useful information: solubility diagrams of solutions containing a polycation (Polymer JR) and sodium alkyl sulfates of various chain lengths showed that the 1:1 stoichiometry of maximum precipitation no longer held when the polymer concentration was lowered beyond a certain critical value determined by the surfactant chain length. The longer the alkyl chain, the lower the critical polymer concentration. From these results, Goddard was able to calculate the adsorption energy per CH_2 group of the alkyl sulfate surfactants.

This chapter discusses the effect of adding a nonionic, anionic, or cationic surfactant to aqueous solutions of Xanthan gum, using data gathered by measuring viscosity and solubility.

3.2. EXPERIMENTAL

3.2.1. Chemicals

Xanthan gum was a sample provided by the Kelco Co. (Clark, NJ). It was purified according to the method described in chapter 2.

Igepal CO-630, a polyoxyethylated nonylphenol with an average of nine ethylene oxides per molecule, was supplied by the GAF Corporation (New York, NY) and was used as supplied.

Sodium dodecylsulfate (SDS) was supplied by Aldrich Chemical Co. Its purity was 98%.

Cetyltrimethylammonium bromide, also supplied by Aldrich, had a 95% purity and was recrystallized twice in hexane/ethanol solvent.

3.2.2. Solubility Measurements

Concentrated solutions of surfactant and polymer were mixed in various ratios and the final concentrations were obtained by adding an appropriate amount of water. The solutions were stirred with a magnetic bar and set aside for several hours. The appearance of the solutions was described as clear (C), turbid (T), small precipitate (SP), or precipitate (P). Ratings were assigned by eye. The points of maximum precipitation were determined by measuring the viscosity of the supernatants. The solubility tests were conducted at room temperature ($23 \pm 2^\circ\text{C}$).

3.2.3. Viscosity Measurements

The solutions' viscosities were measured with an Ostwald viscometer immersed in a temperature-controlled bath kept constant at $25.0^\circ \pm 0.1^\circ\text{C}$. Calibration was done with distilled water.

3.3. RESULTS

3.3.1. Nonionic Surfactant

The effect of the addition of a nonionic polyethyleneoxide surfactant (Igepal) on the viscosity of Xanthan solutions is shown in Figs. 3.1 and 3.2. The viscosity data are plotted in the form of the reduced viscosity:

$$\eta_{\text{red}} = \left(\frac{\eta}{\eta_0} - 1 \right) / c \quad (3-1)$$

with

η = solution viscosity

η_0 = solvent viscosity, taken as that of the pure surfactant solution

c = polymer concentration in g/l

In Fig. 3.1, the polymer concentration is kept constant and equal to 0.10 g/l while increasing amounts of surfactant are added to the solution. The measurements were carried out at pH= 7.0 and pH=2.2. At neutral pH, a small increase in viscosity is observed at surfactant concentrations below $1 \times 10^{-3}\text{M}$, followed by a sharp decrease at higher concentrations. At acidic pH, the reduced viscosity remains constant up to $1 \times 10^{-3}\text{M}$ Igepal, and increases slightly at higher concentrations. Fig. 3.2 shows the effect of adding a fixed amount of surfactant ($1 \times 10^{-2}\text{M}$) to Xanthan solutions of various concentrations, both in the presence of 0.05M NaCl and without

NaCl. Addition of the surfactant results in a decrease in viscosity in the absence of salt, but has no effect on viscosity when the salt is present.

3.3.2. Anionic Surfactant

Figs. 3.3 and 3.4 show the effect of adding various amounts of Sodium dodecylsulfate (SDS) to a 0.10 g/l Xanthan solution. Since the viscosity of the polysaccharide solution is dependent upon its ionic strength, the addition of increasing amounts of SDS decreases the polymer solution viscosity. The similar reduction in viscosity subsequent to addition of equivalent amounts of NaCl (see Fig. 3.3) allows us to rule out any specific interaction between the polymer and the surfactant, however.

Fig. 3.4 shows the viscosities of the same solutions as in Fig. 3.3 after a small amount of CaCl_2 ($2 \times 10^{-4} \text{M}$) has been added. At concentrations less than $1 \times 10^{-4} \text{M}$, the presence of either SDS or NaCl does not affect the viscosity. At higher concentrations, however, addition of SDS results in an increase in viscosity whereas equivalent amounts of NaCl slightly decrease it.

3.3.3. Cationic Surfactant

Fig. 3.5 shows the solubility diagram of mixed solutions of Xanthan and Cetyltrimethylammonium bromide (CTAB). At high polymer concentrations ($>0.1 \text{g/l}$), the points of maximum precipitation could not be determined accurately either visually or through viscosity measurements. Nevertheless, the region in which "P" ratings were assigned corresponds to a solution composition with a polymer/surfactant charge ratio less than the stoichiometric value of 1 (indicated in the diagram by the dashed line). Maximum precipitation is therefore achieved under conditions of excess

surfactant. At lower polymer concentrations, the slope of the maximum precipitation line increases, eventually becoming vertical--and thus independent of the polymer concentration--below 0.05g/l Xanthan. These features are qualitatively similar to those obtained for the Polymer JR/SDS system studied by Goddard (12). But although the polymer JR/SDS precipitates could easily be resolubilized by the addition of excess surfactant, such is not the case for Xanthan/CTAB precipitates: whatever the polymer concentration, complete dissolution of the precipitate could not be achieved by further addition of CTAB. When micellar solutions of surfactant were mixed with dilute Xanthan solutions (less than 0.2g/l), however, precipitation did not occur, presumably because of a significant degree of adsorption of cationic micelles on the polymer molecules. The surfactant concentration required to prevent precipitation was found to be proportional to the amount of Xanthan present in solution; for concentrations greater than 0.2g/l, the limit of solubility of the surfactant (ca. 0.05M) made it impossible to obtain precipitate-free solutions.

Fig. 3.6 shows the effect of adding CTAB on a 0.10g/l Xanthan solution's reduced viscosity. The dashed part of the curve corresponds to the precipitation zone. The addition of equivalent amounts of tetramethylammonium chloride (TMAC) to the Xanthan solution also causes a decrease in viscosity compatible with the effect of salts on polyelectrolyte conformation but is less pronounced than that observed with the addition of the cationic surfactant, especially in the concentration region just prior to precipitation. (Similar effects were reported by Abuin and Scaiano (2) for Dodecyltrimethylammonium chloride/Polystyrene sulfonate systems and by Goddard (1) for SDS/Polymer JR mixtures, although the latter study made

no comparison between the effect of SDS and that of a simple analogous salt on the viscosity of the polymer JR solutions.)

The drastic reduction of solution viscosity in the precipitation zone is due to the removal of most of the polymer from the solution. At maximum precipitation, the viscosity is lowest and nearly equal to that of the solvent. The viscosity increases again in the post-precipitation range, remaining lower with CTAB than that obtained with equivalent amounts of TMAC.

3.4. DISCUSSION

3.4.1. Nonionic Surfactant

The drop in viscosity observed at surfactant concentrations greater than $1 \times 10^{-3} \text{M}$ (Fig. 3.1) is similar to that obtained by Saito (14, 15) with mixed solutions of polyoxyethylene surfactants and polymeric acids. Saito found that nonionic surfactants of this type interact with polyacids (e.g. polyacrylic, polymethacrylic acids) through hydrogen bonding between the acidic protons of the polymer and the ether oxygen atoms of the surfactant. This interaction is further reinforced by hydrophobic attraction between the alkyl chains of the surfactant and hydrophobic segments of the macromolecule. The amount of bound surfactant increases with the total concentration of surfactant. At low concentrations, surfactant molecules bind to the polymer individually, causing a decrease in viscosity as the polymer molecules fold. As the amount of bound surfactant molecules increases, a point is reached at which these molecules start to aggregate, and a much sharper decrease in viscosity is observed. In the case of Xanthan, interaction with Igepal CO-630 through hydrogen bond formation must also be considered; although the carboxylic groups of the

polysaccharide are completely deprotonated at neutral pH, the hydrogen atoms of its hydroxyl groups can form H-bonds. It must be noted, however, that the viscosity drop observed with Xanthan solutions occurs at surfactant concentrations at least one order of magnitude above the cmc of the surfactant, while that observed with polyacid solutions occurs below the cmc. This difference is indicative of a much weaker interaction between Xanthan and the surfactant, which can readily be explained by the fact that hydroxyl groups form weaker H-bonds than do carboxylic groups. Moreover, since Xanthan molecules have a much more hydrophilic character than polyacids, attraction between the polysaccharide and the surfactant alkyl chains should be considered negligible. It seems, therefore, that the very slight increase in viscosity observed in the pre-micellar region could be attributed to a small amount of monomeric surfactant bound to the polysaccharide, with no concomitant effect on its stretched conformation. The amount of bound surfactant probably remains too low for the aggregation of these bound molecules to take place, and only in the micellar region does a more significant interaction between Xanthan and surfactant micelles occur, forcing the former to adopt a more coiled conformation (hence the drop in viscosity).

At pH=2.2, Xanthan molecules are in the ordered conformation, due to a combination of ionic strength and neutralization of the polymer's charged groups. The addition of surfactant hardly affects the viscosity of the solution, although the presence of acidic protons on the macromolecule would be expected to enhance the formation of H-bonds with the surfactant molecules. But these acidic protons can also form intramolecular hydrogen bonds with neighboring hydroxyl groups; Rinaudo and Milas (17) found that the smaller the degree of dissociation of the carboxylic groups of

Xanthan, the more stable the helical conformation. They suggested that intramolecular hydrogen bonding could be responsible for this enhanced stability of the ordered structure. From the observed constancy of the viscosity, it can be deduced that the helical conformation of Xanthan is not affected by the addition of surfactant. This implies, in turn, that the formation of intramolecular H-bonds is more favored than the formation of intermolecular H-bonds (between Xanthan and surfactant). At this point, it is worth noting that, for the same polymer concentration (0.10g/l), and no added surfactant, the viscosity of the Xanthan solution at pH=2.2 is the same as that of Xanthan in 0.01M NaCl (pH=7). The possibility that Xanthan formed intermolecular H-bonds can therefore be ruled out (an increase in viscosity would otherwise be observed). The extent of H-bonding between Xanthan and the nonionic surfactant is therefore considerably reduced, as a consequence of i) the competitive formation of intramolecular H-bonds, and ii) the rigidity of the helical conformation, which restricts the ability of the polymer to wrap around the surfactant micelles.

3.4.2. Anionic Surfactant

The results shown in Fig. 3.3 indicate that the effect of SDS on the viscosity of Xanthan solutions is the same as that of a simple salt, i.e., a decrease in viscosity due to an increase in ionic strength. No specific interaction, therefore, is taking place between Xanthan and SDS.

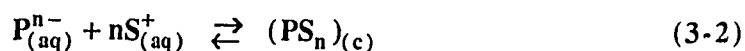
The presence of Ca^{2+} ions in solution, even in such dilute concentration, is sufficient to induce a conformational change--from stretched to helical--in the Xanthan molecules (divalent cations are much more effective than monovalent cations at screening electrostatic repulsions among Xanthan's

carboxylate groups, and less of the former are therefore needed to induce the helical conformation). Under such conditions, addition of NaCl has no effect on the viscosity of the polysaccharide solution, as expected. The addition of SDS, on the other hand, results in a slight increase in viscosity above a surfactant concentration of about $1 \times 10^{-4} \text{M}$. In this concentration region, surfactant micelles are present in significant amount, and it seems likely that the viscosity increase is due to the adsorption of these micelles to the polymer molecules, with the Ca^{2+} ions acting as bridges between the anionic groups of the two compounds.

The absence of interaction between Xanthan and SDS (when Ca^{2+} ions have not been added) was expected, since a number of studies (17, 18) of systems in which polymer and surfactant bear charges of the same sign have come to a similar conclusion. In contrast, no data have been published to date about the effect of divalent ions on such systems.

3.4.3. Cationic Surfactant

The solubility diagram of the Xanthan-CTAB system (Fig. 3.5) shows that maximum precipitation is always obtained under conditions of excess of surfactant (with respect to the 1:1 stoichiometric charge ratio). This clearly indicates that the association between Xanthan and CTAB is relatively weak. The precipitation reaction can be represented by the following equation:



It can be seen that the presence of an excess of surfactant implies that the equilibrium lies to the left-hand side of the above equation.

The overall features of the solubility diagram are similar to those of the solubility diagrams obtained by Goddard (12, 17) for Polymer JR/ Alkyl

sulfates systems. Goddard proposed the following equation to describe the equilibrium at the point of maximum precipitation in these systems:

$$(C_t - C_e) = k[P] \quad (3-3)$$

where C_t and $[P]$ are the total concentrations of surfactant and polymer, respectively, and C_e represents the equilibrium concentration of surfactant required to maintain the existence of the precipitate. The value of C_e is obtained from the position of the vertical part of the precipitation line in Fig. 3.5. This equation allows an interpretation of the precipitation pattern:

At high Xanthan concentrations, C_e is much smaller than C_t and eq. 3-3 reduces to $C_t = k [P]$, hence the linear top portion of the precipitation line. At dilute Xanthan concentrations, $[P]$ tends to zero, and the fraction C_t/C_e thus approaches unity (i.e., virtually all the added surfactant is required to maintain equilibrium with the precipitate), hence the vertical part of the curve.

The comparison between Polymer JR/SDS and Xanthan/CTAB systems also shows several differences in solubility properties and precipitation pattern. Most significant is the fact that Xanthan/CTAB precipitates can never be completely resolubilized through addition of excess surfactant. The "C" ratings that appear in the solubility diagram to the right of "P" ratings on the same horizontal line correspond to clear solutions obtained not by further addition of surfactant to an already precipitated solution, but rather by mixing a Xanthan solution with a micellar surfactant solution. Such clear mixtures could be obtained with dilute Xanthan solutions only (less than 0.1g/l). The minimum surfactant concentration necessary to prevent precipitation increases with the amount of Xanthan in solution. For

Xanthan concentrations greater than 0.1g/l, such minimum surfactant concentration exceeds the solubility limit of the surfactant itself and precipitation can no longer be avoided. From these observations we may conclude that when Xanthan molecules can interact with a significant number of cationic micelles, the resulting polymer-surfactant complex retains a net charge--most likely positive--which prevents it from precipitating. The rheological data show that in such situations, the reduced viscosity of Xanthan remains lower than that of the polysaccharide in its helical conformation. A smaller hydrodynamic radius indicates a more coiled-up conformation for the macromolecule. This result is consistent with the proposed arrangement of Xanthan molecules wrapped around surfactant micelles.

The impossibility of resolubilizing Xanthan/CTAB precipitates, together with the appearance of maximum precipitation at Xanthan/CTAB charge ratios less than unity, seems to confirm the correlation between the two phenomena noted by Goddard in his investigation of a number of cationic polymer/SDS systems (12). He suggested that both properties could result from steric effects due to a high charge density on the polymer molecules. Although Goddard does not state explicitly how such effects would influence the precipitation and resolubilization processes, a causal relationship can indeed be envisaged: if the charged groups on the polymer molecule are separated by a short distance, the access of a surfactant molecule to a free site with adjacent sites already occupied will be hampered, hence the need for an excess of surfactant to compensate for the relative inaccessibility of the few remaining free sites. In the case of Xanthan, steric hindrance definitely plays a role, not only because of an

overall high charge density, but also because of the occurrence on a number of side-chains of a carboxylate group (pyruvate) located in the immediate vicinity of the anionic group borne by the glucuronate residue. On the other hand, the resolubilization process involves the formation of a second layer of bound surfactant ions, with their ionic groups pointing outwards and their alkyl chains in contact with those of the bound surfactant in the first layer (11, 19). In order for this second layer to be formed, the free surfactant molecules must be able to come in contact with the first layer of bound surfactant. In the case of a high charge density polymer, the proximity of the bound surfactant molecules to one another will facilitate the formation of bound aggregates through hydrophobic attraction. This, in turn, will force the polymer molecules to coil around these pseudo-micelles. As a result, the polymer/surfactant precipitate may have most of the bound surfactant located inside the loops of the macromolecule, and therefore relatively inaccessible to the excess surfactant present in solution. This explanation may not hold, however, for polymers lacking the conformational flexibility necessary to accommodate the aggregation of the bound surfactant molecules. The study by Kwak (20) of the interaction between cationic surfactants and a series of anionic polysaccharides shows that the adsorption of Tetradecyltrimethylammonium bromide on Sodium carboxymethylcellulose (which shares with Xanthan a common cellulosic backbone) exhibited very little cooperative effect, i.e., hydrophobic interaction between bound surfactant molecules. The lack of flexibility of Xanthan molecules is also apparent in our viscosity data (Fig. 3.6); in the pre-precipitation region, the reduced viscosity of the Xanthan/CTAB solution is only slightly lower than that of the Xanthan/TMAC solution. As already mentioned in the introduction to this chapter, a significant

hydrophobic interaction between bound surfactant molecules would result in a much greater lowering of the viscosity. (It must be noted that this assessment of the flexibility of Xanthan molecules does not contradict our preceding depiction of Xanthan as wrapping around cationic micelles, which requires only minor conformational changes.)

The relatively weak interaction between Xanthan and CTAB, as illustrated by the solubility and viscosity data, can readily be explained in terms of factors known to affect negatively the interaction between the two compounds, i. e., a high charge density and a conformational rigidity on the part of Xanthan, and a bulky head group on the part of CTAB. These factors do not suffice for a complete interpretation of the solubility properties of Xanthan/CTAB solutions, however, and it is necessary, at this point, to fall back on some detailed local structure (21) of the polymer (for Xanthan it would be the presence of two charged groups on some of the side-chains) in order to account for our unexplained results.

FIGURE 3.1: Reduced viscosity at 25°C of 0.1g/l Xanthan + Igepal CO-630 solutions

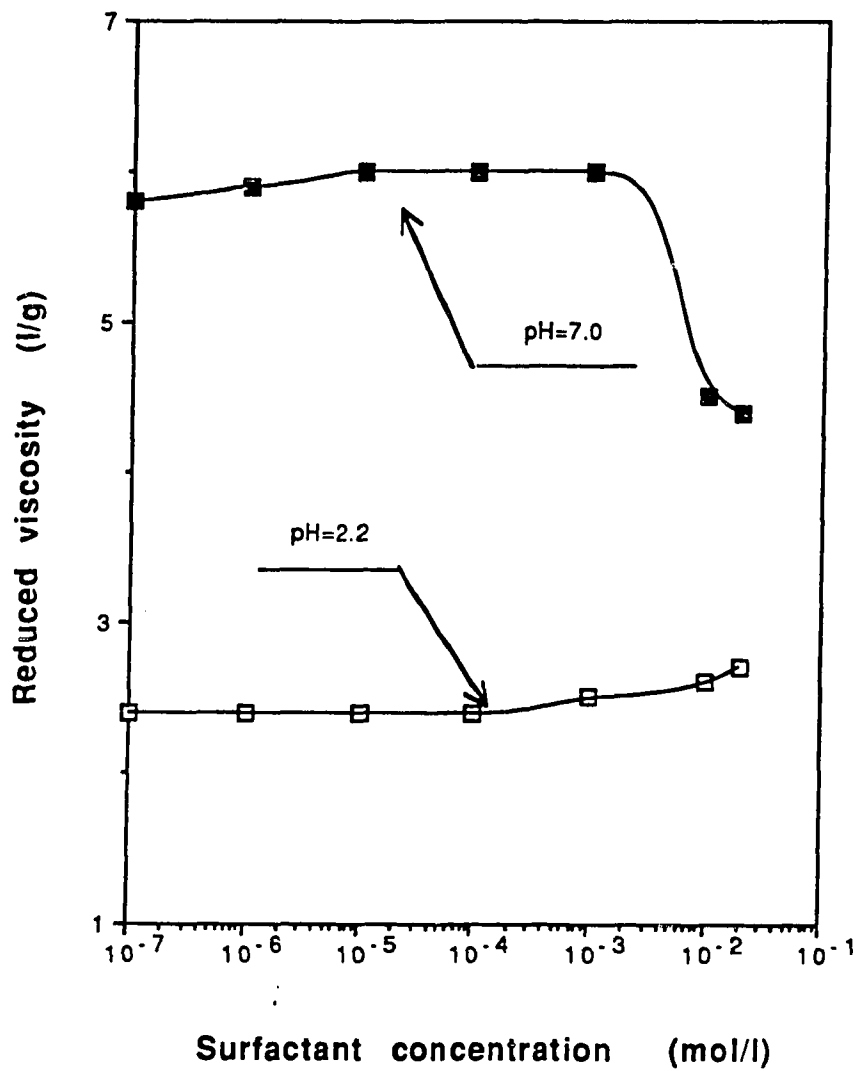
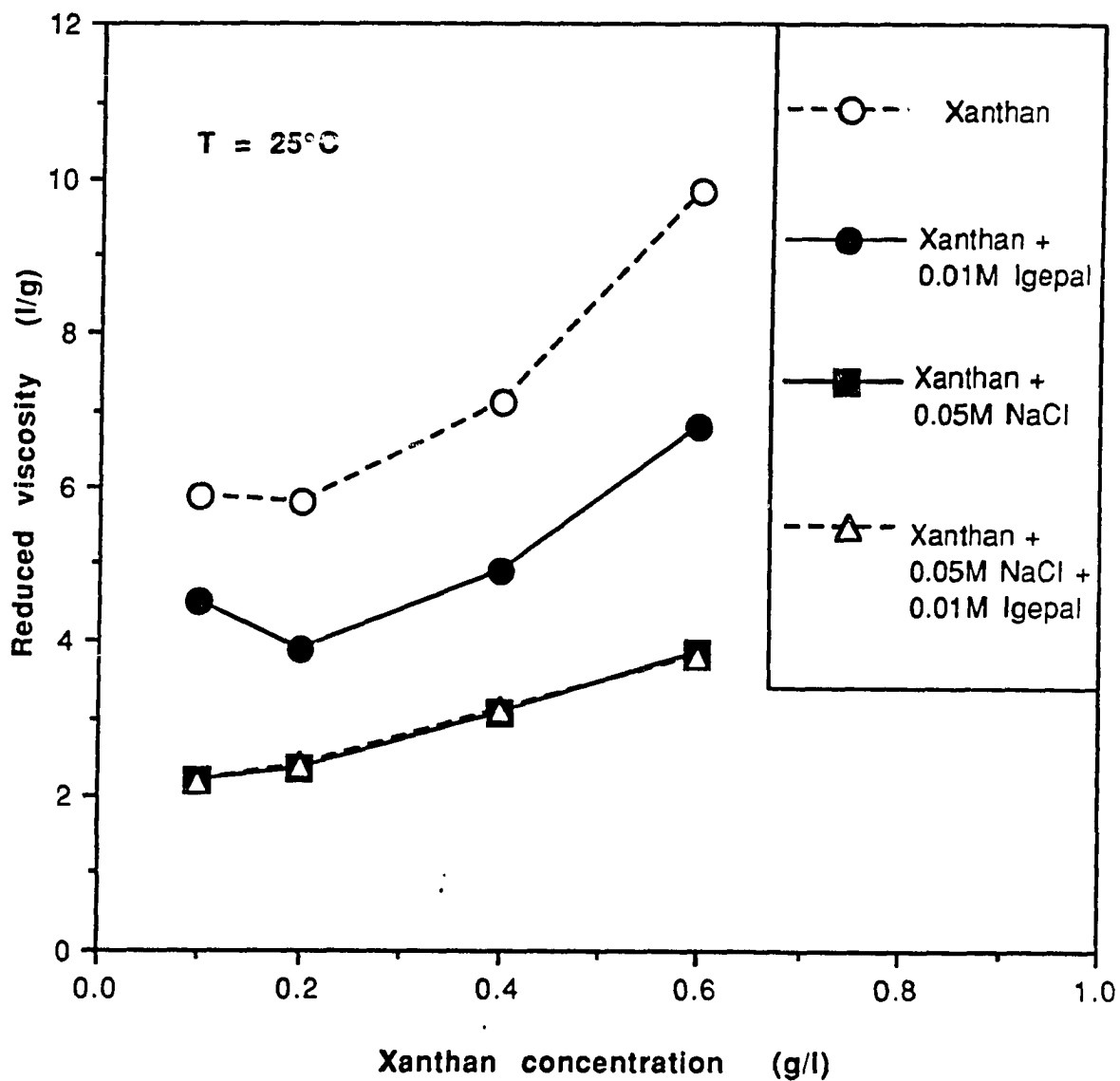


FIGURE 3.2: The effect of adding 0.01M Igepal CO-630 on the reduced viscosity of Xanthan solutions



**FIGURE 3.3: Reduced viscosity at 25°C
of 0.10g/l Xanthan + SDS solutions**

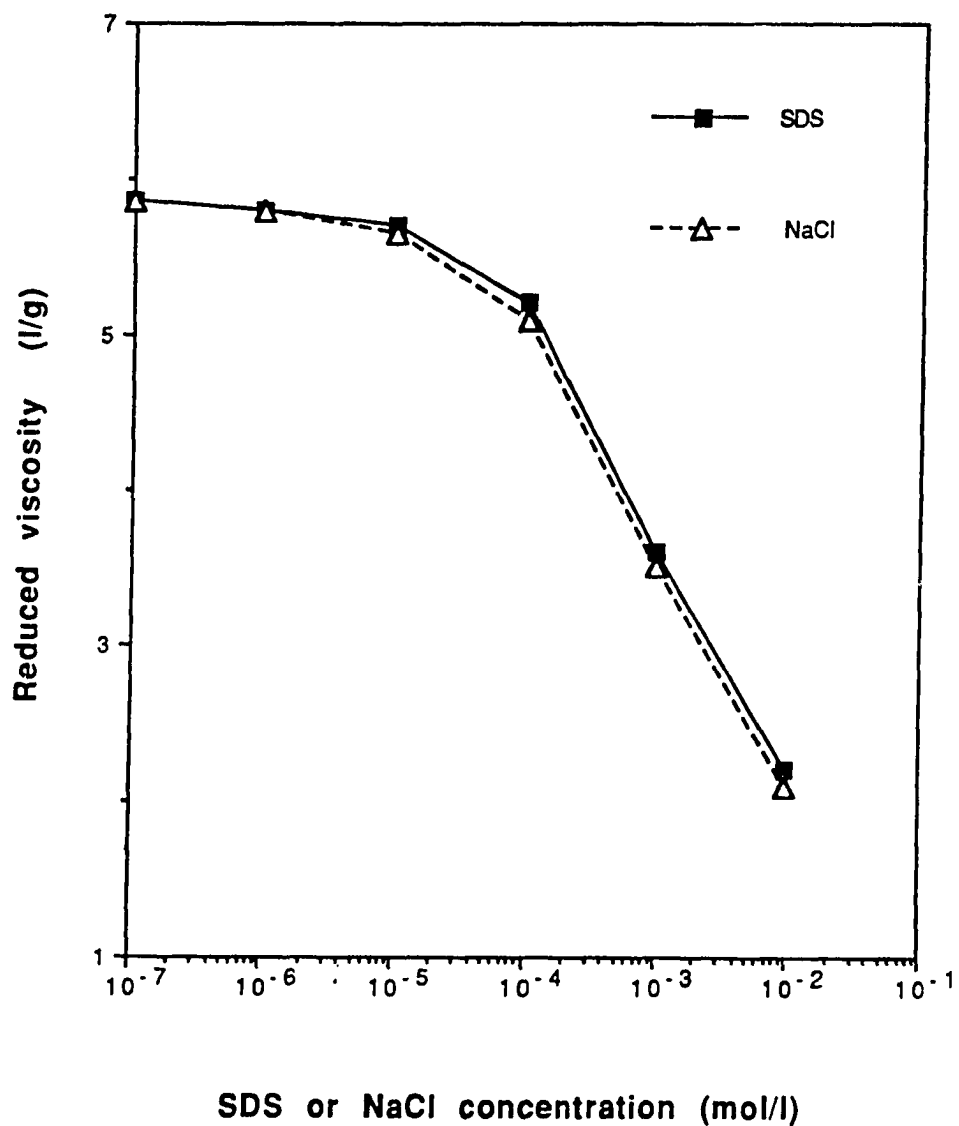


FIGURE 3.4: Reduced viscosity at 25°C of 0.1g/l Xanthan + SDS solutions with 2.0e-4M CaCl₂ added

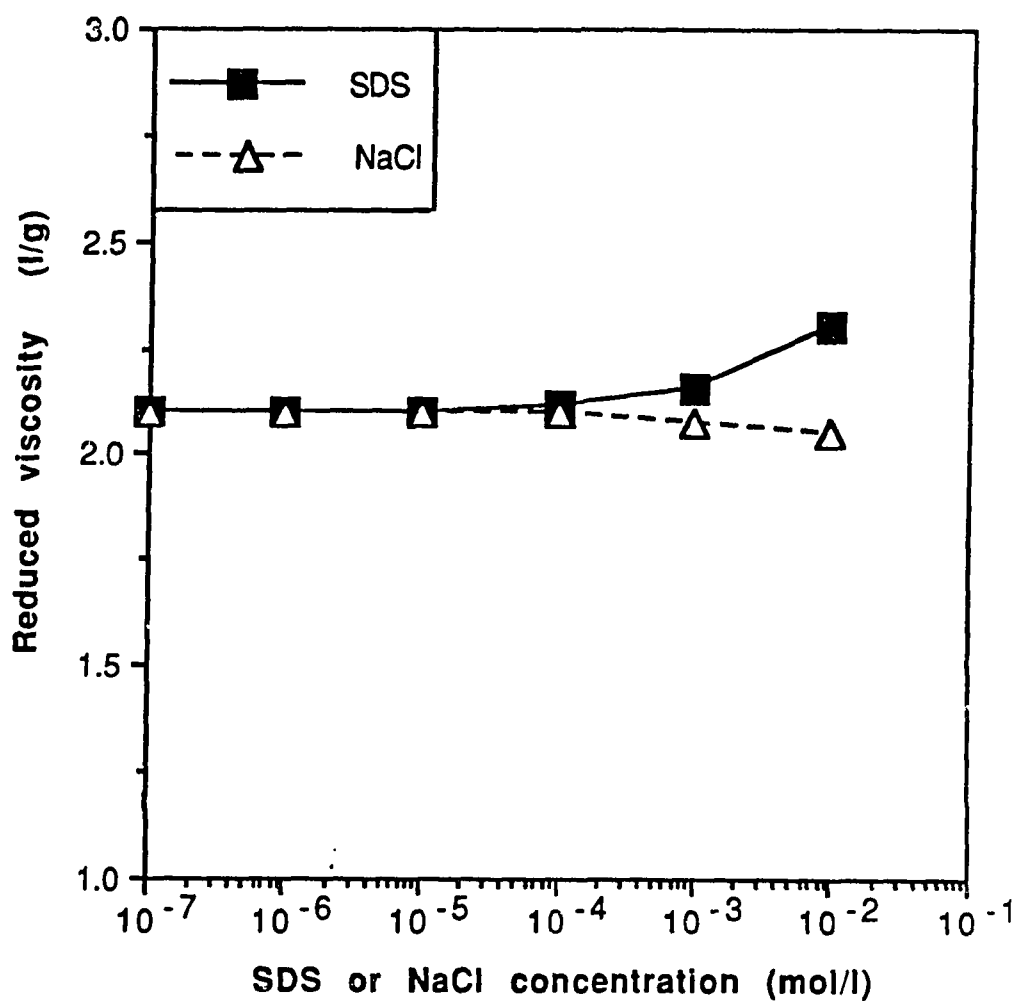


FIGURE 3.5: Solubility diagram of Xanthan + CTAB solutions at 25°C

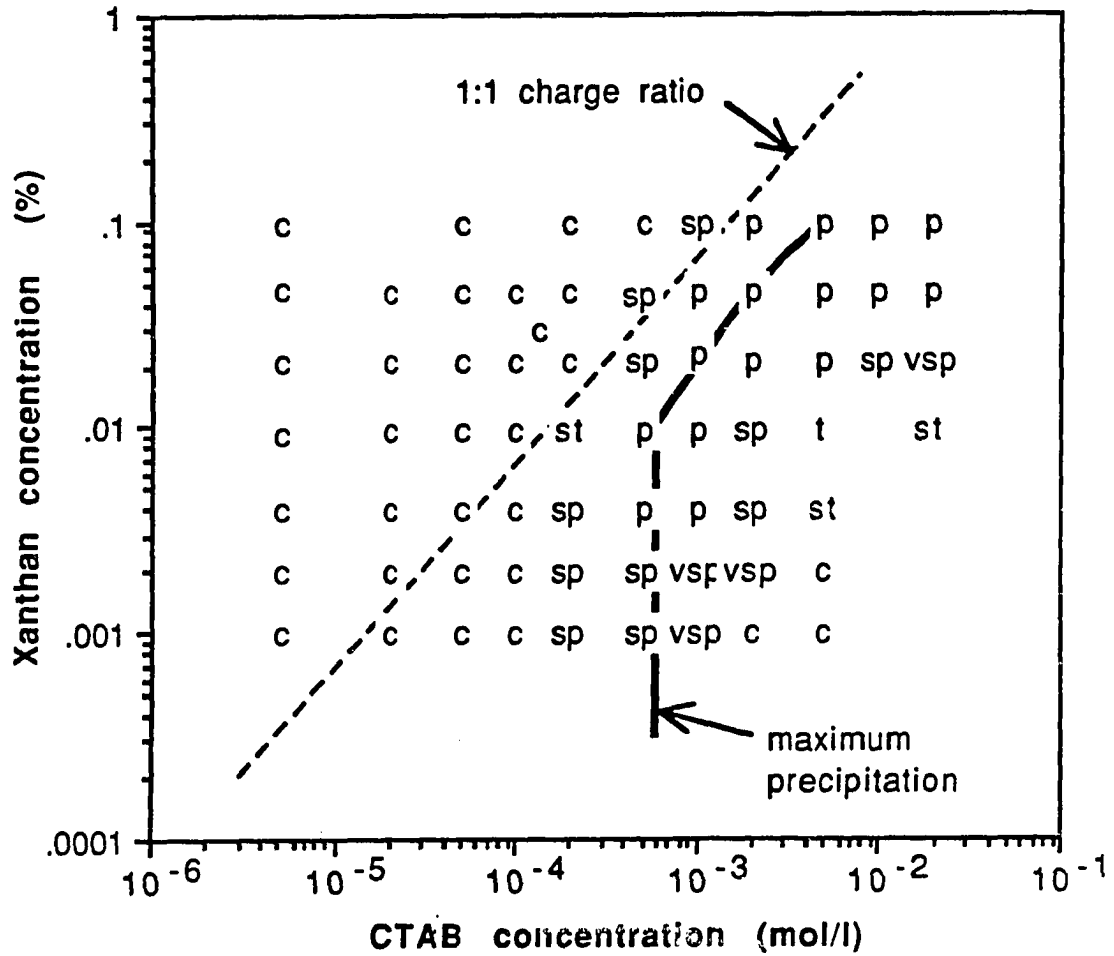
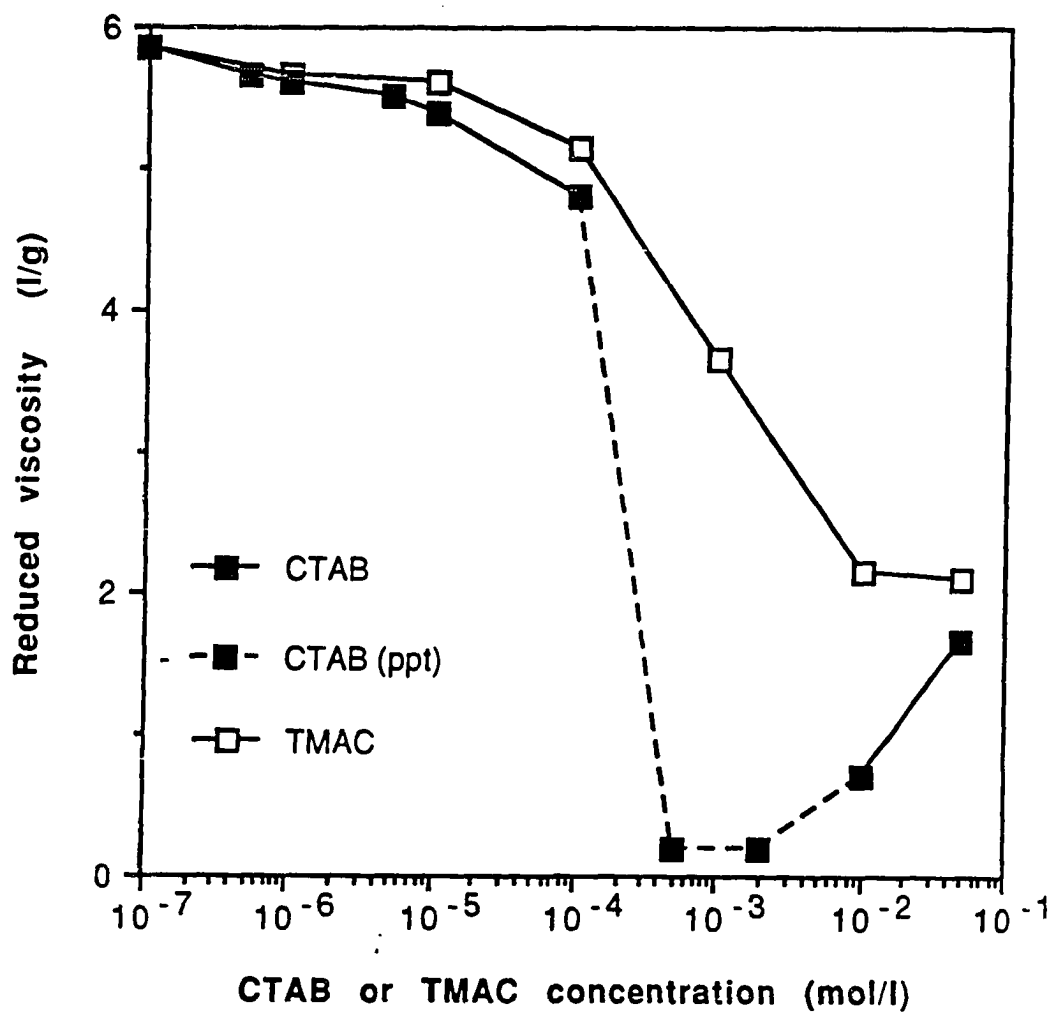


FIGURE 3.6: Reduced viscosity at 25°C of 0.1g/l Xanthan + CTAB solutions



CHAPTER FOUR

SURFACE PROPERTIES OF XANTHAN/SURFACTANT SOLUTIONS

4.1. INTRODUCTION

Surface tension measurement as a means of studying polymer/surfactant interactions was pioneered by Jones (1), who showed that the addition of a fixed amount of Polyethylenoxide, a nonionic polymer, to solutions of SDS resulted in drastic changes in the surface tension at the air/solution interface (Fig. 4.1). Typically, the γ vs $\log c$ curve obtained after addition of a nonionic polymer to the surfactant solution (solid line) is characterized by the existence of a plateau between the concentrations T_1 and T_2 . Above T_2 , the surface tension decreases again, eventually reaching the value corresponding to that for the pure surfactant solution. Jones interpreted the presence of a plateau as evidence for adsorption of the surfactant onto the polymer. Adsorption begins at the concentration T_1 and continues until T_2 , at which point the polymer becomes saturated. Further addition of surfactant results in an increase in free surfactant concentration and subsequent decrease in surface tension, until micelles start to form and γ becomes constant again.

When a charged polymer is added to a solution of an oppositely-charged surfactant, a lowering of the surface tension is observed at surfactant concentrations several orders of magnitude below the critical micelle concentration (Fig. 4.2). Even as precipitation of the polymer/surfactant

complex occurs, the surface tension (dashed curve) remains significantly lower than that of the pure surfactant solution (solid curve), and, as the precipitate is resolubilized by further addition of surfactant, micellization takes place and the two curves eventually coincide. The lowering of the surface tension has been attributed (2) to the fact that adsorption of the surfactant ion onto the polymer decreases its solubility and thereby makes it more surface active.

Goddard (2) measured the surface tension of a series of cationic polymers/SDS solutions, observing that the presence of the charged group on the backbone rather than on the side-chains led to a greater lowering of the surface tension. Buckingham and Lucassen (3) used surface tension measurements to study the interaction between poly-L-lysine, a cationic polypeptide, and SDS. They showed that, above a certain polymer concentration, the surface tension depended on the surfactant concentration alone, making application of the Gibbs equation possible.

Surface tension measurements, however, have most often been used as a means to determine the surface pressure in an insoluble monomolecular film spread over an aqueous substrate. If a water-soluble compound is introduced into the subphase and interacts with the molecules in the monolayer, changes in surface pressure, as well as in surface potential, will be observed. This monolayer technique has been used to study a number of interactions, including those between fatty acids and proteins (4,5), phospholipids and proteins (6), insoluble surfactant films and proteins (7), phospho- and glycolipids and monosaccharides (8,9), and cholesterol and soluble surfactants (10). Goddard (11) observed a drastic increase in the surface pressure of an alkyl sulfate monolayer upon the

introduction of a minute amount (10ppm) of the cationic Polymer JR into the subphase.

Results presented in this chapter, obtained by combining surface tension measurements of Xanthan/surfactant solutions with the monolayer technique, illustrate the effect of Xanthan on the surface properties of anionic, cationic, and nonionic surfactant solutions. Fatty acid monolayers were used as both nonionic and anionic surfactants by varying the pH of the subphase; the cationic surfactant used was a quaternary ammonium compound.

4.2. EXPERIMENTAL

4.2.1. Surface Tension Measurements

Surface tension was measured using the Wilhemy blade method. A sand-blasted platinum blade was attached to a transducer-amplifier (model 311A, Sanborn Co.). The amplified signal was sent to a recorder (Sargent Welsh, model SRG). All glassware was cleaned with potassium dichromate/sulfuric acid solution. Distilled water was used in all preparations.

4.2.2. Chemicals

Palmitic and Arachidic acids were from EM Chemicals (Elmsford, NY).

Stearyl dimethyl benzyl ammonium chloride (SDBAC) was a commercial sample (Ammonyx 4002) from Onyx Chemical Company (Jersey City, NJ) and was of 94% purity. It was further purified by repeated crystallization from a mixture of hexane and ethanol.

Sodium dodecylsulfate, cetyltrimethylammonium bromide, and Xanthan were the same samples as described in the previous chapter (see 3.2.1).

Anhydrous hexane and ethanol were gold-label reagent grades, purchased from Aldrich Chemical Company (Metuchen, NJ).

4.2.3. Monolayer Experiments

The experimental setup is shown in Fig. 4.3. Surface pressures were determined from surface tension measurements using a sand-blasted platinum blade attached to a transducer-amplifier (Model 311A, Sanborn Co.). The amplifier signal was sent to a two-channel recorder (Sargent Welsh, Model DSRG). Surface potential was determined through measurement of the potential between an air-ionizing electrode coated with ^{226}Ra and a silver/silver chloride electrode dipped in the substrate. The air-ionizing electrode was placed one to two millimeters above the surface and connected to an electrometer (Keithley, model 610B). The e.m.f. of the cell consisting of the two electrodes, the electrometer, and the potentiometer (all in series) was measured prior to (V_0) and after (V), the spreading of the monolayer. The difference, $\Delta V = V - V_0$, is the surface potential. The potentiometer was initially set so as to oppose a potential equal to V_0 , allowing the signal sent to the recorder to be read directly as ΔV .

The spreading solutions were prepared as follows. The surfactant to be spread was dissolved in anhydrous hexane (ca. 25mg of solute in 25ml of solvent), and a few drops of ethanol were added, if necessary, to attain complete solubilization.

The subphase solutions were made from deionized water. The pH of the solutions was adjusted by adding either HCl or NaOH. The ionic strength was adjusted by adding NaCl. When the presence of divalent ions was

undesirable, a minute amount of disodium ethylene diamine tetraacetate ($\text{Na}_2\text{-EDTA}$) was added. The solution was foamed in a sintered glass funnel with nitrogen gas in order to remove surface-active impurities, and the pH was then measured again. The temperature of the substrate was regulated by circulating water through a glass cooling coil submerged in the solution.

The surfactant solution was spread evenly on the aqueous substrate with an Agla micrometer syringe. The isotherms of the fatty acids were obtained under rapid compression ($\sim 45 \text{Å}^2/\text{mn}$). The isotherms of the cationic film were obtained at low compression rate ($\sim 3.5 \text{Å}^2/\text{mn}$) in order to assure thermodynamic equilibrium. The equilibrium condition was verified by the fact that a step-wise compression of the film yielded identical values for the surface pressure in the range 0 to 20mN/m. Above 20mN/m, the values obtained by continuous compression were slightly higher than those obtained in the step-wise manner. Each experiment was repeated at least three times, and averaged values were used to plot the curves.

4.3. RESULTS

4.3.1. Surface Tension of Xanthan/Surfactant Solutions

Addition of 0.010% Xanthan to solutions of the nonionic surfactant Tween 60 or of the anionic SDS had no observed effect on the surface tension (Figs. 4.4 and 4.5). Fig. 4.6 shows the surface tension of CTAB solutions at pH=7 and for various surfactant concentrations when 0.010% Xanthan has been added. The surface tension of the polymer-free CTAB solutions is also plotted in order to allow direct comparison. At very dilute surfactant concentrations, the presence of the polysaccharide in solution does not affect the surface tension. As the CTAB concentration is increased

above $1 \times 10^{-7} \text{M}$, a lowering of the surface tension is observed, with the greatest lowering occurring at the onset of precipitation. In the precipitation region, the surface tension rises slightly and a relative maximum is observed at the point of maximum precipitation. In the micellar region, the two curves coincide.

When the solution pH is lowered to 3, the effect of Xanthan is essentially the same as that observed at neutral pH (Fig. 4.7). The departure from the pure surfactant curve, however, occurs at more dilute surfactant concentrations, and the surface tension lowering remains slightly greater throughout the sub-micellar region.

4.3.2. Monolayers

4.3.2.1 Nonionic Films

Pressure and potential isotherms of palmitic acid were obtained at pH=3 and 7, first without the polysaccharide in the subphase and then with 0.01% Xanthan added to it (Figs. 4.8 and 4.9). At pH=3, the palmitic acid is 100% in its undissociated form, while the polysaccharide has about half of its carboxylate groups protonated. At pH=7, the palmitic acid monolayer is slightly charged (about 30% of the acid in its dissociated form), while Xanthan is in its sodium form. Both figures show little or no effect on the fatty acid isotherms when Xanthan is present in the subphase. In the liquid-expanded/gas region, as well as in the incompressible solid region, the isotherms remain the same and the phase transitions from liquid-condensed to solid occur at the same values of area and pressure. The only noticeable change caused by the presence of the polymer is a small increase in surface pressure and potential in the liquid-condensed region.

4.3.2.2. Anionic Films

Palmitic acid films spread on a subphase at pH=10 are predominantly in their dissociated form. The palmitate form is not as insoluble as its protonated counterpart, however, and desorption occurs, especially when dilute salt solutions are used for the subphase. In the present study, desorption was confirmed by the fact that the film could be compressed to areas as low as $10\text{\AA}^2/\text{molecule}$ (Betts and Pethica (12) made the same observation for stearic acid at pH>9 and suggested that formation of a bilayer occurs). In order to avoid desorption, palmitic acid was replaced by arachidic acid (20 C's instead of 16). Figure 4-10 shows the Π -A and ΔV -A isotherms obtained without Xanthan and with 0.010% Xanthan in the subphase. The results in the absence of polymer are in good agreement with the data of Christodoulou (13), except for the value of the film vapor pressure in the L_1 -G transition region (found to be 2mN/m instead of the 5mN/m reported for Christodoulou's study, which used a much higher salt concentration in the subphase). The introduction of 0.010% Xanthan in the subphase did not change the pressure isotherm. The ΔV -A isotherms are also nearly identical, showing only a slight increase in surface potential at large areas.

Fig. 4-11 shows the Π and ΔV isotherms obtained under the same conditions as in Fig. 4-10, except that now no chelating agent has been added to the aqueous substrate. The strong affinity between the carboxylate groups and divalent cations makes even trace amounts of Ca^{2+} in the subphase sufficient to alter radically the pressure and potential isotherms of the fatty acid. In the new Π -A isotherm, which is typical of a condensed film, the "close-packed heads" region has disappeared. The effect of Ca^{2+} on the ΔV -A isotherm is also drastic. The observed decrease in surface

potential, however, is the reverse of what would have been expected on electrostatic grounds. Goddard (14) reported a similar change for stearic monolayers at pH=10 when small amounts of Ca^{2+} or Mg^{2+} were added to the subphase.

When 0.010% Xanthan has been added, a significant increase in surface pressure is observed at areas below $35\text{\AA}^2/\text{molecule}$, and the collapse pressure is about 5mN/m greater. The presence of the polymer also increases the surface potential by as much as 20mV .

4.3.2.3. Cationic Monolayers

In Figs. 4-12 and 4-13 are shown the pressure and potential isotherms of the quaternary ammonium surfactant (SDBAC) spread on 0.40g/l xanthan subphase solutions at pH=3 and pH=7, respectively. The pressure isotherm (without Xanthan in the subphase) is the same at both pH's and is typical of an ionized monolayer with a "close-packed heads" region at large surface areas. The transition from expanded to condensed phase did not cause any discontinuity in the slope of the curve. The values of the collapse area and pressure are $45\text{\AA}^2/\text{molec.}$ and 36mN/m , respectively. The ΔV -A isotherms show a quasi-linear dependency of the surface potential on the molecular area with a slope of 2.0mV per $\text{\AA}^2/\text{molec.}$ at pH=3 and 2.3mV per $\text{\AA}^2/\text{molec.}$ at pH=7. The data of Davies (15) obtained for octadecyltrimethylammonium chloride on 0.01M NaCl substrate yield a value of 2.5mV per $\text{\AA}^2/\text{molec.}$

Upon addition of 0.40g/l Xanthan, the pressure isotherms show a substantial expansion between ca. 60 and $180\text{\AA}^2/\text{molec.}$ The increase in surface pressure occurs at both pH's and is most pronounced around

$90\text{\AA}^2/\text{molec.}$ It vanishes near the collapse point as well as at very large areas. The ΔV -A isotherms show much less dramatic changes: the presence of the polymer in the subphase causes a slight increase in surface potential at both acidic and neutral pH's, the effect being smaller in the latter case. Fig. 4-14 shows the increase in surface pressure observed upon addition of Xanthan in the subphase plotted as a function of the initial surface pressure, i.e. the surface pressure measured when the subphase contains no polymer. It is apparent that the pressure increase is slightly greater at acidic pH than it is at neutral pH.

The effect of temperature is shown in Figs. 4-15 and 4-16. In the temperature range investigated, 10 to 31°C , the pressure isotherms obtained for a subphase containing 0.040% Xanthan show very little variation. Fig. 4-16 shows the pressure increase $\Delta\Pi$ due to 0.040% Xanthan as a function of the film initial pressure, for different temperatures. At all temperatures, a maximum pressure increase is obtained around $\Pi=10\text{mN/m}$, which corresponds to a surface area of 90 to $95\text{\AA}^2/\text{molec.}$

The effect of Xanthan concentration on the pressure isotherm is shown in Figs. 4-17 through 4-20. When $\Delta\Pi$ is plotted against the logarithm of the polymer concentration for a fixed pressure and temperature (Figs. 4-21 through 4-24), a linear relationship is observed at low polymer concentrations. At higher concentrations (above ca. 0.01%), the values of $\Delta\Pi$ level off and become almost constant.

4.4. DISCUSSION

4.4.1. Nonionic and Anionic Surfactants

The lack of observed effect of Xanthan on the surface tension of the nonionic and anionic surfactant solutions was expected, since the absence of interaction between polymer and nonionic surfactant or between polymer and surfactant bearing a charge of the same sign is well documented (16-18). The monolayer experiments with palmitic acid also show no interaction between the uncharged film and the polysaccharide. The small changes observed in the ΔV -A isotherms fall within the range of experimental error. It is conceivable, however, that the presence of polymer molecules beneath the insoluble film slightly modifies the structure and orientation of water molecules, thereby causing a small increase in the vertical component of the dipole moment of these molecules. The possibility for Hydrogen bonding between the carboxylic groups of the fatty acid molecules and the hydroxyl groups of the polysaccharide could also be considered as a way to account for the small increase in surface pressure observed at neutral pH (Fig. 4-9). Johnston et al. (19, 20) have shown that the compression isotherms of cationic surfactant and phospholipid monolayers were expanded when monosaccharides (glucose, galactose, mannose, etc.) were introduced in the subphase. They suggested that the sugar molecules are coordinated to the ionic headgroups of the lipids through Hydrogen bonds, and that the driving force was entropic in nature: a single sugar molecule can form an H-bond for each of its hydroxyl groups, thereby replacing several water molecules in the hydration shell of the ionic groups and increasing the overall entropy of the system. It must be noted, however, that the significant increases in surface area obtained by Johnston's group corresponded to sugar concentrations at least 300 times greater than the

concentrations of Xanthan used in our experiments. In the case of very dilute Xanthan concentrations, these effects can be considered negligible.

Similar conclusions can be drawn in the case of an anionic monolayer (Fig. 4-10), except for the situation in which divalent cations are available at the interphase. The increase in surface pressure (Fig. 4-11) observed in this case indicates clearly that the simultaneous presence of Ca^{2+} and Xanthan affects the environment of the ionized fatty acid molecules. The strong affinity of Ca^{2+} for the carboxylate groups of both Xanthan and arachidic acid suggests that the divalent cation acts as a bridge between the anionic groups of the two compounds, which results in the penetration of certain segments of the polymer molecule into the interface and, as a consequence, in an increase in surface pressure. The number of such penetrating segments probably remains small, since the surface pressure increase is not observed at areas greater than $35\text{\AA}^2/\text{molec.}$ The strength of the interaction, however, is confirmed by the increase in the collapse pressure. An alternative explanation could also be considered, i.e., Xanthan acts as a chelating agent itself, thereby removing the Ca^{2+} ions from the surface. This hypothesis can be ruled out, however, since the addition of an excess of Ca^{2+} to the subphase yielded a compression isotherm similar, if not identical, to that shown in Fig. 4-11.

The effect on the surface potential isotherm, although indicating significant modifications of the interface as well, does not lend itself to a straightforward interpretation, since it presupposes an explanation for the effect of Ca^{2+} alone on ΔV . When the divalent ion is present in the subphase, without Xanthan, the surface potential at areas greater than ca. $45\text{\AA}^2/\text{molec.}$ is nearly zero, indicating that Ca^{2+} has effectively penetrated the plane of the negatively charged head groups of the fatty acid. Using the

schematic representation of Davies (15), shown in Fig. 4-25, the cation can be pictured as being somewhere around the plane CD. Upon compression, ΔV becomes increasingly negative, suggesting that Ca^{2+} ions are being squeezed out and relocated beneath the plane CD. In this context, the less negative values of ΔV obtained with Xanthan in the subphase would tend to indicate that the squeezing-out of Ca^{2+} ions is being opposed by the presence of the polymer segments adsorbed at the interface, possibly because of steric hindrance.

4.4.2. Cationic Surfactant

The effect of Xanthan on the surface tension of CTAB solutions is relatively small compared to that obtained by Goddard for a series of cationic polymers on SDS solutions (2). It is, however, consistent with his finding that polymers having their charged groups located on the side chain rather than on the backbone have a smaller effect on the surface tension. Moreover, the stiffness of Xanthan's backbone, whether in the stretched or in the helical conformation, definitely restricts the extent of the interaction. Comparing the change in the compression isotherm of the cationic monolayer due to the addition of 0.10g/l Xanthan (1000 ppm) with that obtained by Goddard for the Polymer JR/eicosylsulfate system (21) makes the limited effect of Xanthan on the surface properties of the cationic surfactant even more apparent. In Goddard's results, the overall features of the Π -A isotherm of the anionic monolayer are completely altered by the mere introduction of 10ppm of the cationic polymer into the subphase; a significant pressure increase is observed even at very high surface areas, and the film collapses at a much higher pressure. In contrast, the effect of Xanthan on the cationic film Π -A isotherm is not only quantitatively much

smaller, but also qualitatively noteworthy for preserving the shape of the isotherm. At very large surface areas, the presence of Xanthan in the subphase results in a slight decrease instead of an increase in surface pressure. Above ca. 30mN/m the compression isotherm is no longer affected by the introduction of Xanthan in the subphase, and the collapse pressure is unchanged. These results lead us to conclude that the interaction between Xanthan and the cationic surfactant is weak, and that the monolayer expansion is primarily due to the replacement of a number of chloride counterions by carboxylate ions of Xanthan, with very little or no penetration of segments of the macromolecule into the hydrophobic region of the monolayer (above the plane CD in Fig. 4-25). The magnitude of the surface pressure increase is quite consistent with such a mechanism. Christodoulou and Rosano (13) showed that the compression isotherm of stearic acid spread on solutions of various alkali metal hydroxides was very much influenced by the nature of the metal cation, which acts as counterion to the carboxylate groups of the fully ionized monolayer. The potassium and cesium forms of the stearate monolayer, for instance, yield Π -A isotherms that are almost identical in shape, with the latter one displaced to greater surface areas. The difference in surface pressures measured at the same molecular area can be as great as 15mN/m. In the case of Xanthan, it is doubtful that all chloride ions could be replaced by carboxylate groups, if only on steric grounds. The ion exchange results in such a drastic change in the environment of the surfactant headgroup, however, that the replacement of even a small fraction of the chloride ions could conceivably bring about the observed increases in surface pressure.

The fact that the effect on the surface tension and on the cationic film pressure is greater at acidic pH than it is at neutral pH may seem

surprising, since under the former condition a number of the polysaccharide's charged groups (about half) have been neutralized. This charge neutralization gives a more hydrophobic character to the macromolecule, however, thereby enhancing the surface activity of the polymer-surfactant complex. Similarly, Rosano (7) found that the increase in surface pressure of an anionic film due to the penetration of a positively charged protein was maximal at the isoelectric point.

The effect of temperature on the magnitude of the surface pressure increase is quite small for the range of temperatures investigated. This is consistent with a mechanism involving primarily electrostatic forces of attraction. In contrast, were hydrophobic interactions to play a significant role in the process, the compression isotherms would be affected markedly by changes in temperature.

The plots of $\Delta\Pi$ vs Π shown in Figs. 4-22 through 4-24 recall similar results obtained by Pethica (22) for the penetration of a water-soluble surfactant into an insoluble monolayer. Pethica (22) and later Alexander (23) used the Gibbs equation of adsorption to derive expressions allowing the computation of the surface concentration of the penetrating species at constant temperature and monolayer surface concentration. These expressions cannot be applied directly to our experimental data, given the differing mechanisms involved. The counterion exchange results not only in the occurrence of a new component in the monolayer, but also in a change in the concentration of the original insoluble component. An exact quantitative treatment of the interaction of Xanthan with the cationic monolayer would be possible only if the monolayer experiments were conducted in conjunction with experimental methods (e.g., radiotracer techniques) that would independently provide information about the surface

concentration of one of the monolayer components. On the other hand, a number of simplifications can be made, that will allow a thermodynamic treatment of the interaction. As already discussed, the increase in surface pressure can be safely attributed to the penetration of carboxylate groups of Xanthan into the monolayer, thus displacing some of the chloride counterions. Following Fowkes (24), the insoluble monolayer can be treated as a distinct phase, and at equilibrium, the partial molar free energy of the carboxylate groups in the monolayer and in the bulk phase must be equal:

$$\mu_B(\text{COO}^-) = \mu_M(\text{COO}^-) \quad (4-1)$$

where

$$\mu_B(\text{COO}^-) = \mu_B^0 + RT \text{Ln} a_B \quad (4-2)$$

$$\mu_M(\text{COO}^-) = \mu_M^0 + RT \text{Ln} a_M + \int_{\Pi_i}^{\Pi_{\text{eq}}} \bar{A}_P d\Pi \quad (4-3)$$

with \bar{A}_P the partial molar surface area of the COO^- groups, and Π_i and Π_{eq} , the initial surface pressure and the equilibrium surface pressure, respectively. Assuming that both the bulk phase and the monolayer are ideal solutions, equation (1) becomes:

$$\mu_B^0 + RT \text{Ln} c = \mu_M^0 + RT \text{Ln} X_P + \int_{\Pi_i}^{\Pi_{\text{eq}}} \bar{A}_P d\Pi \quad (4-4)$$

where c and X_P denote the bulk concentration and the surface molar fraction of carboxylates, respectively. Equation (4) can be rewritten as follows:

$$\mu_M^0 - \mu_B^0 = \Delta \bar{G}_{\text{pen}}^0 = RT \text{Ln} \left(\frac{c}{X_P} \right) - \int_{\Pi_i}^{\Pi_{\text{eq}}} \bar{A}_P d\Pi \quad (4-5)$$

where $\Delta \bar{G}_{\text{pen}}^0$ represents the partial molar standard free energy change of Xanthan's carboxylate groups upon penetration into the monolayer. The

quantities \bar{A}_P and X_P can be computed by applying the Gibbs' equation of adsorption. At constant temperature and pressure, it can be written as

$$d\Pi = RT\Gamma_M d\ln a_M + RT\Gamma_{Cl} d\ln a_{Cl} + RT\Gamma_P d\ln a_P \quad (4-6)$$

where Γ is the surface concentration, and the subscripts M, Cl, and P refer to the insoluble cation, the chloride ion, and the anionic group of the polymer, respectively. If the experiment is carried out in the presence of an excess of salt (e.g., NaCl), and the bulk phase is again assumed to be an ideal solution, equation (6) becomes:

$$d\Pi = RT\Gamma_M d\ln a_M + RT\Gamma_P d\ln c \quad (4-7)$$

Pethica (22) showed that when the monolayer is in or near the condensed region, equation (7) can be reduced to

$$d\Pi = \frac{\hat{A}_M}{\hat{A}_M - \bar{A}_M} RT\Gamma_P d\ln c \quad (4-8)$$

with \hat{A}_M the area per molecule of M as spread on the trough, and \bar{A}_M , the partial molar area of M. The latter is assumed to be equal at a given surface pressure to the molar area of M at the same pressure when the polymer has not been added to the subphase. \bar{A}_P and X_P can then be computed by using the following expressions:

$$\bar{A}_P = \frac{\hat{A}_M - \bar{A}_M}{\hat{A}_M \Gamma_P} = RT \left(\frac{\partial \Pi}{\partial \ln c} \right)^{-1} \quad (4-9)$$

and

$$X_P = \frac{\hat{A}_M - \bar{A}_M}{\hat{A}_M - \bar{A}_M + \bar{A}_P} \quad (4-10)$$

Figure 4.26 shows the values obtained for $\Delta \bar{G}_{pen}^0$ as a function of the initial surface pressure and for different temperatures. At very low and very high

initial surface pressures, values could not be computed due to the unreliability of the data, $\Delta\Pi$ being in these regions of the order of the experimental error. The values of $\Delta\bar{G}_{\text{pen}}^0$ vary only slightly with Π_1 , and at all temperatures a small minimum is observed around 10 to 15mN/m. In figure 4.27 are shown the variations of $\Delta\bar{G}_{\text{pen}}^0$ with temperature. At all values of Π_1 a linear relationship is observed, allowing the direct computation of the standard change of enthalpy, $\Delta\bar{H}_{\text{pen}}^0$, and of the standard change of entropy, $\Delta\bar{S}_{\text{pen}}^0$. Values for the former are found to be in the range 30 to 35kJ/Eq, while $\Delta\bar{S}_{\text{pen}}^0$ varies from 180 to 203 J/Eq.K. These thermodynamic values indicate that the penetration process is entropically favorable while enthalpically unfavorable. It is worth mentioning that Kwak et al. (25) have obtained similar values for the interaction between dodecyltrimethylammonium bromide (DTAB) and the anionic polysaccharide dextran sulfate, although through an entirely different approach. In their study surfactant binding was determined by means of a solid-state-surfactant selective electrode, and the resulting experimental binding isotherms were interpreted in terms of the model developed by Schwarz (26) and Satake (27) (see section 1.3.3.2.). In the range 5 to 35°C their calculated values of the standard free energy of surfactant binding by the polymer varied from -22.6 to -25.9kJ/mol, and they found the corresponding ΔH^0 and ΔS^0 to be constant and equal to 8.3kJ/mol and 112J/mol K, respectively. Although the similarity in the values of the change in standard free energy obtained by the two methods should be seen as probably coincidental since different standard states have been used, the fact that both approaches agree as far as the enthalpic and entropic nature of the polymer/surfactant interaction is reassuring when considering the

number of assumptions made in the present study. The much greater value of ΔH^0 obtained in the case of the Xanthan/SDBAC system can be interpreted as the consequence of a greater steric hindrance: the head group of SDBAC is bulkier than that of DTAB and the polysaccharide dextran whose backbone consists of α -D(1-6) glucoside linkages is more flexible than Xanthan.

In conclusion, the results obtained in this study seem to validate the thermodynamic approach that was chosen. It remains to be seen, however, whether it is applicable to other polymer/surfactant systems, and if it is, whether it can provide a sensitive tool for analyzing the various factors that influence polymer/surfactant interactions.

FIGURE 4.1: Schematic Illustration of the effect of a neutral polymer on the surface tension of solutions of an ionic surfactant

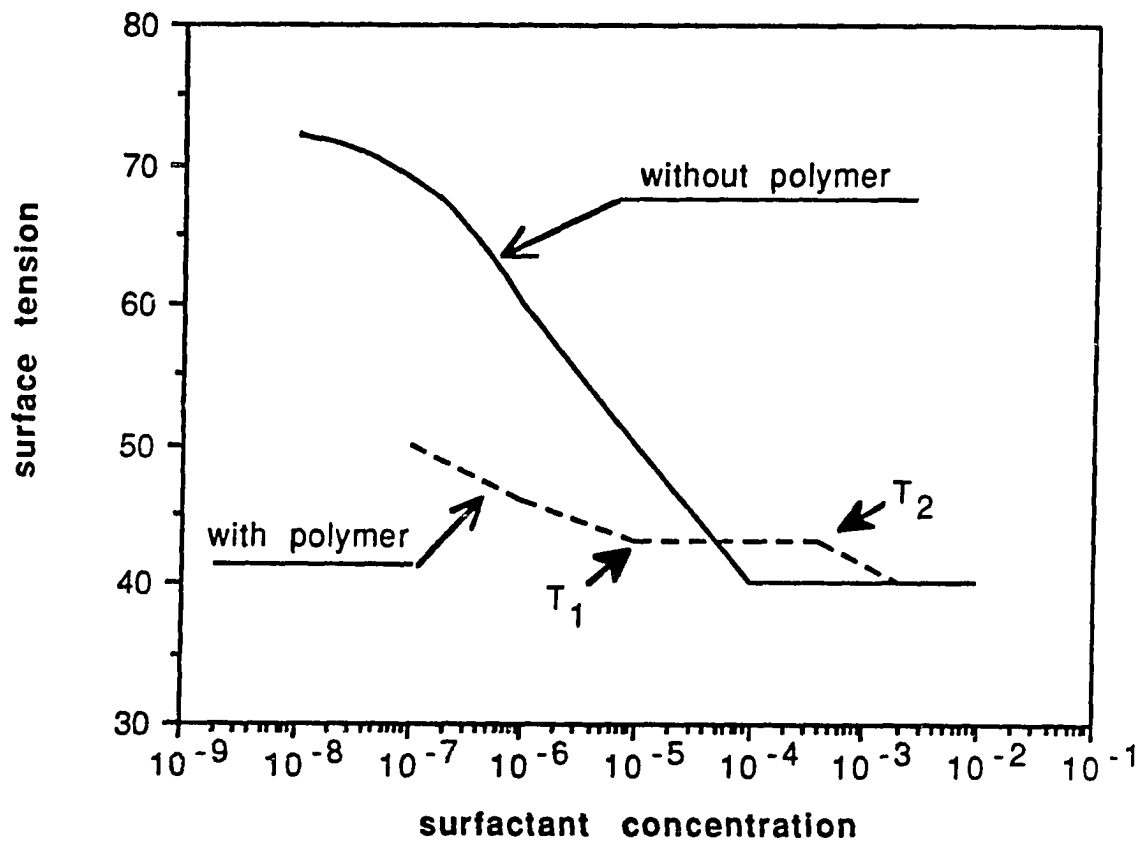


FIGURE 4.2: Schematic illustration of the effect of an anionic polymer on the surface tension of solutions of a cationic surfactant

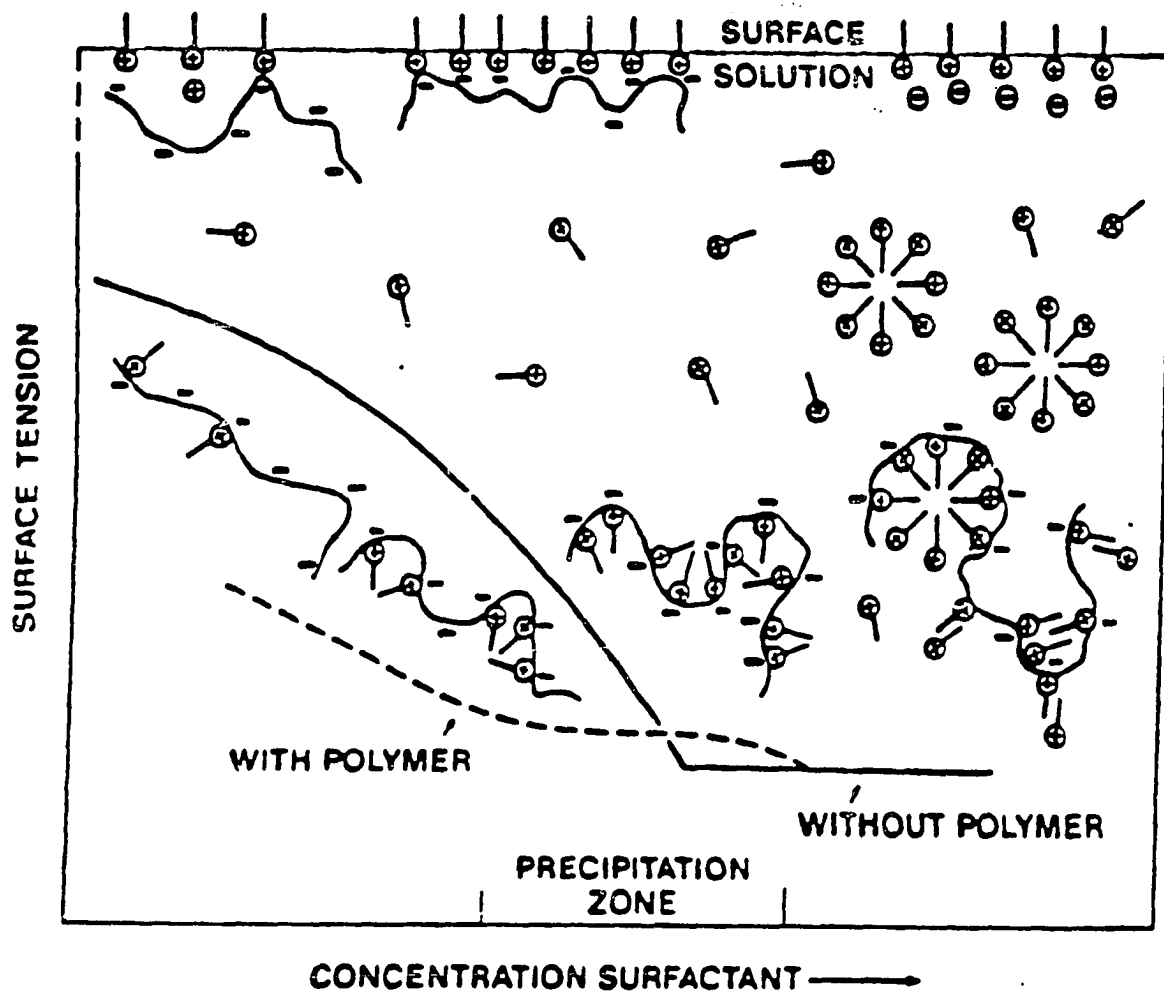
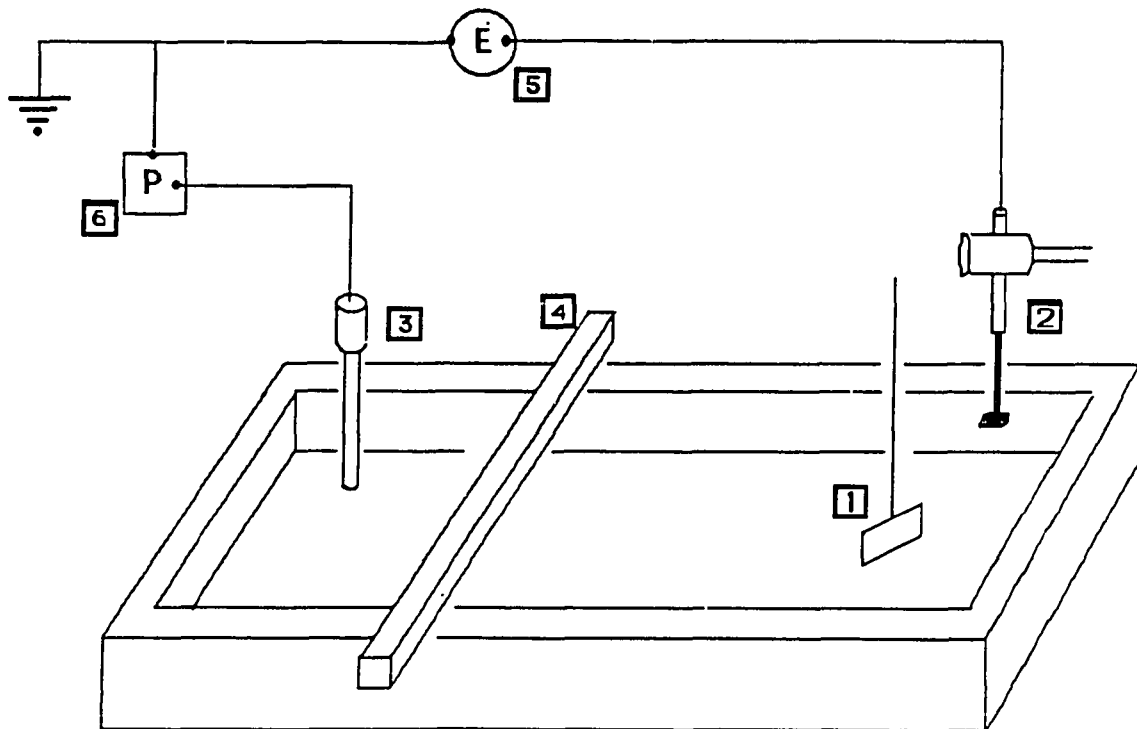


FIGURE 4.3: Experimental apparatus for measuring the surface pressure and surface potential



LEGEND:

- 1: WETTABLE BLADE**
- 2: RADIOACTIVE ELECTRODE**
- 3: TROUGH ELECTRODE**
- 4: MOVING BARRIER**
- 5: ELECTROMETER**
- 6: POTENTIOMETER**

FIGURE 4.4: Surface tension at 25°C of Tween 60 + 0.10g/l Xanthan solutions

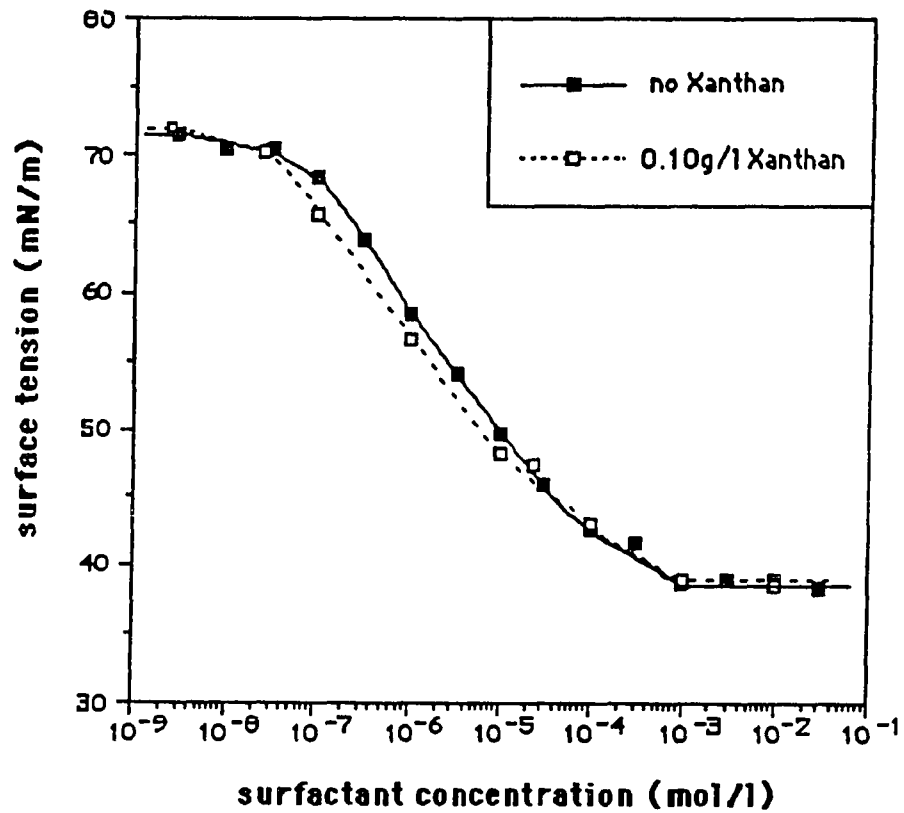


FIGURE 4.5: Surface tension at 25°C of SDS + 0.10g/l Xanthan solutions

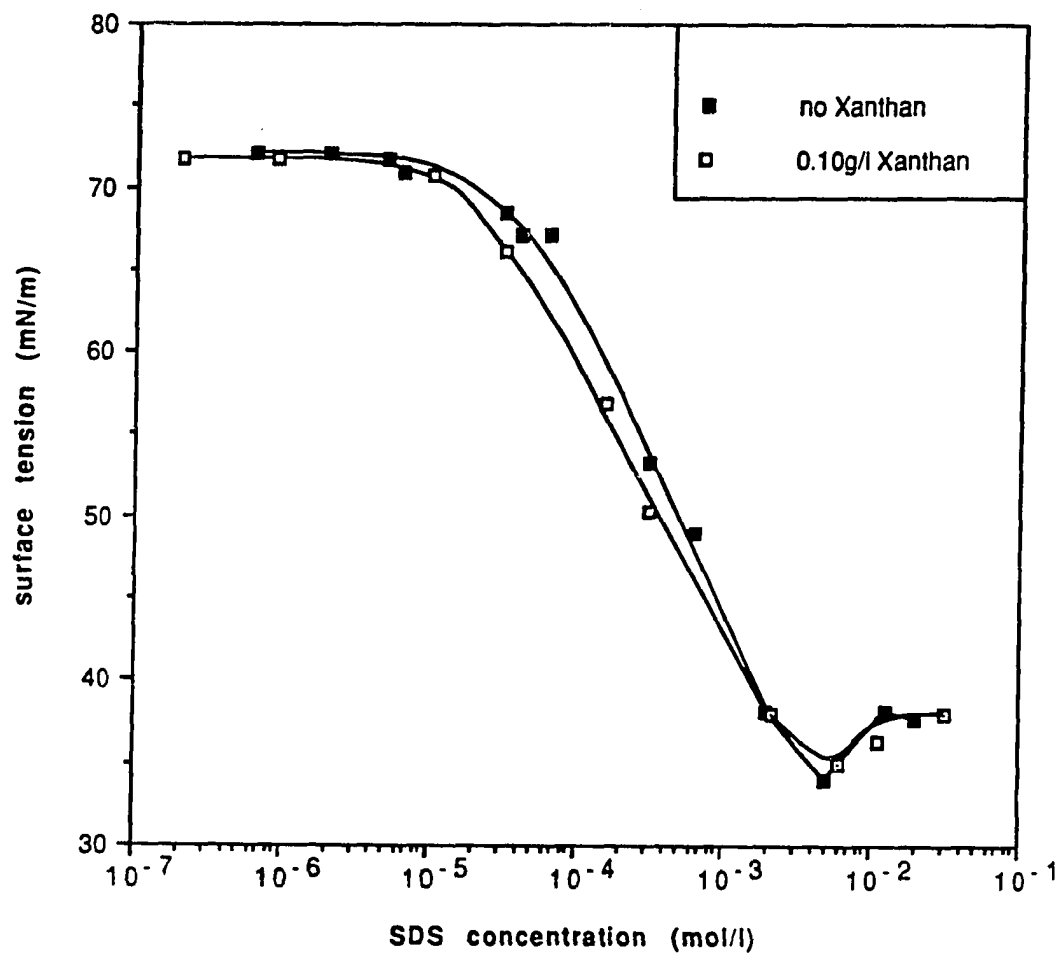


FIGURE 4.6: Surface tension at 25°C of CTAB + 0.01g/l Xanthan solutions at pH=7

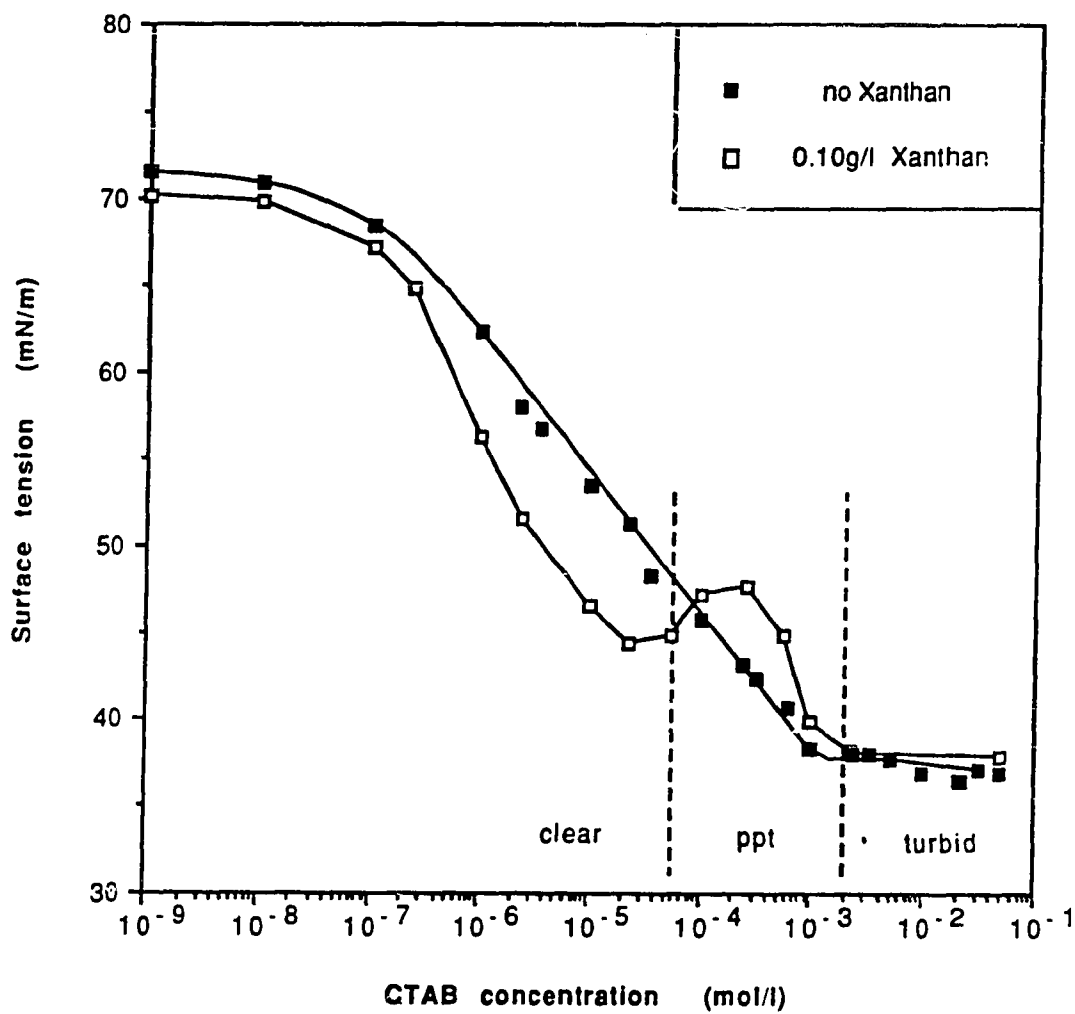


FIGURE 4.7: Surface tension at 25°C of CTAB + 0.10g/l Xanthan solutions. pH=3

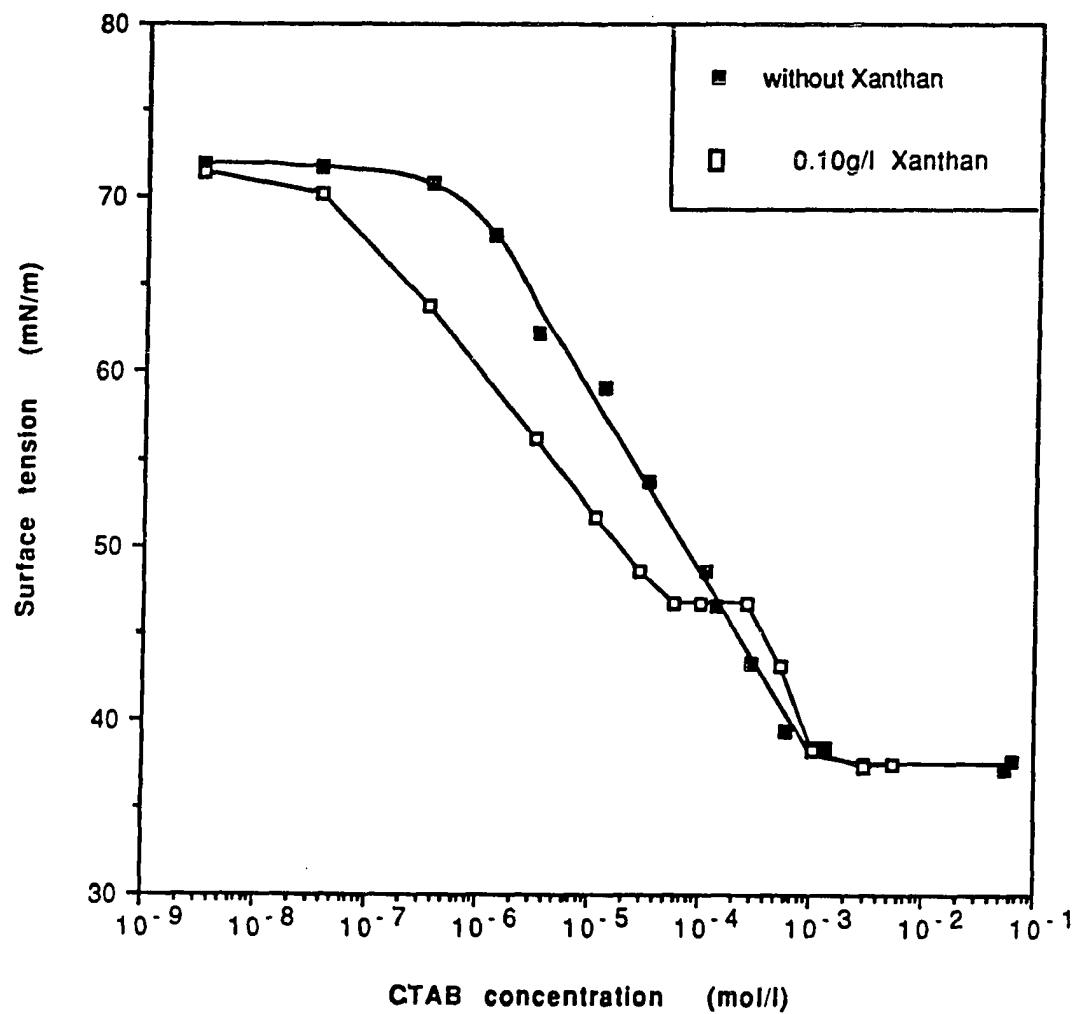


FIGURE 4.8: Π -A and ΔV -A isotherms of palmitic acid at pH=3 on 0.10g/l Xanthan subphase. T=25°C

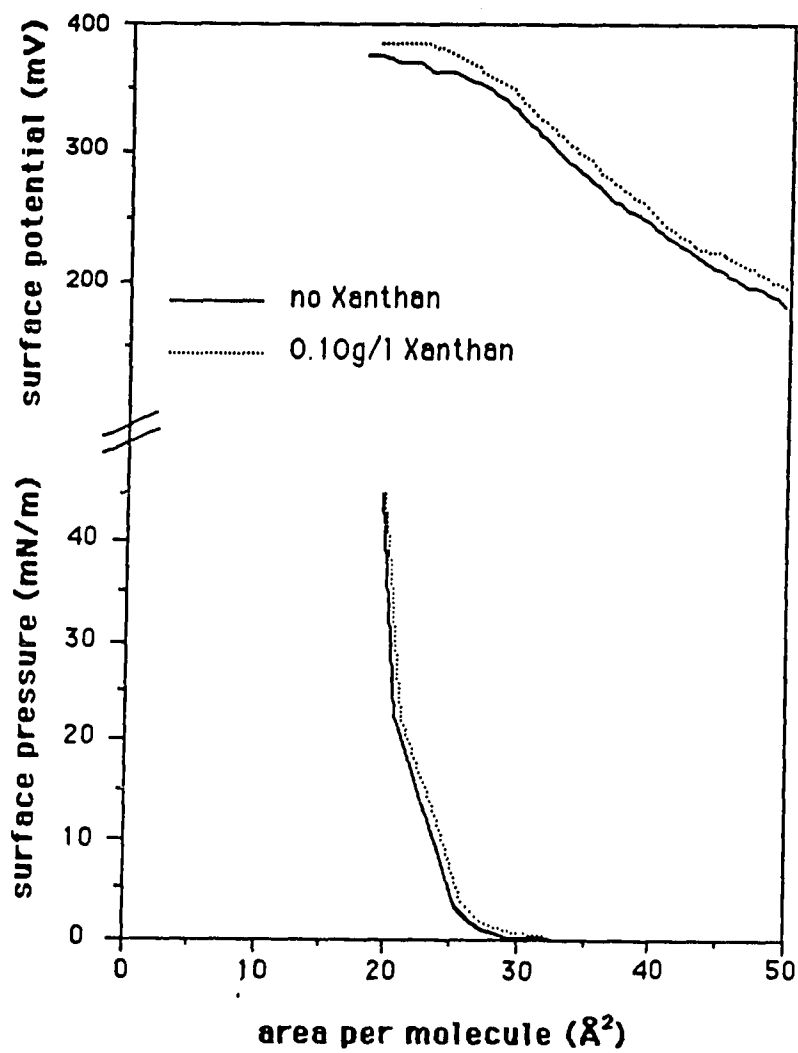


FIGURE 4.9: Π -A and ΔV -A isotherms of palmitic acid at pH=7 on 0.10g/l Xanthan subphase. T=25°C

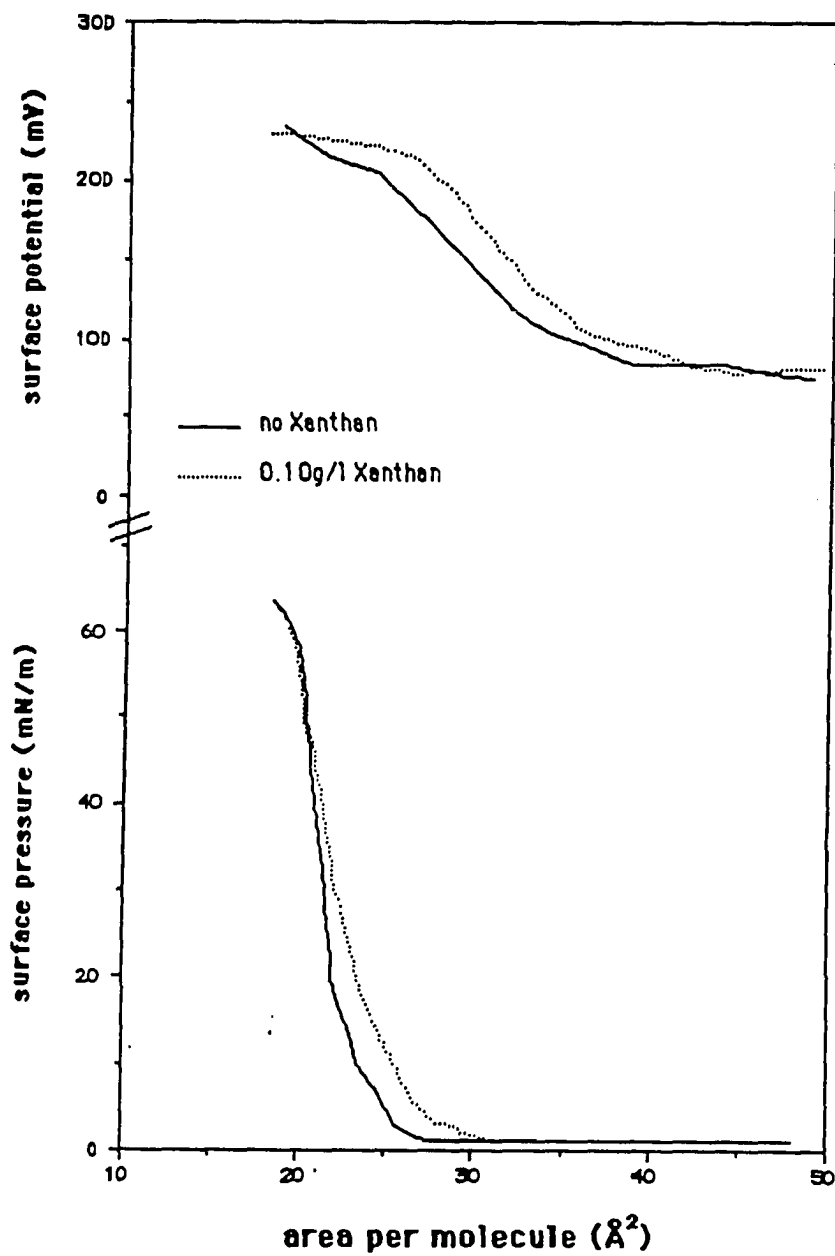


FIGURE 4.10: Π -A and ΔV -A isotherms of arachidic acid at pH=10 on 0.10g/l Xanthan. T=25°C

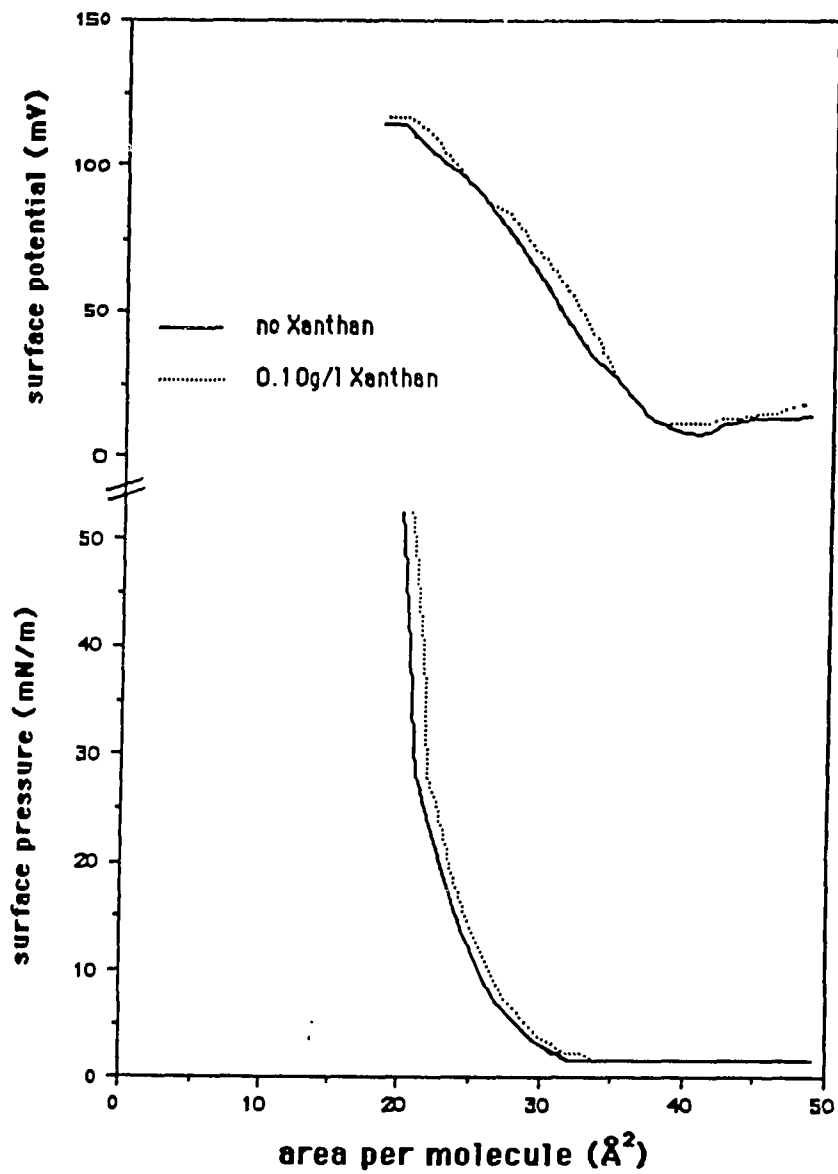


FIGURE 4.11: Π -A and ΔV -A isotherms of arachidic acid on 0.10g/l Xanthan + CaCl subphase at pH=10. T=25°C

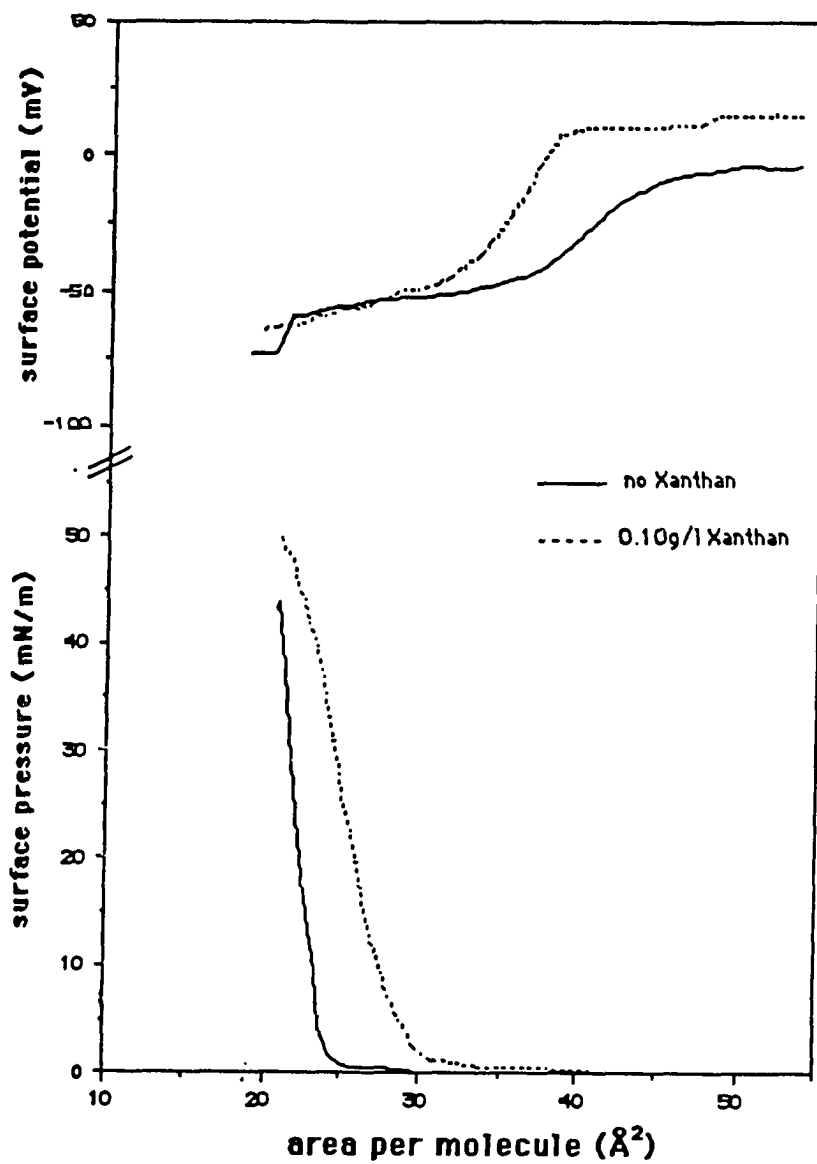


FIGURE 4.12: Π -A and ΔV -A isotherms of SDBAC on 0.04g/l Xanthan subphase at pH=3. T=25°C

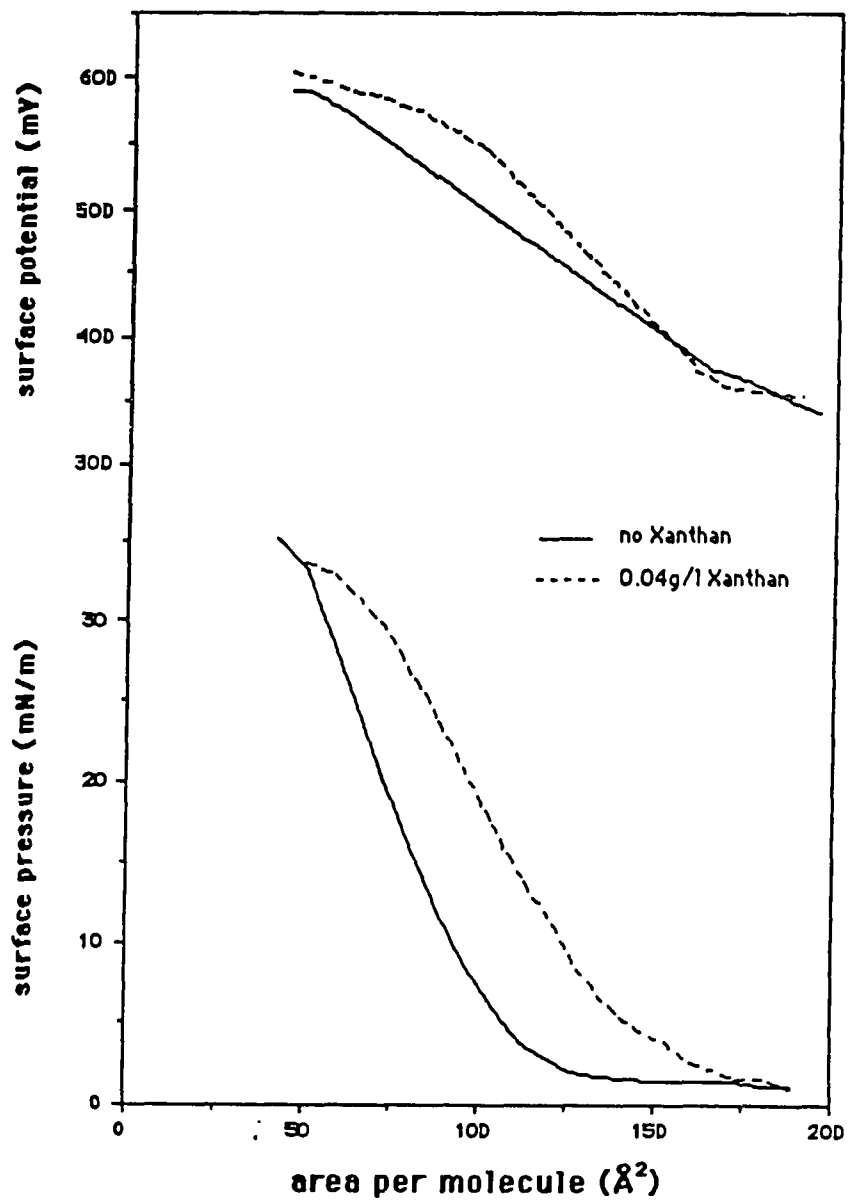


FIGURE 4.13: Π -A and ΔV -A isotherms of SDBAC on 0.04g/l Xanthan subphase at pH=7. T=25°C

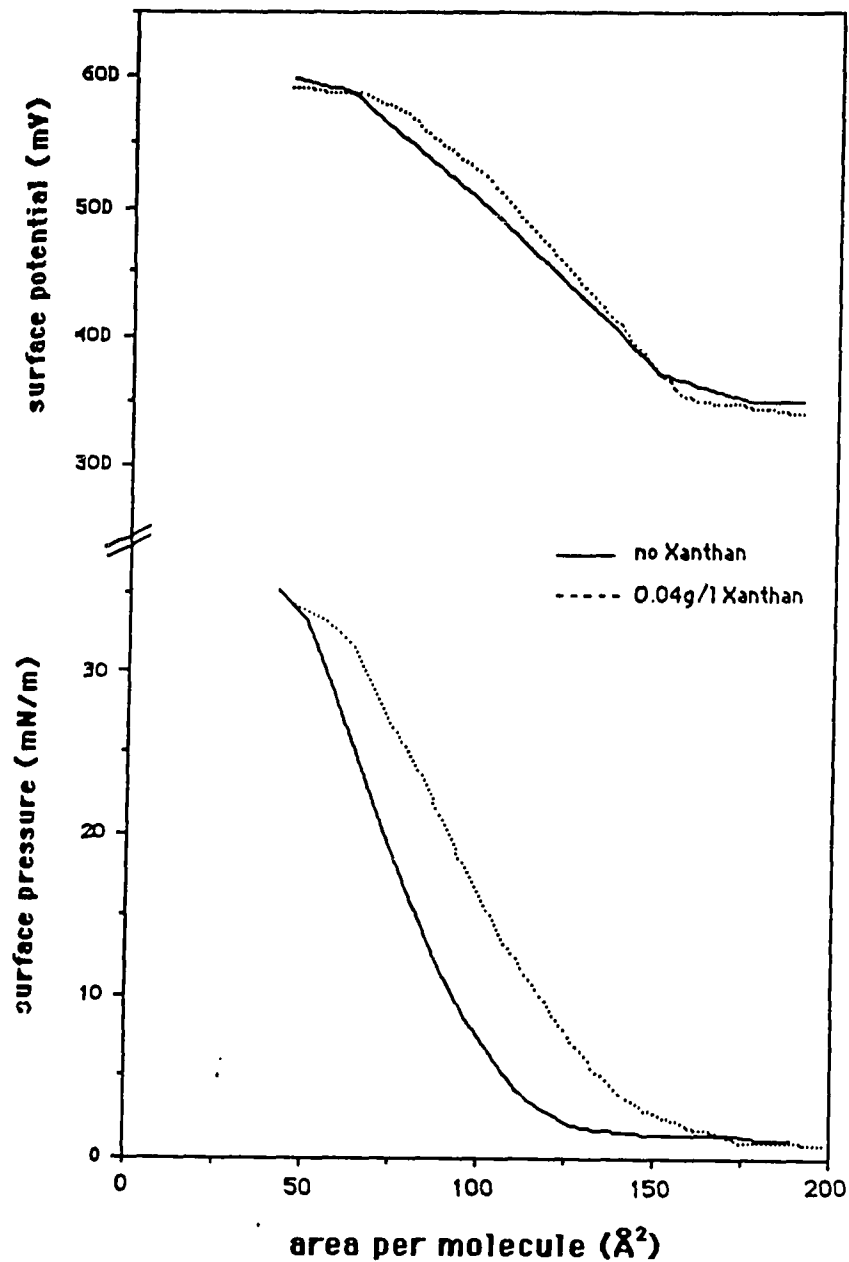


FIGURE 4.14: Plots of the increase in surface pressure vs. the initial pressure for a 0.04g/l Xanthan subphase at pH=3 and pH=7. T=25°C

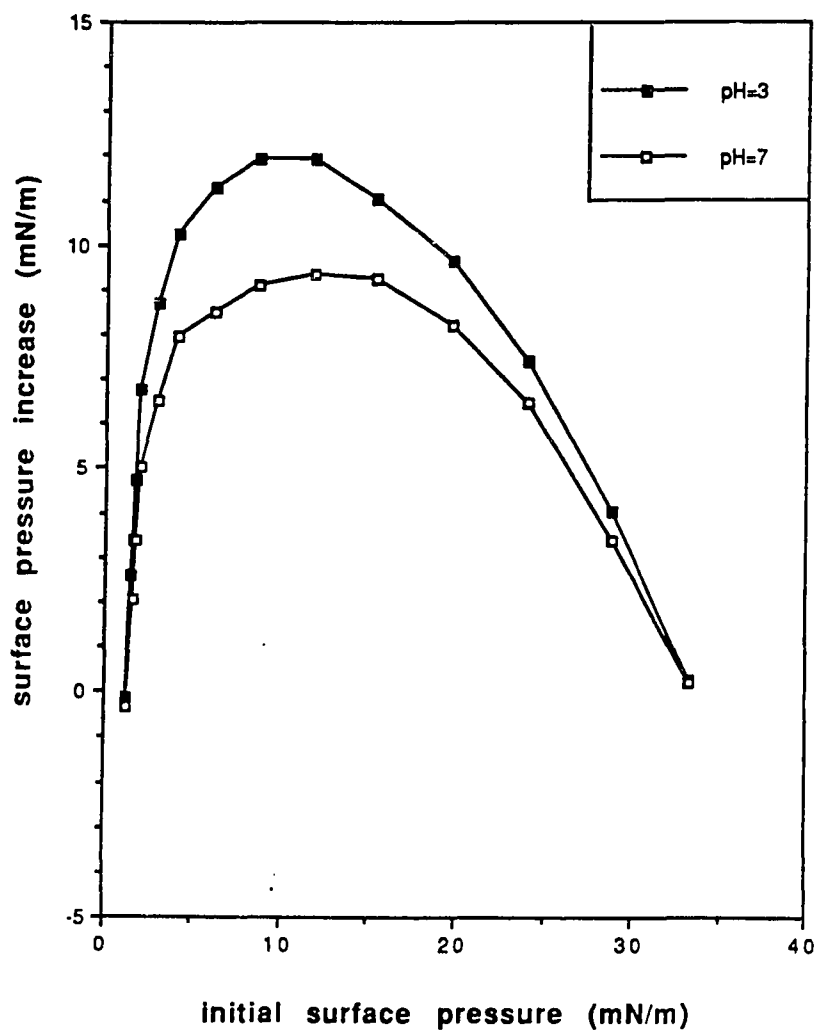


FIGURE 4.15: Π -A Isotherms of SDBAC on 0.4g/l Xanthan subphase at different temperatures

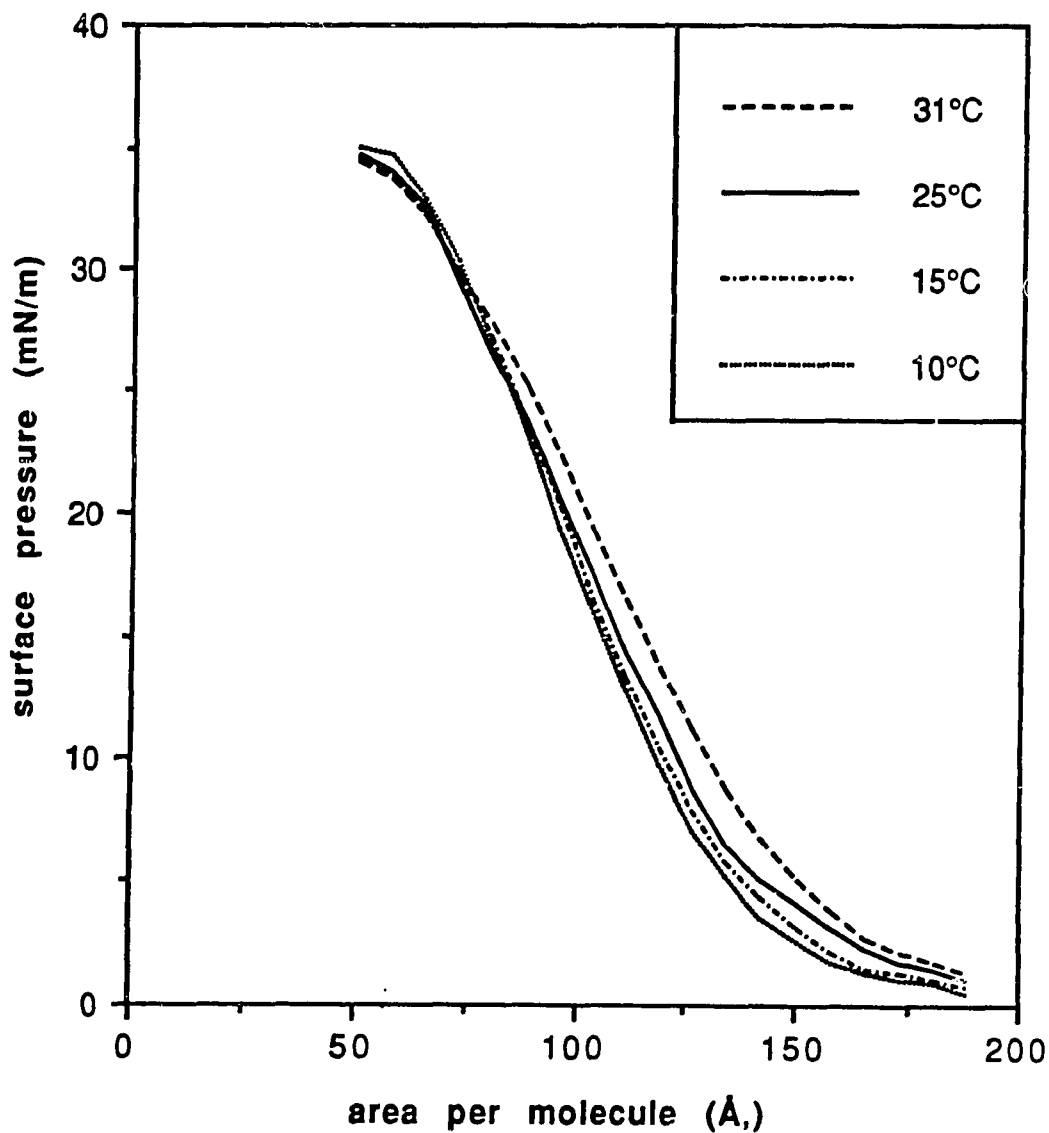


FIGURE 4.16: Plots of the surface pressure increase vs. the initial surface pressure at different temperatures, when 0.4g/l Xanthan has been added to the subphase

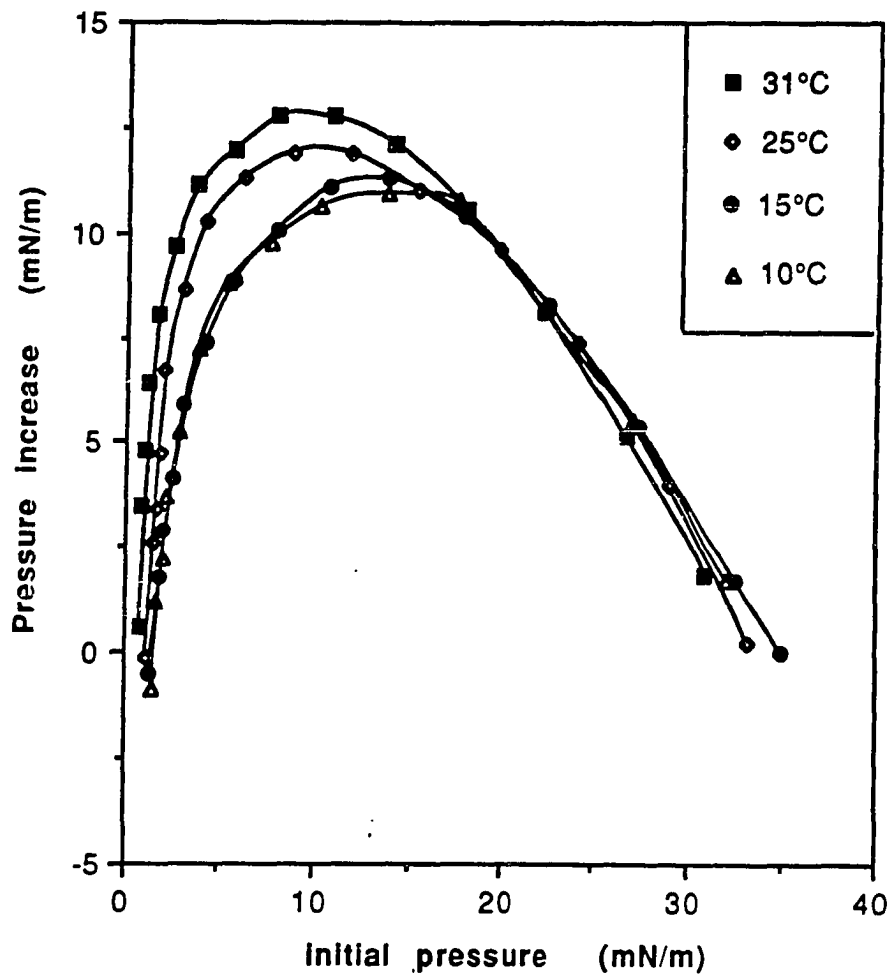


FIGURE 4.17: Plots of the increase in surface pressure vs. the initial film pressure at 10°C

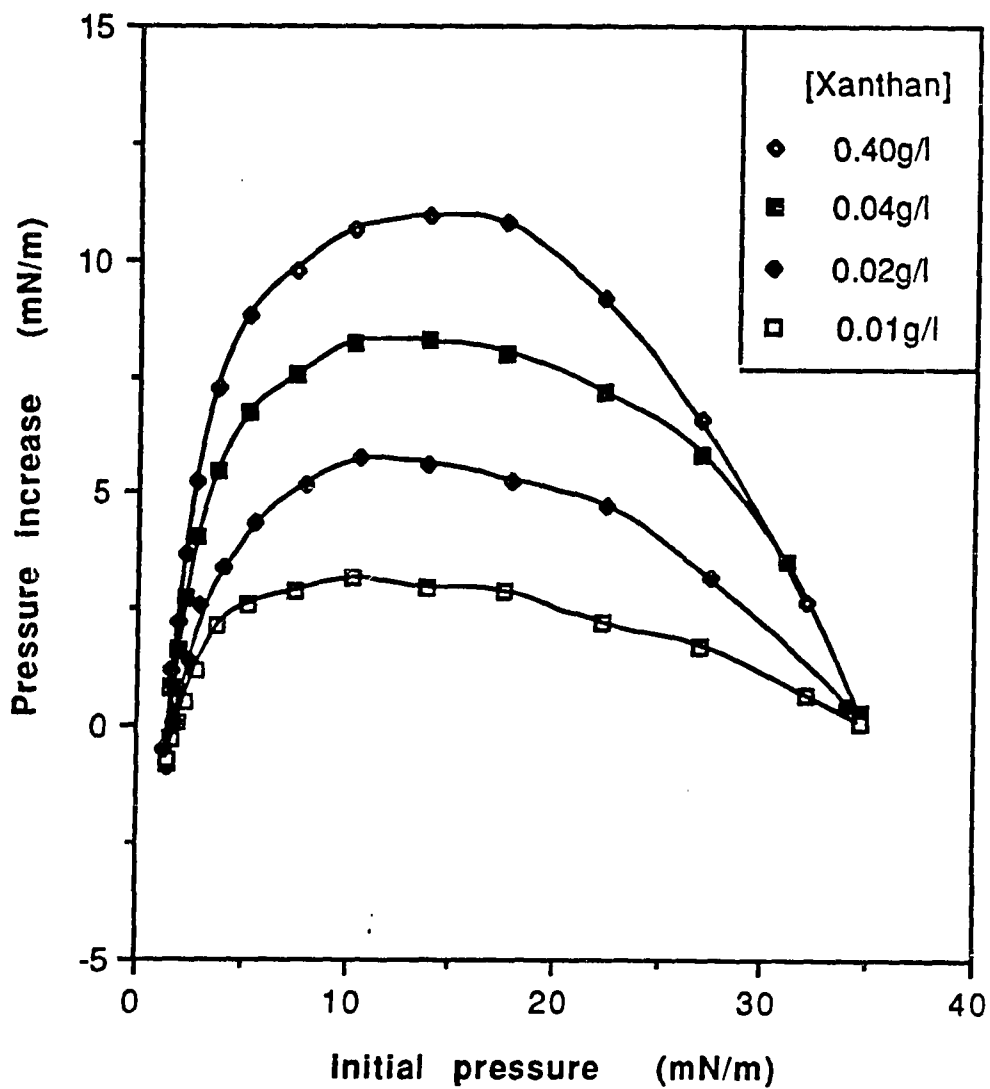


FIGURE 4.18: Plots of the increase in surface pressure vs. the initial film pressure at 15°C

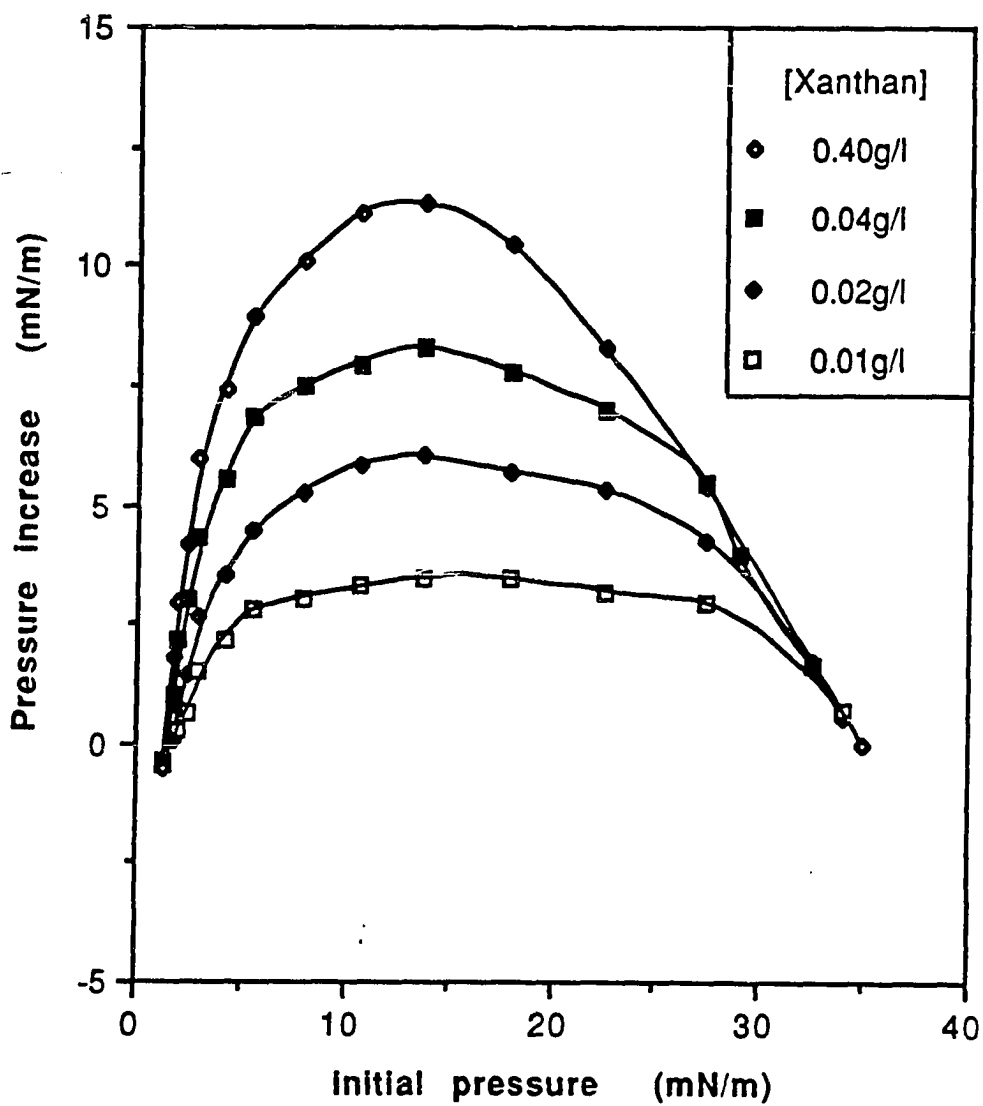


FIGURE 4.19: Plots of the increase in surface pressure vs. the initial film pressure at 25°C

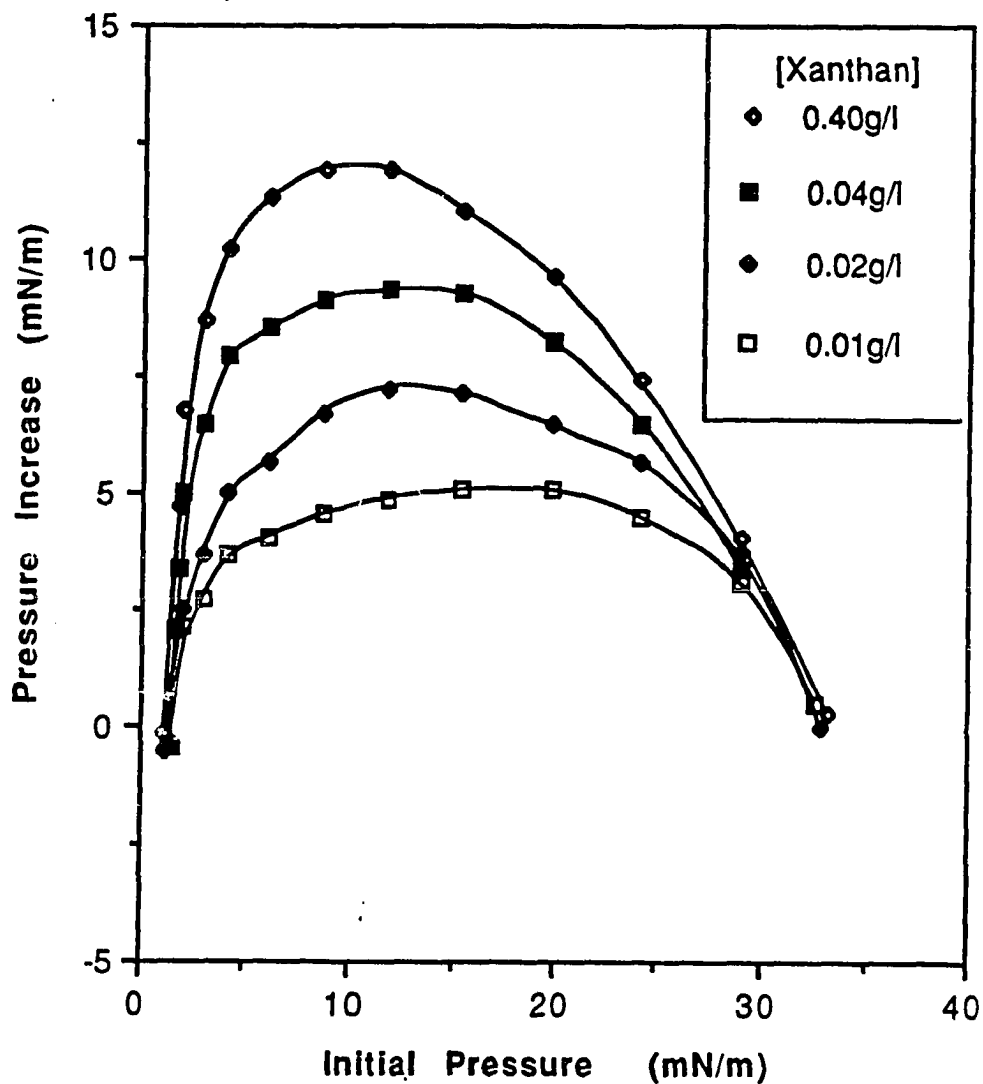


FIGURE 4.20: Plots of the increase in surface pressure vs. the initial film pressure at 31°C

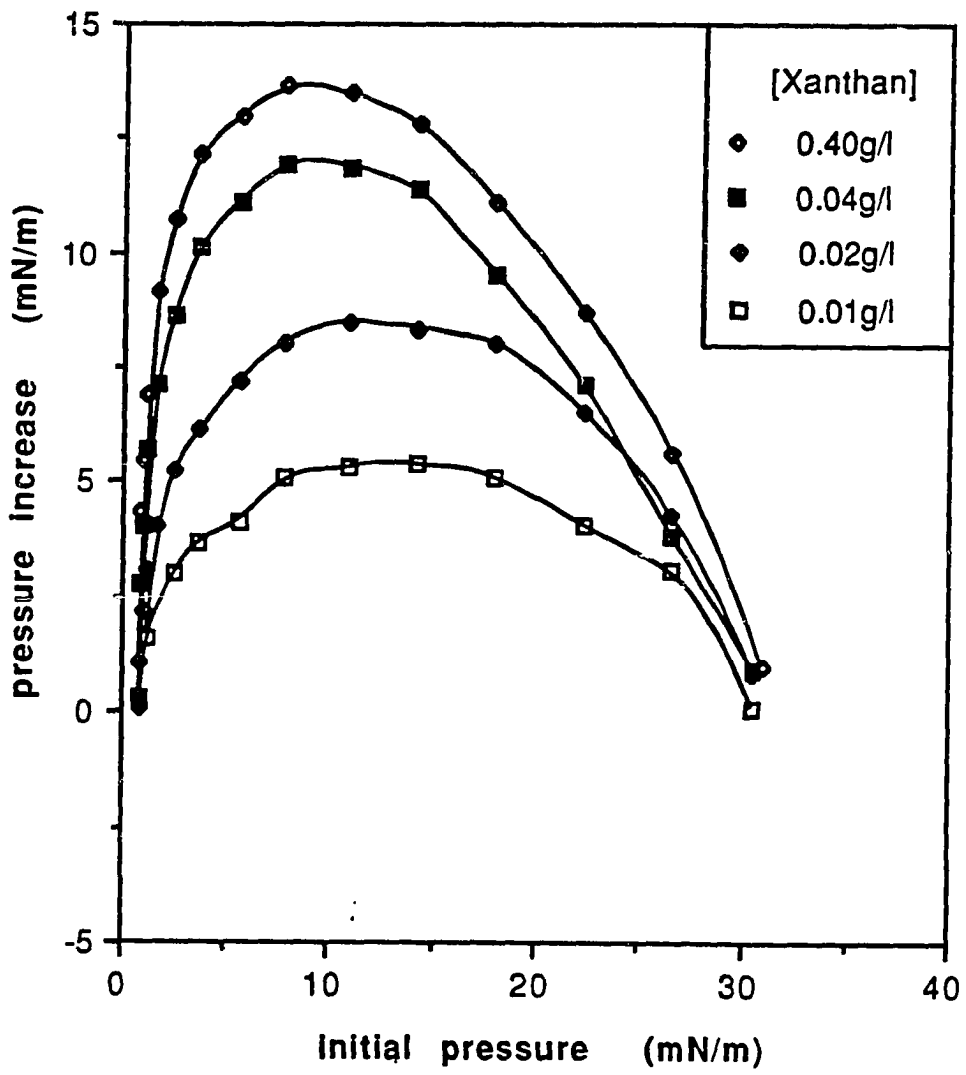


FIGURE 4.21: Plots of the increase in surface pressure vs. the concentration of Xanthan in the subphase at 10°C and constant initial pressure

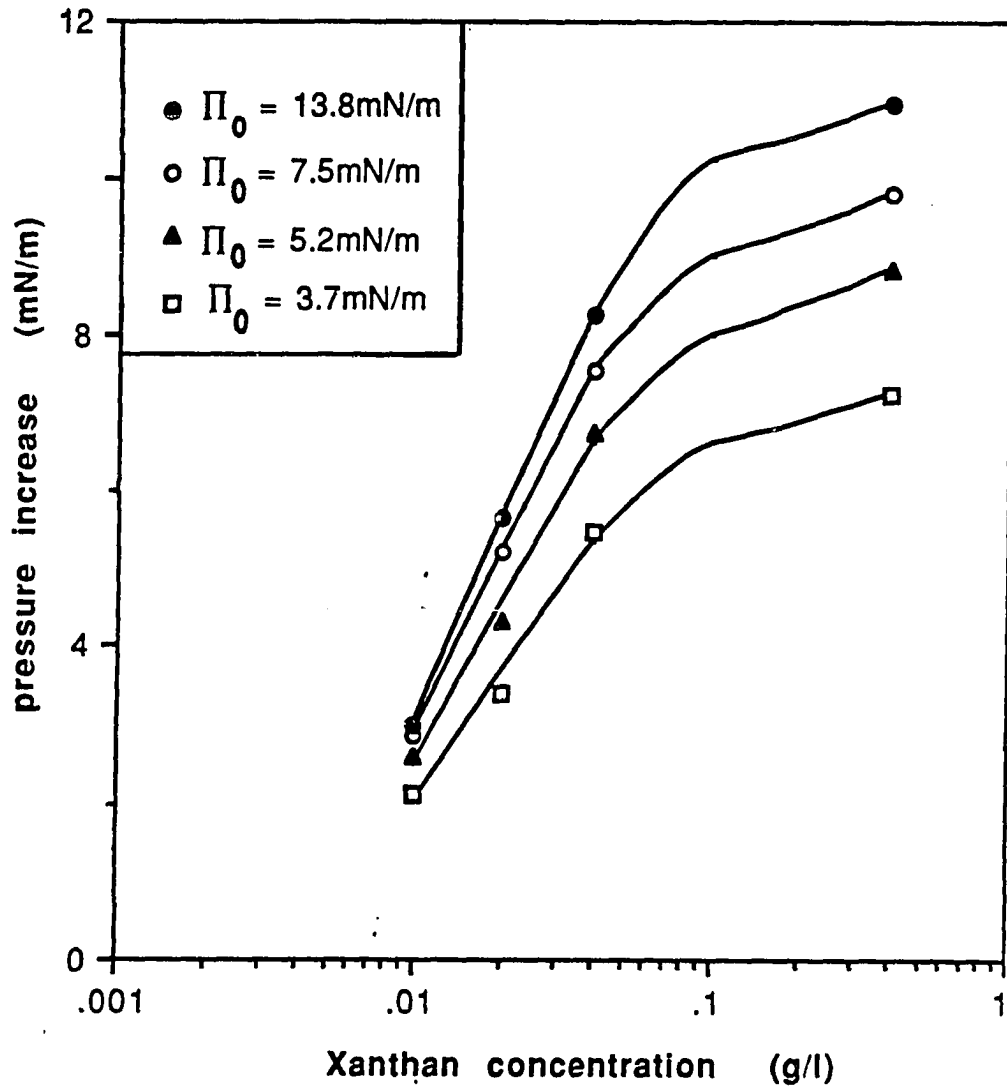


FIGURE 4.22: Plots of the Increase in surface pressure vs. the concentration of Xanthan in the subphase at 15°C and constant initial pressure

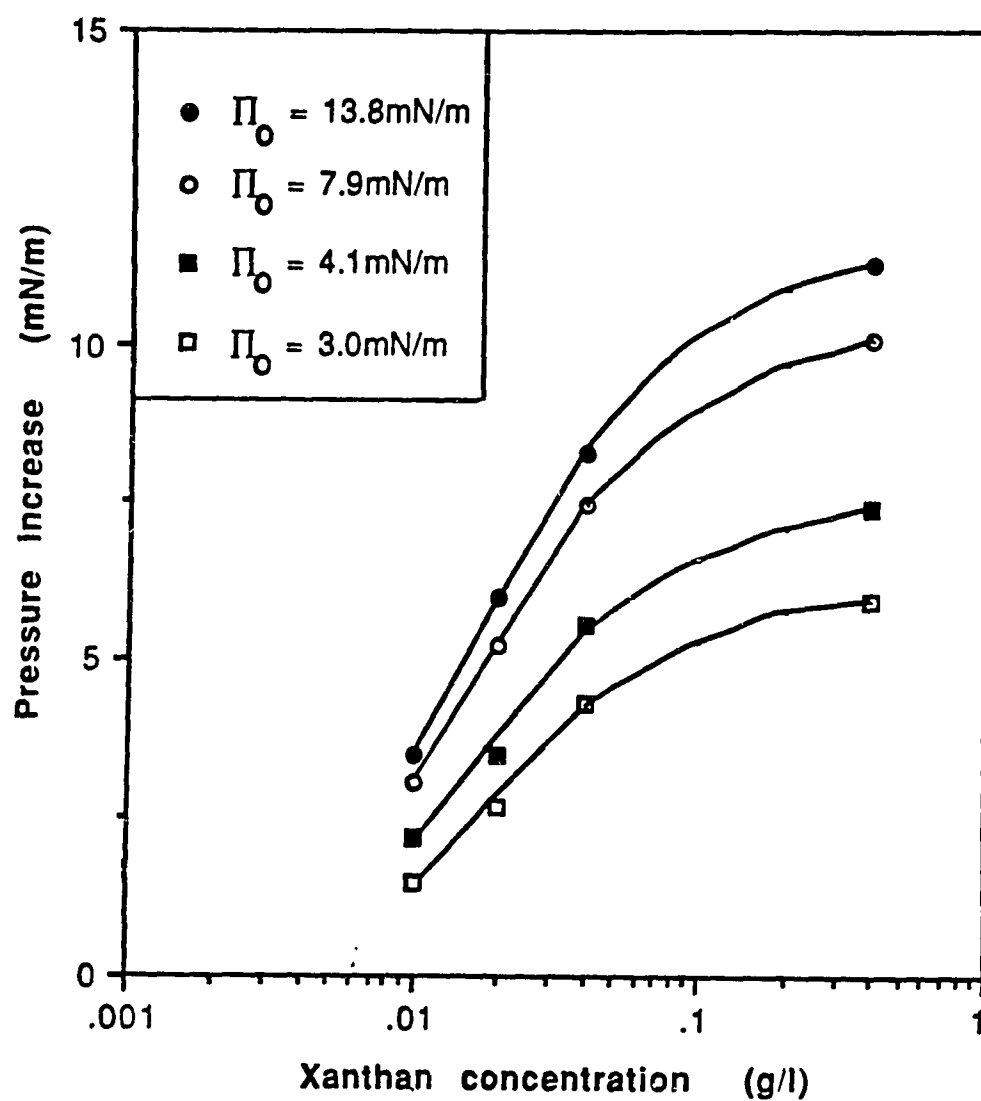


FIGURE 4.23: Plots of the increase in surface pressure vs. the concentration of Xanthan in the subphase at 25°C and constant initial pressure

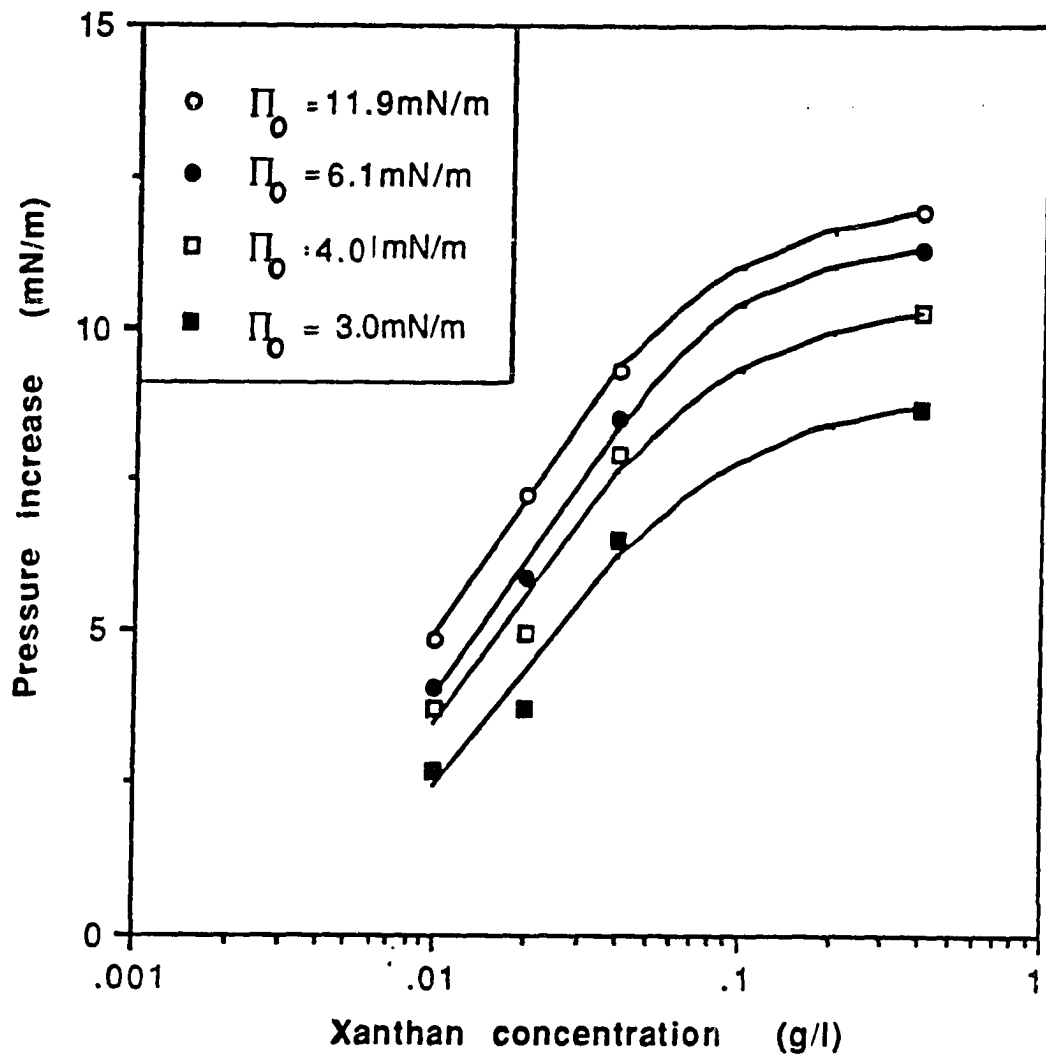


FIGURE 4.24: Plots of the increase in surface pressure vs. Xanthan concentration at a constant initial pressure. T=31°C

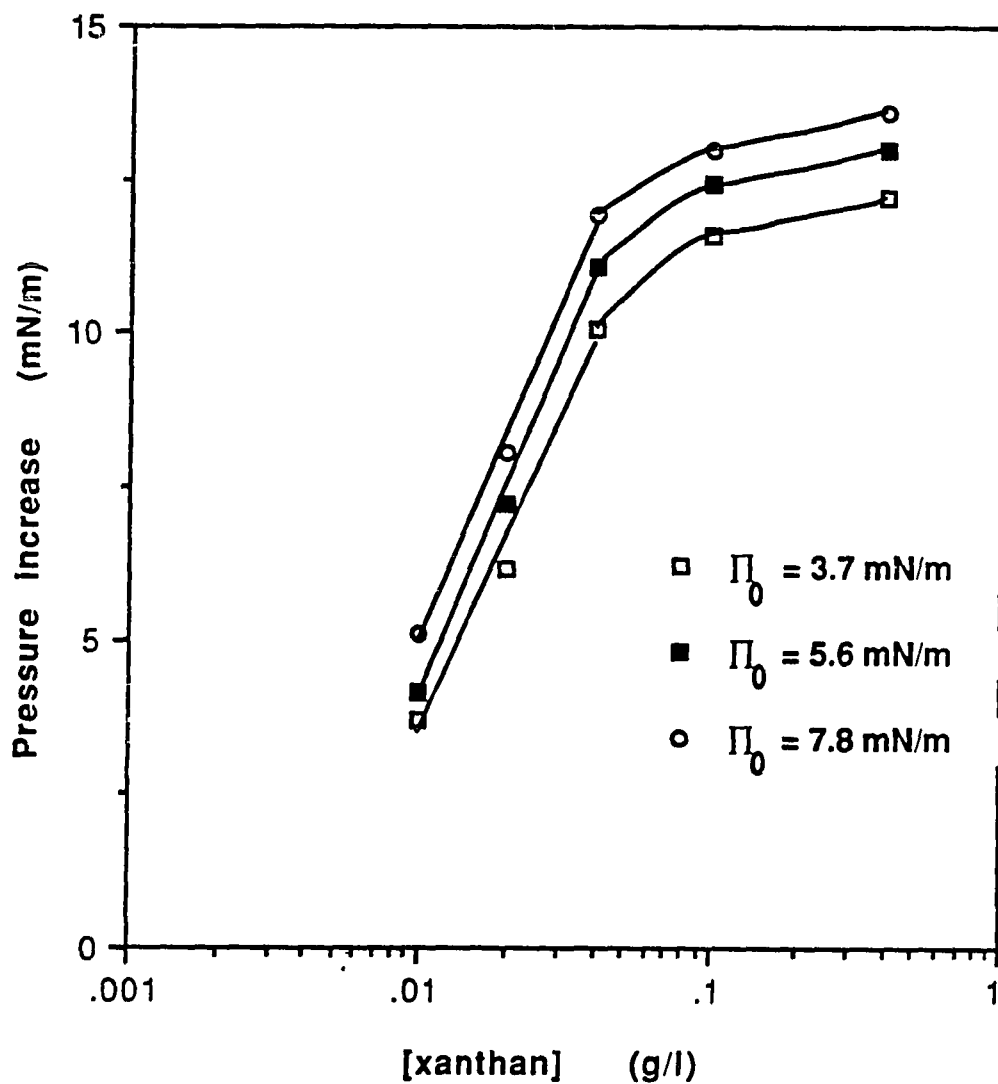


FIGURE 4.25: Schematic illustration of the arrangement of detergent ions at the air-water interface

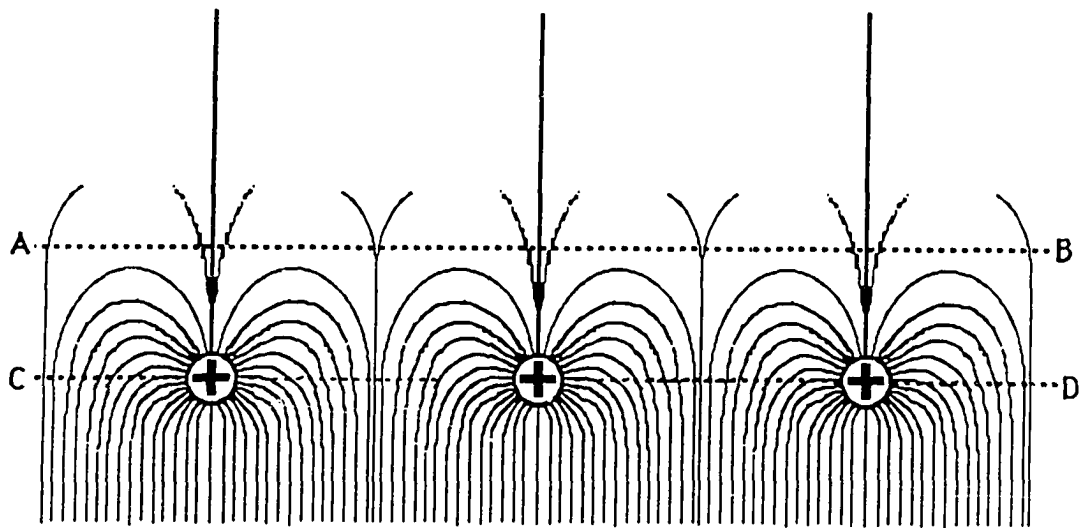


Figure 4.26: Change in standard free energy of penetration vs. the initial surface pressure.

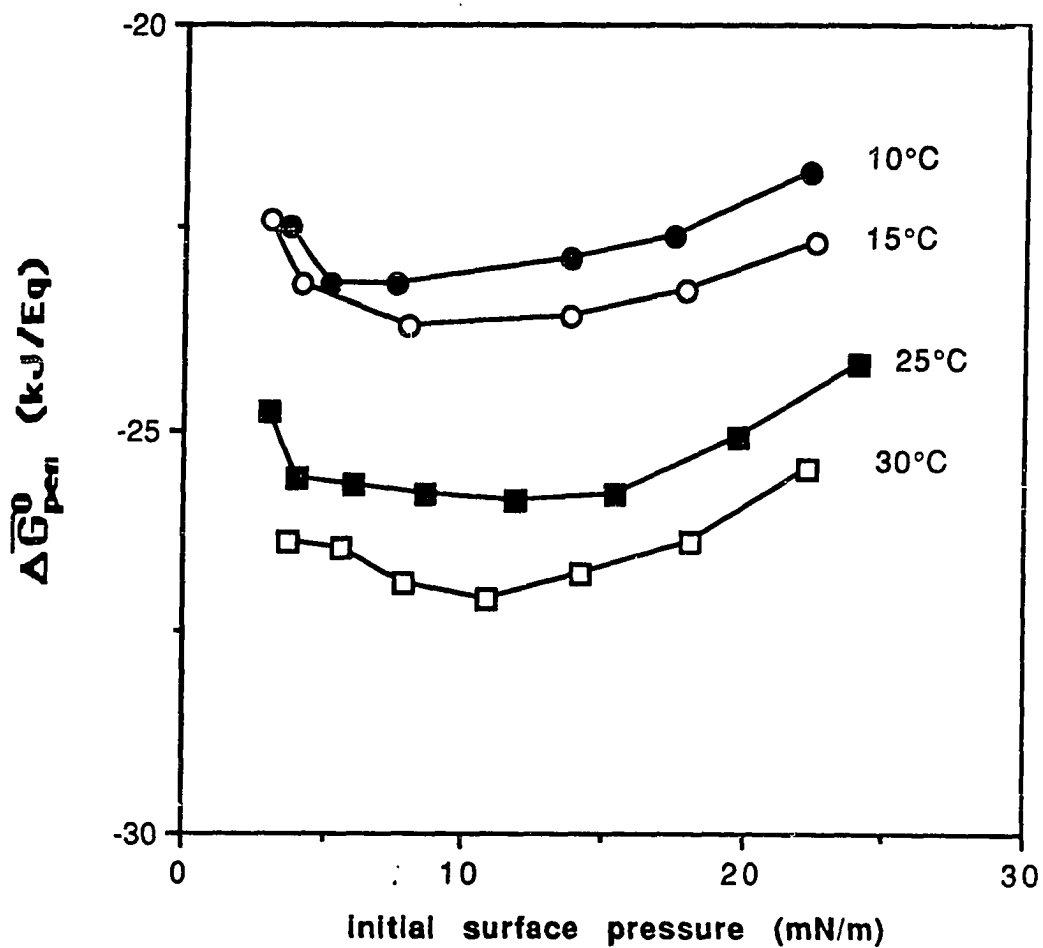
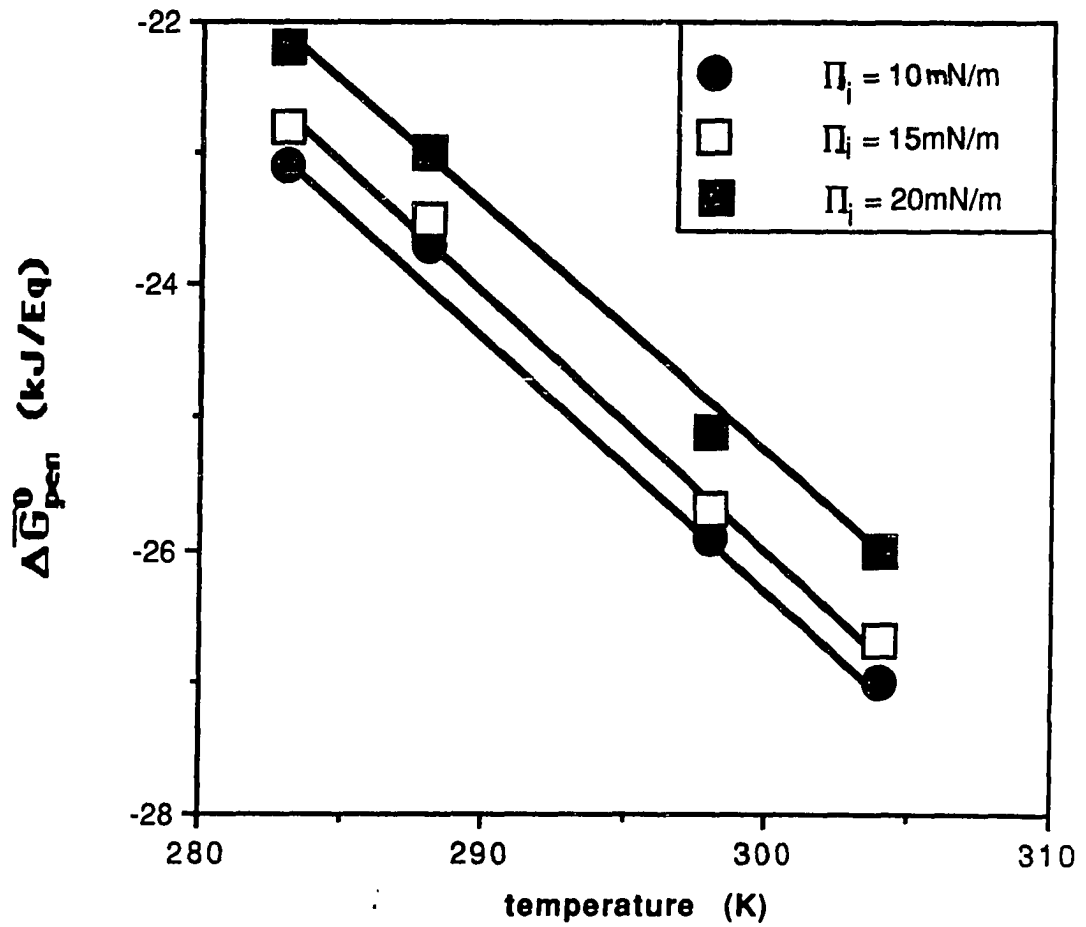


Figure 4.27: Partial free energy of penetration of Xanthan vs. temperature



REFERENCES

CHAPTER ONE

- 1) Breuer, M.M.; Robb, I.D., *Chem. Ind.*, 13, 531 (1972)
- 2) Robb, I.D., *Anionic Surfactants, Physical Chemistry of Surfactant Action*, Lucassen-Reynders, Ed.; M. Dekker, NY, 109 (1981)
- 3) Steinhardt, J.; Reynolds, J.A., *Multiple Equilibria in Proteins*, Academic, NY, 1969
- 4) Everett, D.H., *Pure Appl. Chem.*, 31, 579 (1972)
- 5) Hartley, G.S., *Aqueous Solutions of Paraffin chain Salts*, Hermann, Ed.; Paris, 1936
- 6) Debye, P., *J. Phys. Chem.*, 53, 1 (1949)
- 7) Debye, P., *Ann. N.Y. Acad. Sci.*, 51, 573 (1949)
- 8) Reich, I., *J. Phys. Chem.*, 60, 257 (1956)
- 9) Overbeek, J.T.G.; Stigter, D., *Rec. Trav. Chim.*, 75, 1263 (1956)
- 10) Hoeve, C.A.J.; Benson, G.C., *J. Phys. Chem.*, 61, 1149 (1957)
- 11) Poland, D.C.; Scheraga, H.A., *J. Colloid. Interf. Sci.*, 21, 273 (1966)
- 12) Tanford, C., *J. Phys. Chem.*, 78, 2469 (1974)

- 13) Nagarajan, R.; Ruckenstein, E., *J. Colloid. Interf. Sci.*, 60, 221 (1977)
- 14) Israelachvili, J.N.; Mitchell, D.J., *J. Chem. Soc. Faraday Trans. II*, 72, 1525 (1976)
- 15) Hill, T.L., *Thermodynamics of Small Systems*, Vol.1 and 2, Benjamin, Ed.; NY, 1964
- 16) Mukerjee, R., *Micellization, Solubilization and Microemulsions*, Mittal Ed.; Plenum, NY, 1977
- 17) Nagarajan, R.; Ruckenstein, E., *J. Colloid. Interf. Sci.*, 91, 500 (1983)
- 18) Nagarajan, R.; Ruckenstein, E., *J. Colloid. Interf. Sci.*, 71, 580 (1979)
- 19) Hall, D.G.; Pethica, B.A., *Non-Ionic Surfactants*, Schick, M.J., Ed.; M. Dekker, NY, 1967
- 20) Goddard, E.D.; Pethica, B.A., *J. Chem. Soc.*, 2659 (1951)
- 21) Saito, S., *Colloid. Polym. Sci.*, 257, 266 (1979)
- 22) Jones, M.N., *J. Colloid. Interf. Sci.*, 23, 36 (1967)
- 23) Saito, S., *J. Colloid. Sci.*, 15, 283 (1960)
- 24) Knox, W.J.; Parshall, T.O., *J. Colloid. Interf. Sci.*, 33, 16 (1970)
- 25) Goddard, E.D.; Hannan, R.B., *J. Soc. Cosmet. Chem.*, 26, 461 (1975)

- 26) Gravsholt, S., Proc. 5th Int. Congr. Surf. Active Subst., Barcelona, 1968, Vol.2, p993
- 27) Shirahama, K., Colloid. Polym. Sci., 252, 978 (1974)
- 28) Cabane, B., J. Phys. Chem., 81, 1639 (1977)
- 29) Cabane, B., Solution Behavior of Surfactants, Mittal & Fenders, Edit., Vol.1, Plenum, NY, NY, p.661 (1982)
- 30) Zana, R.; Lang, J., Polym. Prepr. A.C.S. Div. Polym., 23, 39 (1982)
- 31) Gilanyi, T.; Wolfram, E., Colloids and Surfaces, 3, 181 (1985)
- 32) Goddard, E.D.; Hannan, R.B., J. Colloid. Interf. Sci., 55, 73 (1976)
- 33) Hayakawa, K.; Kwak, J.C.T., J. Phys. Chem., 86, 3866 (1982)
- 34) Hayakawa, K.; Santerre, J.P.; Kwak, J.C.T., Macromolecules, 16, 1642 (1983)
- 35) Hayakawa, K.; Kwak, J.C.T.; Malovikova, A., J. Phys. Chem., 88, 1930 (1984)
- 36) Muller, N.; Smith, M.L., J. Colloid. Interf. Sci., 52, 507 (1975)
- 37) Nagarajan, R., Colloids and Surfaces, 13, 1 (1985)
- 38) Ruckenstein, E.; Huber, G.; Hoffman, F., Langmuir, 3, 382 (1987)
- 39) Hall, D.G., J. Chem. Soc., Faraday Trans. I, 77, 1121 (1981)
- 40) Hall, D.G., J. Chem. Soc., Faraday Trans. I, 81, 885 (1985)

- 41) Jones, M.N.; Manley, P.; Midgeley, P.J.W., *J. Colloid. Interf. Sci.*, 82, 257 (1981)
- 42) Cabane, B.; Duplessis, R., *Colloids and Surfaces*, 13, 19 (1985)
- 43) Francois, J.; Dayantis, J.; Sabbadin, J., *Eur. Polym. J.*, 21, 165 (1985)
- 44) Sasaki, T.; Kushima, K.; Matsuda, K.; Suzuki, H., *Bull. Chem. Soc. Jpn*, 53, 1864 (1980)
- 45) Satake, I.; Yang, J.T., *Biopolymers*, 15, 2263 (1976)
- 46) Schwartz, G., *Eur. J. Biochem.*, 12, 442 (1970)
- 47) Zimm, B.H.; Bragg, J.K., *J. Chem. Phys.*, 31, 526 (1959)
- 48) Manning, G.S., *J. Chem. Phys.*, 51, 924 (1969)
- 49) Delville, A., *Chem. Phys. Letters*, 118, 617 (1985)

CHAPTER TWO

- 1) Sandford, P.A.; *Adv. Carbohydr. Chem. & Biochem.*, 36, 265 (1979)
- 2) Lilly, V.G.; Wilson, H.A.; Leach, J.G.; *Appl. Microbiol.*, 6, 105 (1958)
- 3) *Bergey's Manual of determinative bacteriology*, 8th Ed., p.243, Buchanan, R.E. & Gibbons, N.E., ed; The Williams & Wilkins Co., Baltimore, Md (1974)

- 4) Jeanes, A.; Pittsley, J.E.; Senti, F.R.; *J. Appl. Polym. Sci.*, Vol. V, 17, 519 (1961)
- 5) Jeanes, A.; *J. Polym. Sci., Symp. No 45*, 209 (1974)
- 6) Publication ARS-NC-51 of the USDA Agricultural Research Service (Nov. 1976)
- 7) Dintzis, F.R.; Babcock, G.E.; Tobin, R.; *Carbohyd. Res.*, 13, 257 (1970)
- 8) Jansson, P.E.; Kenne, L.; Lindberg, B.; *Carbohyd. Res.*, 45, 275 (1975)
- 9) Melton, L.D.; Mindt, L.; Rees, D.A.; Sanderson, G.R.; *Carbohyd. Res.*, 46, 245 (1976)
- 10) Cadmus, M.C.; Rogovin, S.P.; Burton, K.A.; Pittsley, J.E., Knutson, C.A.; Jeanes, A.; *Can. J. Microbiol.*, 22, 942 (1976)
- 11) Cadmus, M.C.; Knutson, C.A.; Lagoda, A.A.; Pittsley, J.E.; Burton, K.A.; *Biotechnol. Bioeng.*, 20, 1003 (1978)
- 12) Rees, D.A.; *Biochem. J.*, 126, 257 (1972)
- 13) Holzwarth, G.; *Biochemistry*, Vol.15, 19, 4333 (1976)
- 14) Morris, E.R.; Rees, D.A.; Young, G.; Walkinshaw, M.D.; Darke, A.; *J. Mol. Biol.*, 110, 1 (1977)
- 15) Milas, M.; Rinaudo, M.; *Carbohyd. Res.*, 76, 189 (1979)
- 16) Dove, W.F.; Davidson, N.; *J. Mol. Biol.*, 5, 467 (1962)

- 17) Schildkraut, C.; Lifson, S.; *Biopolymers*, 3, 195 (1965)
- 18) Smith, I.H.; Symes, K.C.; Lawson, C.J.; Morris, E.R.; *Int. J. Biol. Macromol.*, 3, 129 (1981)
- 19) Frangou, S.A.; Morris, E.R.; Rees, D.A.; Richardson, R.K.; Ross-Murphy, S.B.; *J. Polym. Sci.: Polym. Lett.*, 20, 531 (1982)
- 20) Flory, P.J.; *Proc. Roy. Soc. Ser. A*, 234, 50 (1956)
- 21) Sandford, P.A.; Pittsley, J.E.; *A.C.S. Symp. Ser.*, 45, 192 (1977)
- 22) Maret, G.; Milas, M.; Rinaudo, M.; *Polym. Bull.*, 4, 291 (1981)
- 23) Moorhouse, R.; Walkinshaw, M.D.; *A.C.S. Symp. Ser.*, 45, 90 (1977)
- 24) Okuyama, K.; Arnott, S.; *A.C.S. Symp. Ser.*, 141, 411 (1980)
- 25) Holzwarth, G.; Prestige, E.B.; *Science*, 197, 757 (1977)
- 26) Holzwarth, G.; *Carbohydr. Res.*, 66, 173 (1978)
- 27) Southwick, J.G.; Mc Donnell, M.E.; *Macromol.*, Vol.2, 2, 305 (1979)
- 28) Paradossi, G.; Brant, D.; *Macromol.*, 15, 874 (1982)
- 29) Norton, I.T.; Goodall, D.M.; *J. Chem. Soc. Chem. Commun.*, 545 (1980)
- 30) Norton, I.T.; Goodall, D.M.; Frangou, S.A.; Morris, E.R.; Rees, D.A.; *J. Molec. Biol.*, 175, 371 (1984)

- 31) Manning, G.; J. Chem. Phys., 51, 924 (1969)
- 32) Manning, G.; Annu. Rev. Phys. Chem., 23, 117 (1972)
- 33) Manning, G.; J. Phys. Chem., 79, 262 (1975)
- 34) Zimm, B.H.; Bragg, J.K.; J. Chem. Phys., 31, 526 (1959)
- 35) Morris, V.J.; Franklin, D.; I'anson, K., Carbohydr. Res., 121, 13 (1983)
- 36) Milas, M.; Rinaudo, M.; Lambert, F.; Vincendon, M.; Macromolecules, 16, 816 (1983)
- 37) Holzwarth, G.M., in "Solution Properties of Polysaccharides", Ed. Brant, D.A., ACS Symp. Series No.150, Amer. Chem. Soc., Washington, DC, p.15
- 38) Southwick, J.G.; Jamieson, A.M.; Blackwell, J., Carbohydr. Res., 99, 117 (1982)
- 39) Rinaudo, M.; Milas, M., Biopolymers, 17, 2663 (1978)
- 40) Mandelkern, L.; Flory, P.J.; J. Chem. Phys., 20, 212 (1952)
- 41) McDonnell, M.E.; Jamieson, A.M., J. Appl. Polym. Sci., 21, 3261 (1977)
- 42) Southwick, J.G.; Hoosung, L.; Jamieson, A.M.; Blackwell, J., Carbohydr. Res., 84, 287 (1980)

CHAPTER THREE

- 1) Goddard, E.D.; Hannan, R.B., *Micellization, Solubilization and Microemulsions*, Vol.2, K.L. Mittal, Ed., Plenum, NY, NY
- 2) Abuin, E.B.; Scaiano, J.C., *J. Am. Chem. Soc.*, 106, 6274 (1984)
- 3) Goddard, E.D.; Leung, P.S., Ananthapadmanabhan, K.P., *Colloids and Surfaces*, 13, 63 (1985)
- 4) Zana, R.; Yiv, S.; Strazielle, C.; *J. Colloid. Interf. Sci.*, 80, 208 (1981)
- 5) Cabane, B., *J. Phys. Chem.*, 81, 1639 (1977)
- 6) Goddard, E.D.; Leung, P.S.; Glinka, C.J.; *Colloids and Surfaces*, 13, 47 (1985)
- 7) Maeda, H.; Kato, H.; Ikeda, S.; *Biopolymers*, 23, 1333 (1984)
- 8) Satake, I.; Yang, J.T.; *Biopolymers*, 15, 2263 (1976)
- 9) Musabekov, K.B.; Omarova, K.I.; Izimov, A.I.; *Acta Phys. Chem.*, 29, 89 (1983)
- 10) Bekturov, E.A.; Kudaibergenov, S.E.; Kanapyanova, G.S.; *Polym. Bull.*, 11, 551 (1984)
- 11) Goddard, E.D.; Pethica, B.A.; *J. Chem. Soc.*, 2659 (1951)
- 12) Goddard, E.D.; Hannan, R.B.; *J. Am. Oil Chem. Soc.*, 54, 561 (1977)

- 13) Vanlerberghe, G; Handjani-Vila, R.M.; Poubeau, M.C.; Proc. 7th Int. Congr. Surf. Act. Agents, Moscow, 1976, V.M. Zimina, Ed., Moscow, p. 791
- 14) Saito, S.; Taniguchi, T., J. Colloid Interf. Sci., 44, 114 (1972)
- 15) Saito, S., Colloid Sci., 257, 266 (1979)
- 16) Milas, M.; Rinaudo, M., in "Solution Properties of Polysaccharides", Ed. Brant, D.A., ACS Symp. Series No. 150, Amer. Chem. Soc., Washington, DC, p.25
- 17) Goddard, E.D., Phillips, T.S., Hannan, R.B., J. Soc. Cosmet. Chem., 26, 461 (1975)
- 18) Schwuger, M.J., Lange, H., Tenside, 5, 257 (1968)
- 19) Goddard, E.D.; Hannan, R.B., J. Colloid Interf. Sci., 55, 73 (1976)
- 20) Kwak, J.C.T.; Hayakawa, K., J. Phys. Chem., 86, 3866 (1982)
- 21) Kwak, J.C.T.; Hayakawa, K.; Santerre, J.P., Macromolecules, 16, 1642 (1983)

CHAPTER FOUR

- 1) Jones, M.N., J. Colloid Sci., 23, 36 (1967)
- 2) Goddard, E.D.; Hannan, R.B., J. Am. Oil Chem. Soc., 54, 561 (1977)

- 3) Buckingham, J.H.; Lucassen, J.; Hollway, F., *J. Colloid Interf. Sci.*, 67, 423 (1978)
- 4) Birdi, K.S., *J. Colloid Interf. Sci.*, 57, 228 (1976)
- 5) Eley, D.D.; Hedge, D.G., *J. Colloid Sci.*, 12, 419 (1957)
- 6) Buckelew, A.R.; Colacicco, G., *Biochimica Biophysica Acta*, 233, 7 (1971)
- 7) Chen, S.S.; Rosano, H.L., *J. Colloid Interf. Sci.*, 61, 207 (1977)
- 8) Johnston, D.S.; Coppard, E.; Parera, G.; Chapman, D., *Biochemistry*, 23, 6912 (1984)
- 9) Johnston, D.S.; Coppard, E.; Chapman, D., *Bioch. Bioph. Act.*, 815, 325 (1985)
- 10) Pethica, B.A.; Anderson, P.J., *Trans. Far. Soc.*, 51, 1402 (1955)
- 11) Goddard, E.D.; Hannan, R.B., *J. Colloid Interf. Sci.*, 55, 73 (1976)
- 12) Pethica, B.A.; Betts, J.J., 1581 (1956)
- 13) Christodoulou, A.P.; Rosano, H.L., *Adv. Chem.*, 84, 210 (1968)
- 14) Goddard, E.D.; Ackilli, J.A., *J. Colloid Sci.*, 18, 585 (1963)
- 15) Davies, J.T., *Proc. Roy. Soc. (London)*, 208A, 224 (1951)
- 16) Schwuger, M.J.; Lange, H., *Tenside*, 5, 257 (1968)
- 17) Chatterjee, R.; Mitra, S.P.; Chatteraj, D.K., *Ind. J. Biochem. Biophys.*, 16, 22 (1979)

- 18) Goddard, E.D.; Phillips, T.S.; Hannan, R.B., *J. Soc. Cosm. Chem.* 26, 461 (1975)
- 19) Johnston, D.S.; Coppard, E.; Chapman, D., *Biochim. Biophys. Act.*, 815, 325 (1985)
- 20) Johnston, D.S.; Coppard, E.; Parera, G.V.; Chapman, D., *Biochemistry*, 23, 6912 (1984)
- 21) Goddard, E.D.; Hannan, R.B., *J. Colloid Interf. Sci.*, 55, 73 (1976)
- 22) Pethica, B.A., *Trans. Farad. Soc.*, 51, 1402 (1955)
- 23) Alexander, D.M.; Barnes, G.T., *J.C.S. Faraday*, 1, 76 (1980)
- 24) Fowkes, F.M.,
- 25) Kwak, J.C.T.; Santerre, J.P.; Hayakawa, K., *Colloid Surf.*, 13, 35 (1985)
- 26) Schwartz, G., *Eur. J. Biochem.*, 12, 442, (1970)
- 27) Satake, I.; Yang, J.T., *Biopolymers*, 15, 2263 (1976)